NTNU

Norwegian University of
Science and Technology

MultiPhase Permanent Magnet Synchronous Generators for Offshore Wind Enegy System

Control of six phase PMSG- six leg converter system

Nahome Alemayehu Ayehunie

Master of Science in Electric Power Engineering
Submission date: July 2011
Supervisor: Tore Marvin Undeland, ELKRAFT

Norwegian University of Science and Technology
Department of Electric Power Engineering

NTNU
Norwegian University of
Science and Technology

Control of Multiphase PMSG for Offshore Wind

Vector Control of Six Phase PMSG

Nahome Alemayehu Ayehunie

Master of Science in Electric Power Engineering

Submission Date: July 2011

Supervisor: Tore M. Undeland,

Norwegian University of Science and Technology

Department of Electric Power Engineering

Preface

First of all I would like to express my sincere gratitude to Professor Tore Undeland, my supervisor, for giving me the chance to explore the field of Power Electronics towards the project. And his encouragement and guidance based on his myriad experience of the field are also invaluable for me.

I would like to thank Temesgen Haileslassies, PhD student and Rabah Zaimeddine, Post doc, for their continuous, sometimes long discussion and sharing ideas with me.

This work would not be successful without the help from Sverre, PhD student. I would also like to thank sachin thopati, master student.

I would like to thank all service laboratory staff for their support from the first day of the project up to the last week.

The encouragement and moral that I have got from my officemates and friends are invaluable, so I am deeply indebted to them.

Finally, I would like to thank my parents for their love and support.

Nahome Alemayehu Ayehunie

Trondheim, Norway

July 2011

Summary

The three phase permanent magnet synchronous generator with full scale converter arrangement has gained significant market share in win energy turbine topology. This is because of the advancement in production of superior magnetic properties and steady decline in price of the magnets. Permanent magnet synchronous generators are of compact in size and light in weight. They become attractive for offshore wind application. But offshore wind energy system has to be not only light weight and compact in size but also **reliable** operation. The majority of failures of wind turbines are the electrical systems. To increase the reliability of the ordinary three phase wind energy system, a six phase wind energy system is proposed: a six phase permanent magnet synchronous connected to six leg converter.

To harness the maximum energy from the wind, the viable option is using variable speed wind turbine. Variable speed operation of drive is achieved by suitable control of generator-converter system.

This project deals with the design, simulation and implementation vector control of six phase permanent magnet synchronous generator-converter system. Step by step approach is used to tackle the problem. First the dynamic modeling of six phase permanent magnet in different references frames is studied. Then the time average and switching model of a six leg converter is presented. The different modulation technique of six leg converter is studied. Last the design or tuning of control parameters for the speed and current controllers are done. Dc link voltage control design is also done.

After having the theoretical base, the majority of the work is done in preparation of laboratory setup, understanding of FPGA platforms and fighting with sporadic practical problem.

Finally, it is of great personal success to be able to model, and control in the laboratory a low speed Non Standard Six Phase PMSG having 33.27 degree separations between the phase groups.

Contents

Acronyms

AC, ac	Alternating Current
ADC	Analog to Digital Converter
CAN	Controller Area Network
DC, dc	Direct Current
DRAM	Dynamic Random Access Memory
DSP	Digital Signal Processor
EV	Electric Vehicle
emf	Electromotive force
EWEA	European Wind Energy Association
FOC	Field Oriented Control
FPGA	Field Programmable Gate Array
FRC	Fully-Rated Converter
IGBT	Insulated Gate Bipolar Transistor
IP	Intellectual Property
IPMSG	Interior-mount Permanent Magnet Synchronous Generator
MPPT	Maximum-Point Power Tracking
PI	Proportional Integrator
PM	Permanent Magnet
PMSG	Permanent Magnet Synchronous Generator
PMSM	Permanent Magnet Synchronous Machine
PWM	Pulse Width Modulation
PWM-VSC	Pulse Width Modulation - Voltage Source Converter
RMS	Root Mean Square
SMPMSG	Surface-Mount Permanent Magnet Synchronous Generator
SVPWM	Space Vector Pulse Width Modulation
TTL	Transistor-Transistor Logic
UPF	Unity Power Factor
VSC	Voltage Source Converter

List of Figures

List of Tables

1 Introduction

In this chapter brief introduction about wind energy trends and technology; off shore wind energy and its potential to support green power and green house gas emission reduction. The problem description and related literature review history is discussed. The scope and limitation of the project work is also revealed.

1.1 Wind Energy System

The ambition to tackle climate and energy crisis boosts the utilizing and market growth of renewable energy sources. To mention, the European Union has set a binding target of 20% of its energy supply to come from renewable resources by the year 2020. To meet this target, more than one-third of European electrical demand needs to be renewable, and wind power is expected to deliver 12% to 14% (180 GW) of the total demand. Thus wind energy will play a leading role in providing a steady supply of indigenous and green power [1].

The annual installed capacity of wind is increasing fast. As it can be seen in Figure 1-1, the installed wind capacity is more than doubling every third year.

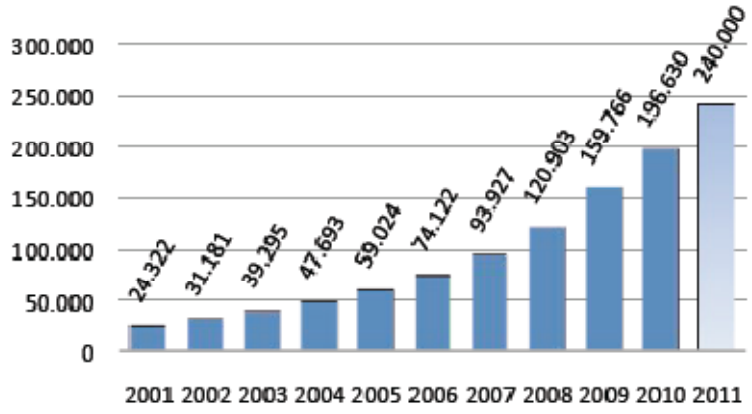

Figure 1-1 World Total Wind Power Installed Capacity in MW, [2]

The long term benefits of wind energy are enormous if environmental factors are considered in the light of increasing pollution by the use of fossil-fuels, for example the Gulf of Mexico oil spill in 2010 is a recent witness.

Based on the average energy mix of the European Union, it is assumed that 1 TWh of wind power displaces 0.667 Mt of CO_2.

The Wind Power

The wind power captured by the turbine P_t is given by

$$P_t = \frac{1}{2} C_p(\beta, \lambda) \rho A v_\omega^3 \qquad (1.1)$$

Where, C_p is the power coefficient, β is pitch angle, λ is tip speed ratio ρ is the air density, A is the area swept out by the turbine blades and v_ω is wind speed.

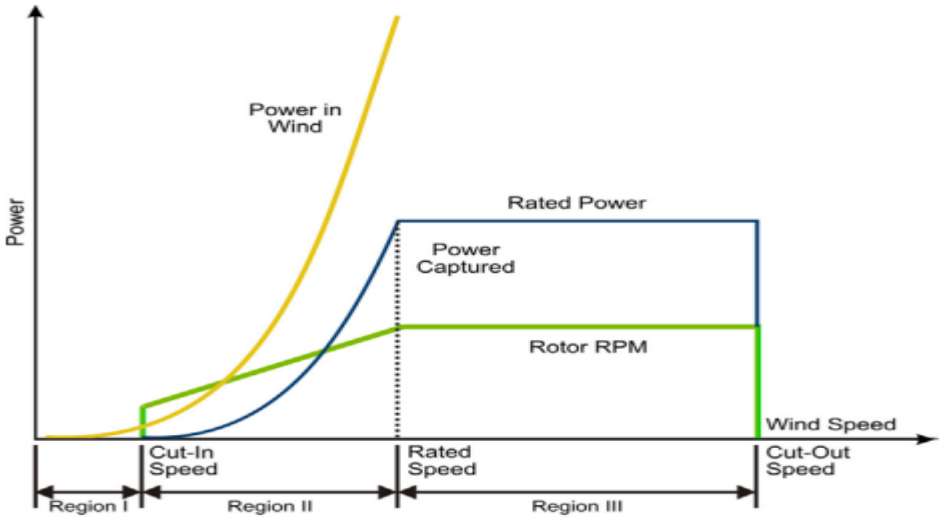

Figure 1-2 Wind Power, Turbine Power and Rotor speed in different operating regions

In region I the wind speed is too slow to derive the turbine and produce valuable energy. The cut-in speed is 4-5 m/s in modern wind turbines.

When the wind speed is above the cut-out speed, 22-25m/s, the turbines must stop operation to prevent overloads and damage to the turbine's components.

In region III, the wind speed is strong enough to produce the rated or maximum power. Pitch control mechanism is used to keep output turbine power constant.

In Region II the turbine has to operate at the maximum possible efficiency by adjusting the speed of the generator. Generally two basic schemes of wind turbine control system can be considered.

Fist method is constant tip-speed ratio scheme. It is based on the fact that the maximum energy is extracted from the wind when the optimal tip speed ratio is achieved. The rotor power coefficient as a function of tip speed ratio and pitch angle is shown in Figure 1-3.

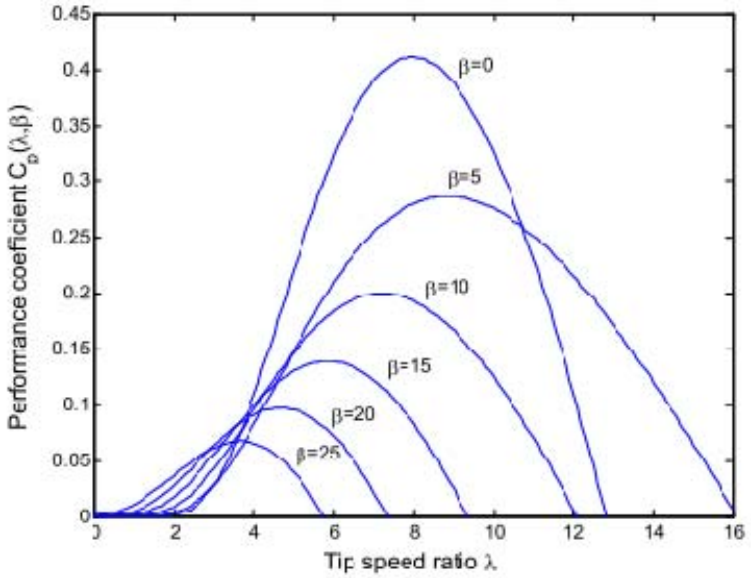

Figure 1-3 Power coefficient as function of λ and β

Second method is Maximum Point Power Tracking (MPPT) scheme. It is based on the fact that the power versus speed curve has a single well defined peak , $dP/dw = 0$. This scheme is insensitive to errors in wind velocity measurement [3].

Therefore, region II is the main interest of this project: to insure the maximum power transfer from the wind (offshore) to grid by controlling the wind generator. The vector control method is used for the control purpose.

1.2 Offshore Wind

Offshore wind farms offer significant energy production advantages over onshore farms with respect to wind quality and available area of deployment. Wind traveling over large bodies of water tends to be more uniform with higher velocity than onshore wind, which encounters obstructions such as forests that create eddy currents. The consistency and quality of offshore wind makes it relatively easy for utility operators to predict and manage. However, there are big both technological and financial challenges to put wind turbines out on a sea and to integrate them to the grid.

The offshore wind industry is flourishing. European Wind Energy Association statistics show that on average in 2008, over 1 MW was installed per day, reaching a total of 1,471 MW worldwide by the end of the year, shown in Figure 1-4

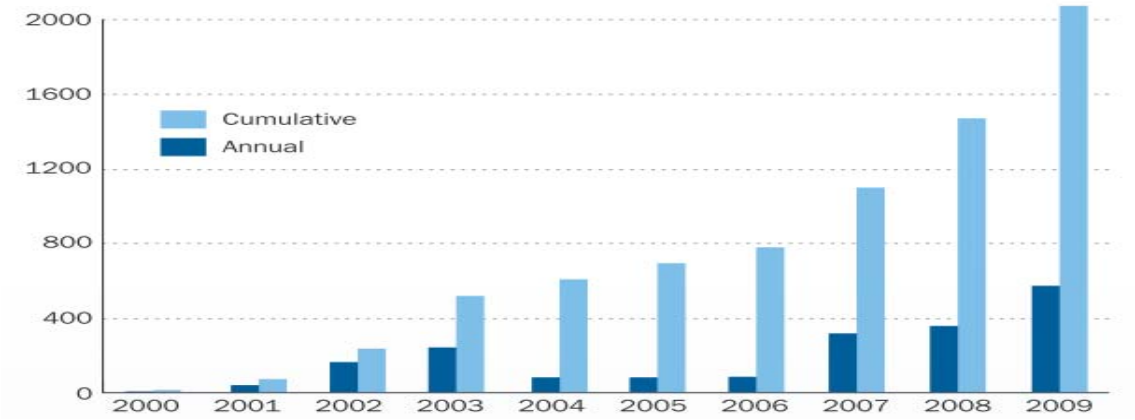

Figure 1-4 Annual and Cumulative installed offshore capacity in Megawatts (MW), [4]

There are over 100 GW of offshore wind projects already being planned. These projects would produce 10% of the EU's electricity whilst avoiding 200 million tones of CO2 emissions each year. EWEA has a target of 40 GW of offshore wind in the EU by 2020 and 150 GW by 2030 [4].

1.3 Problem Description

The three phase permanent magnet synchronous generator with full scale converter arrangement has gained significant market share in win energy turbine topology. This is because of the advancement in production of superior magnetic properties and steady decline in price of the magnets. Permanent magnet synchronous generators are of compact in size and light in weight. Permanent magnet synchronous generators are also more stable in normal operation range and they do not need external excitation. All these make them attractive for offshore wind application.

But offshore wind energy system has to be not only light weight but also **reliable**. The majority of failures of wind turbines are known to be the electrical systems. To increase the reliability of the ordinary three phase wind energy system, six phase wind energy system is proposed as shown in Figure 1-5.

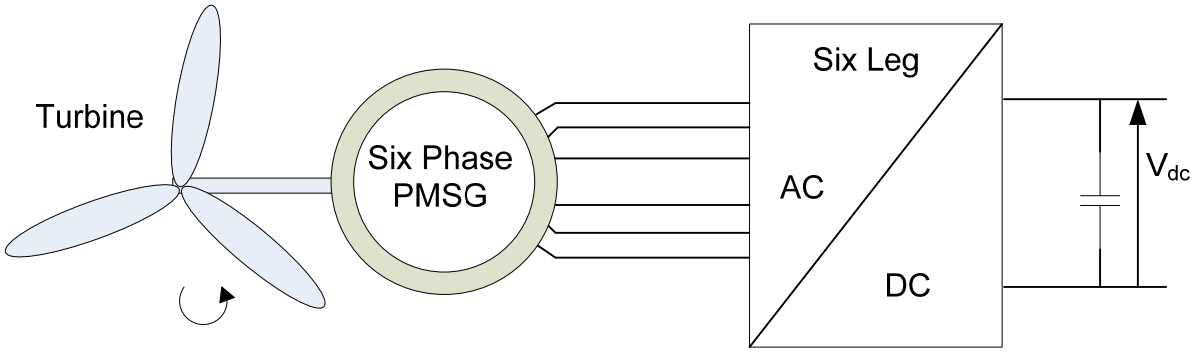

Figure 1-5 Proposed topology

Besides their reliability, Six phase machines with asymmetric arrangement have many advantage over three phase machines; such as lower torque ripple, lower dc link current(lower capacitance), and lower total harmonic. By selecting special control and switching technique of the converter, stator losses of the generator and dc link current can further be reduced.

The objective of this project is to design, simulate and implement the vector control six phase permanent magnet synchronous generator connected to six-leg converter. Six-leg converter is equivalent to having two three phase converters connected to a common dc link.

1.4 Literature Review

In the late 1920's, the limitations in the circuit breaker capabilities and the needs of enormous to limit fault current brought to birth of multiphase machines [5]. In 1930, the theory and design limitations of dual stator winding generators were presented [6]. Later, Robert [7] had shown that stray losses due to phase harmonics can be materially reduced by means of two separate stator windings displaced 30^0 from each other.

In 1973, Fuchs and Rosenberg [8] presented the mathematical model of dual stator winding separated by any arbitrary angle using the dual orthogonal transformation. In the same year,[9] the use of multiple inverters connected to a multiphase machine with appropriate winding displacements showed significant improvement in system performance compared to three phase converter feed induction machines. Later inverter fed multiphase induction machines, six phase synchronous machines with AC and DC connection, and inverter fed synchronous motors were introduced[11]-[13].

The development of power electronics devices and the advancement in DSP modules boomed the study and research on the multiphase machines. Multiphase machine drives has been used as in Electric Vehicles (EV), hybrid EV, aerospace, ship propulsion, and high-power

applications in which the requirements are not cost oppressive when compared to the overall system [14]. Levi [15] did a thorough survey related to Multiphase drives in various subcategories including the application of Multiphase machines for power generation.

Multi phase PMSG for large power applications had not obtained much attention because of the high price and the lower quality of magnetic materials. It has now turned out with steady decrease in the price of the magnet and by the technology advancement which brings very high quality magnetic material.

In [16] parallel connection of converters to multiphase PMSG with a modular way was investigated to allow the use of classical converters. The control of multiphase PMSG for wind was also presented in [17] when the two set of three phase windings are controlled independently by using two independent converters.

In this paper, the control of multiphase machine is simulated using space vector decomposition technique so that two set of three phase windings are controlled together using one six phase converter. This helps to reduce the number of controller to be used, to improve the total harmonic distortion and to reduce the current ripples. In addition, using one six leg converter gives additional degree of control freedom which can be used either for loss minimization. But because the complexity of vector space decomposition, this modulation method is done one space vector modulation for the two converters is used.

1.5 Scope and Limitation of the Work

Scope of the work includes

- Modeling and simulation of six phase generator and converter
- Vector control or Field Oriented Control of six phase PM machine
- Dc link voltage control
- Implementation and laboratory test of vector control of the generator and dc link voltage control

Limitations:

- Wind turbine model is not included.
- Grid side converter is not studied

1.6 Report Layout

For the implementation of the control of six-phase PMSG the project is organized as follows

Chapter1- shows the general fact of wind energy system, offshore wind energy and literature review about multiphase machines

Chapter 2- deals with modeling of six phase generator in synchronous rotating frame

Chapter 3- deals with converts and modulation scheme for ordinal and six- leg converter

Chapter 4- is about the control, which combines the modeling of generator and converter; different control modes and dc link control

Chapter 5 – describes experimental setup.

Chapter 6- in this chapter, controllers are designed, simulated and implemented in the laboratory and the results are presented

Chapter 7-concludes the report with recommendations for further work

2 Multiphase PMSG

In this chapter dynamic modeling of six phase permanent magnet synchronous machines are discussed. The physical parameters of the machine in stationary stator reference frame are given. Next, the modeling of the machine in synchronous rotating reference frame is studied. The two phase component transformation or vector space decomposition modeling of the machine is presented.

2.1 Introduction

The permanent magnet synchronous machine is a regular synchronous machine where the DC excitation is replaced by permanent magnets. Excitation losses may reach up to 5% in small machines [18].Having permanent magnets in the rotor circuit. These losses in the rotor are eliminated. The PMSG has a smaller physical size, higher reliability and power density per volume ratio. Because of these advantages, the PMSG are becoming an interesting solution for wind turbine applications. However, the drawback of the PMSGs is their lack of voltage control because of their constant excitation. Therefore, there have to be converters to support voltage control for PMSG. But for variable speed wind turbine operation it is inevitable to use converters for grid integration and have already been a standard.

Based on the rotor construction, PMSG can be either surface mounted permanent magnet synchronous generators SPMSG or interior mounted permanent magnet synchronous generators IPMSG. Interior mounted rotor is built with the magnets inserted in cavities in the rotor structure. This creates saliency which results in reluctance torque component.

Based on the magnetic flux orientation, PMSG can be group as a radial flux and an axial flux machine. Radial flux machine is constructed by placing stator around the rotor in such a way to produce radial directed flux. In axial flux machine, the stator and the rotor are placed such that the air gap is perpendicular to the direction of rotation there by the main flux crosses the air gap in axial direction of rotation. Only Radial flux PMSG is studied here.

Based on the arrangement of stator windings, PMSG can also be divided as distributed winding and concentrated winding. The generator that is available in the laboratory is concentrated winding machine, therefore the modeling and control focus on this type of machine.

Based on the number of phases, machines in general can be two phase, three phase or multiphase (greater than three). Three phase machines have been studied for long time and are widely available in numerous applications.

Multi phase machines provides several advantages such as

- Reduced amplitude and increased frequency of pulsating torque
- Lower current per phase for the same rated voltage
- Lower dc-link current harmonics converter fed system
- Higher reliability and
- Higher degree of freedom

The six phase synchronous machine has two identical stator windings which are assumed balanced star connected. Commonly, the two sets of winding can have a phase shift of 0, 30 and 60 degrees. Zero degree phase shift is exactly similar to three phase system. Sixty degree phase shift forms symmetrical arrangement and can be reduced to three phase system because two phases of different stars are always collinear. Thirty degree phase shift forms unsymmetrical arrangement which cannot be further simplified. The thirty degree phase shift arrangement is optimal with respect to voltage harmonic distortion and torque pulsation [7]. Therefore, thirty degree phase shift between star connections has been preference arrangement and also in this project. But, the actual machine used for implementation in the laboratory has 33.2725 degree separation between the two three phase groups.

2.2 Modeling Assumptions and Physical Parameters

In developing the mathematical model the following assumptions are made:

- The set of three-phase stator winding is symmetrical.
- The capacitance of all the windings can be neglected.
- Each of the distributed windings may be represented by a concentrated winding.
- The change in the inductance of the stator windings due to rotor position is sinusoidal and does not contain higher harmonics.
- Hysteresis loss and eddy current losses are ignored.
- The magnetic circuits are linear (not saturated) and the inductance values do not depend on the current.

The arrangement of the windings of the machine is represented by their axis of flux lines as shown in Figure 2-1.

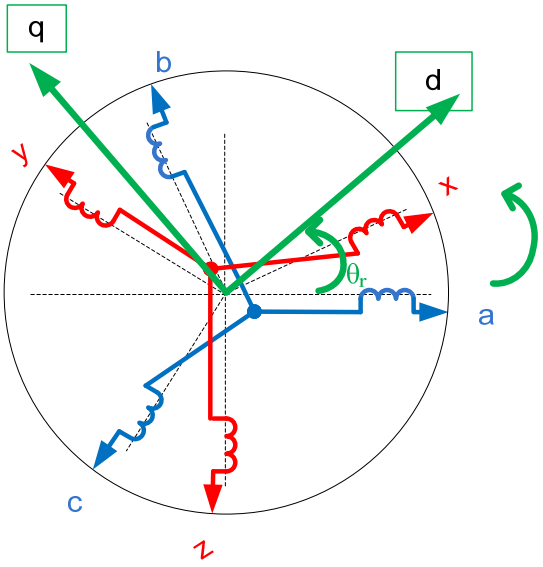

Figure 2-1 Six-phase machine windings axis of flux lines

Mathematical model of six phase machines, like any other machine, can be started from the basic the stator voltage equation which is given in matrix form as

$$[V_s] = [R_s][I_s] + \frac{d[\lambda_s]}{dt} \qquad (2.1)$$

Where, $[V_s] = \begin{bmatrix} V_a & V_b & V_c & V_x & V_y & V_z \end{bmatrix}^T$, $[I_s] = \begin{bmatrix} I_a & I_b & I_c & I_x & I_y & I_z \end{bmatrix}^T$, $[\lambda_s] = \begin{bmatrix} \lambda_a & \lambda_b & \lambda_c & \lambda_x & \lambda_y & \lambda_z \end{bmatrix}^T$ are stator voltage, stator current and stator flux linkages of machine respectively, and the stator resistances are given $[R_s] = diag\begin{bmatrix} R_a & R_b & R_c & R_x & R_y & R_z \end{bmatrix}^T$

For magnetically coupled stator windings, the stator linkage flux is the sum of all fluxes around it. This is represented by the following matrix equation:

$$[\lambda_s] = [L_s][I_s] + [\lambda_{sPM}] \qquad (2.2)$$

λ_{sPM} is the flux linkage of the Permanent Magnet (PM) which links the stator windings can be written as:

$$[\lambda_{sPM}] = \lambda_{PM}\left[cos\theta_r \;\; cos\left(\theta_r - \frac{2\pi}{3}\right) \;\; cos\left(\theta_r + \frac{2\pi}{3}\right) \;\; cos\left(\theta_r - \frac{\pi}{6}\right) \;\; cos\left(\theta_r - \frac{5\pi}{6}\right) \;\; cos\left(\theta_r - \frac{3\pi}{2}\right)\right]^T \qquad (2.2.1)$$

Where λ_{PM} the permanent magnet flux linkage, and θ_r is the angle between magnetic axis of phase and rotor as shown in Figure 2-1.

The inductance matrix L_s includes the self inductance and the mutual inductances of all the stator windings, and is given by

$$[L_s] = \begin{bmatrix} L_{aa} & L_{ab} & L_{ac} & L_{ax} & L_{ay} & L_{az} \\ L_{ba} & L_{bb} & L_{bc} & L_{bx} & L_{by} & L_{bz} \\ L_{ca} & L_{cb} & L_{cc} & L_{cx} & L_{cy} & L_{cz} \\ L_{xa} & L_{xb} & L_{xc} & L_{xx} & L_{xy} & L_{xz} \\ L_{ya} & L_{yb} & L_{yc} & L_{yx} & L_{yy} & L_{yz} \\ L_{za} & L_{zb} & L_{zc} & L_{zx} & L_{zy} & L_{zz} \end{bmatrix} \quad (2.3)$$

In the case of salient pole machine, the self-inductance of each stator phase winding will reach a maximum value whenever the rotor d-axis aligns with the axis of the phase winding because the reluctance of the linkage flux path is minimum. This minimum reluctance condition occurs twice during each rotation of the rotor so that the stator self-inductances are represented by a constant component and a single periodic component, the higher harmonics neglected [19]. As of the form

$$\begin{aligned} &L_{ii} = L_l + L_1 + L_2\, cos(2\theta_i),\ for\ \ i = a, b, c, x, y, z \\ &\theta_a = \theta_r\,, \theta_b = \theta_r - \frac{2\pi}{3}\ and\ \theta_c = \theta_r + \frac{2\pi}{3} \\ &\theta_x = \theta_a - \frac{\pi}{6}\,, \theta_y = \theta_b - \frac{\pi}{6}\ and\ \theta_z = \theta_c - \frac{\pi}{6} \end{aligned} \quad (2.3.1)$$

Where,

L_l is leakage inductance a of stator winding.

L_1 is the constant component of the magnetizing inductance of a stator winding.

L_2 is amplitudes of the second harmonics of the magnetizing inductance.

As each of the stator windings is shifted in space relative to the others by 120^o the mutual inductance between each of the stator windings is negative. When the rotor d-axis is midway between axes of two of the windings, the magnitude of the inductance is maximum, [19].

Therefore, ignoring the mutual leakage inductance, the mutual inductance within the phase group can be written as

$$
\begin{aligned}
L_{ab} &= L_{ba} = -\frac{1}{2}L_1 - L_2\cos 2(\theta_r - \frac{\pi}{3}) \\
L_{bc} &= L_{cb} = -\frac{1}{2}L_1 - L_2\cos 2(\theta_r - \frac{\pi}{2}) \\
L_{ca} &= L_{ac} = -\tfrac{1}{2}L_1 - L_2\cos 2(\theta_r + \tfrac{\pi}{3}) \\
L_{xy} &= L_{yx} = -\frac{1}{2}L_1 - L_2\cos 2(\theta_r - \frac{\pi}{2}) \\
L_{yz} &= L_{zy} = -\frac{1}{2}L_1 - L_2\cos 2(\theta_r - \frac{\pi}{6}) \\
L_{zx} &= L_{xz} = -\tfrac{1}{2}L_1 - L_2\cos 2(\theta_r + \tfrac{\pi}{6})
\end{aligned}
\qquad (2.3.2)
$$

The effect of mutual leakage inductance of the two groups of three phase windings voltage harmonic distortion and torque pulsation is appeared to be negligible when the separation of the two set of windings is 30^o,[12] Therefore, the mutual coupling inductances between the two groups can be written

$$
\begin{aligned}
L_{ax} &= L_{xa} = \frac{\sqrt{3}}{2}L_1 - L_2\cos 2(\theta_r + \frac{\pi}{12}) \\
L_{ay} &= L_{ya} = -\frac{\sqrt{3}}{2}L_1 - L_2\cos 2(\theta_r - \frac{5\pi}{12}) \\
L_{az} &= L_{za} = 0 + L_2\cos 2(\theta_r + \tfrac{\pi}{4}) \\
L_{bx} &= L_{bx} = 0 - L_2\cos 2(\theta_r - \frac{5\pi}{12}) \\
L_{by} &= L_{zb} = \frac{\sqrt{3}}{2}L_1 - L_2\cos 2(\theta_r + \frac{\pi}{4})
\end{aligned}
\qquad (2.3.3)
$$

$$L_{bz} = L_{zb} = -\frac{\sqrt{3}}{2}L_1 - L_2 \cos 2(\theta_r - \frac{\pi}{6})$$

$$L_{cx} = L_{cx} = -\frac{\sqrt{3}}{2}L_1 - L_2 \cos 2(\theta_r + \frac{\pi}{4})$$

$$L_{cy} = L_{yc} = 0 - L_2 \cos 2(\theta_r - \frac{\pi}{12})$$

$$L_{cz} = L_{zc} = \frac{\sqrt{3}}{2}L_1 - L_2 \cos 2(\theta_r - \frac{5\pi}{12})$$

Having the above mathematical representation of the inductances the stator winding of six phase machine, the modeling of surface mounted concentrated winding machine on synchronous rotating frame will be discussed latter. The modeling of six phase machines on synchronous rotating frame can be done in two ways. First, considering the six phase machine as two ideally separated three phase machine. Second, considering the machine as it is and using six phase symmetrical component transformation.

2.3 Dynamic Modeling in Dual Synchronous Rotating Frame

The mutual inductances between stator coils of single layer concentrated windings are very small compared to their corresponding self inductances. For surface mounted PMSG the inductance is independent of rotor position considering no saliency ($L_2 \sim 0$). Taking the above presumable assumptions, the stator inductance matrix of six-phase SPMSG with concentrated windings is reduced to

$$[L_s] = \begin{bmatrix} L_{aa} & & & & & \\ & L_{bb} & & & & \\ & & L_{cc} & & & \\ & & & L_{xx} & & \\ & & & & L_{yy} & \\ & & & & & L_{zz} \end{bmatrix} \qquad (2.4)$$

$$L_{ii} = L_l + L_1 \,, for \;\; i = a, b, c, x, y, z$$

Six phase machine variables in stationary reference frame can be obtained using Clark Transformation and Modified Clark Transformation with respect $(\alpha 1, \beta 1, o1)$ and $(\alpha 2, \beta 2, o2)$ respectively as seen in Figure 2-2.

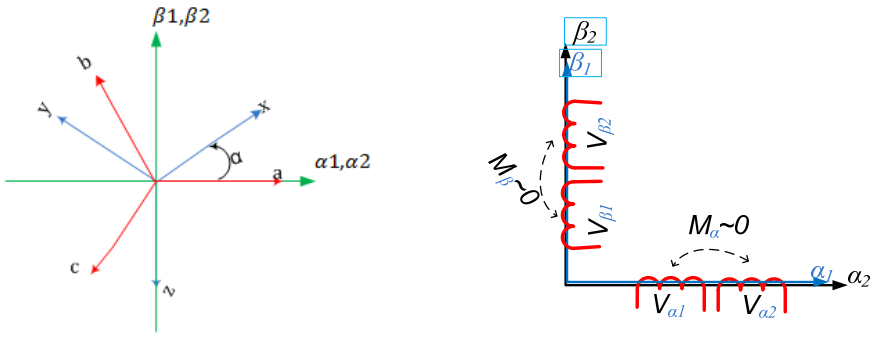

Figure 2-2 Dual Stationary Reference Frame

The stator voltage equation which is by equation Equations (2.1) is split in half, and Clarke and inverse Clarke transformations on voltage, stator current and stator flux linkages of phase group 1 $(a, b, c) - \alpha\beta o1$, and modified Clarke and inverse modified Clarke transformations on voltage, stator current and stator flux linkages of phase group 2 $(x, y, z) - \alpha\beta o2$. Then the equivalent stator linkage flux in stationary frames is

$$\lambda_{\alpha 1} = L_\alpha I_{\alpha 1} + \lambda_{PM} \cos\theta_r$$

$$\lambda_{\beta 1} = L_\beta i_{\beta 1} + \lambda_{PM} \sin\theta_r \qquad (2.5)$$

$$\lambda_{\alpha 2} = L_\alpha I_{\alpha 2} + \lambda_{PM} \cos\theta_r$$

$$\lambda_{\beta 2} = L_\beta I_{\beta 2} + \lambda_{PM} \sin\theta_r$$

The voltage equations in stationary frame become

$$V_{\alpha 1} = R_s I_{\alpha 1} + L_\alpha \frac{dI_{\alpha 1}}{dt} - \omega_r \lambda_{PM} \sin\theta_r$$

$$V_{\beta 1} = R_s I_{\beta 1} + L_\alpha \frac{dI_{\beta 1}}{dt} + \omega_r \lambda_{PM} \cos\theta_r \qquad (2.6)$$

$$V_{\alpha 2} = R_s I_{\alpha 2} + L_\alpha \frac{dI_{\alpha 2}}{dt} - \omega_r \lambda_M \sin\theta_r$$

$$V_{\beta 2} = R_s I_{\beta 2} + L_\alpha \frac{dI_{\beta 2}}{dt} + \omega_r \lambda_M \cos\theta_r$$

The voltage equations, Equation (2.5), are dependent on the rotor position. In order to eliminate the rotor position dependence and time varying equation, synchronous rotating frame transformation is employed. Synchronous rotating frame is also called rotor reference frame.

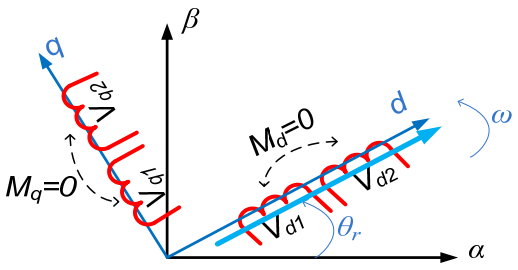

Figure 2-3 Stator windings in synchronous rotating reference frame

Appling Angle Transformation on Equations (2.4) and (2.5), then the corresponding model equivalent model of the machine on synchronous rotating frame

$$\begin{aligned}\lambda_{d1} &= L_d I_{d1} + \lambda_{PM}\\ \lambda_{q1} &= L_q I_{q1}\\ \lambda_{d2} &= L_d I_{d2} + \lambda_{PM}\\ \lambda_{q2} &= L_q I_{q2}\end{aligned} \qquad (2.7)$$

The voltage equations then

$$\begin{aligned}V_{d1} &= R_s I_{d1} + L_d \frac{dI_{d1}}{dt} - \omega_r L_q I_{q1}\\ V_{q1} &= R_s I_{q1} + L_q \frac{dI_{q1}}{dt} + \omega_r L_d I_{d1} + \omega_r \lambda_M\\ V_{d2} &= R_s I_{d2} + L_d \frac{dI_{d2}}{dt}\ pI_{d2} - \omega_r L_q I_{q2}\\ V_{q2} &= R_s I_{q2} + L_q \frac{dI_{q2}}{dt}\ pI_{q2} + \omega_r L_d I_{d2} + \omega_r \lambda_M\end{aligned} \qquad (2.8)$$

The equivalent circuit

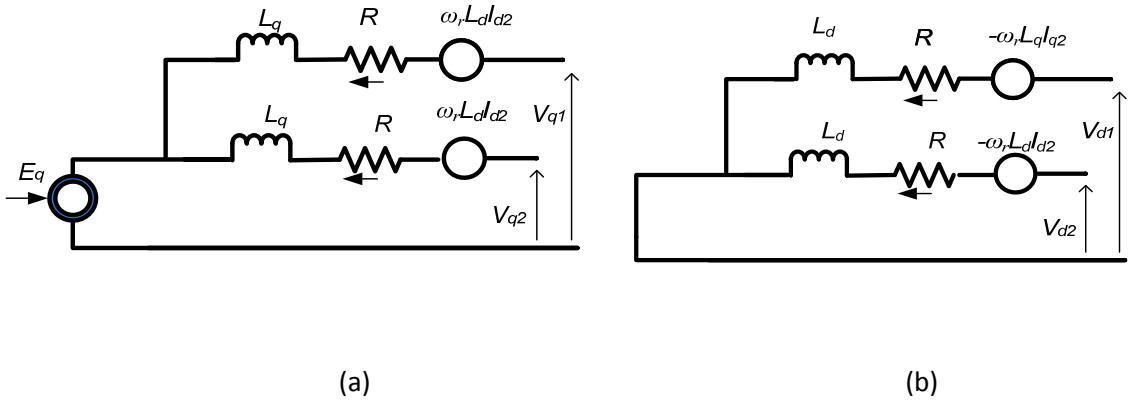

(a) (b)

Figure 2-4 Equitant circuit of six phase PMSG, (a) q axis (b) d axis

Electromagnetic Torque

The electromagnetic torque is the most important output variable that determines the mechanical dynamics of the machine such as the rotor position and speed.

The electro-magnetic torque expression can be calculated from the air gap power P_{ag}. The air gap power is the part of input power which does not contribute to resistive loss, P_{loss}, or rate of change of stored energy in the inductances. The rate of change of stored magnetic energy could only be zero in steady state.

The total air gap flux contributes to the electromechanical torque,

$$P_e = \frac{3}{2}\begin{bmatrix} I_{d1} \\ I_{q1} \end{bmatrix}^T \begin{bmatrix} V_{d1} \\ V_{q1} \end{bmatrix} + \frac{3}{2}\begin{bmatrix} I_{d2} \\ I_{q2} \end{bmatrix}^T \begin{bmatrix} V_{d2} \\ V_{q2} \end{bmatrix},\ P_e\text{-}electrical\ power$$

$$P_{ag} = P_e - P_{loss} - P_{rateChangeStoredMagnetic} \qquad (2.9)$$

$$P_{ag} = \frac{3}{2}\omega_r\, \lambda_{PM}(I_{q1} + I_{q2})$$

And if there are P poles, the electrical torque M_e is

$$M_e = \frac{P_{ag}}{\omega_m} = \frac{P}{2}\frac{3}{2}\lambda_{PM}(I_{q1} + I_{q2}) = K_T\,(I_{q1} + I_{q2}) \qquad (2.10)$$

$$K_T = \frac{P}{2}\frac{3}{2}\lambda_{PM}$$

The toque expression given above is analogous to that of dc machine or that of three phase AC machines in d-q plane.

2.4 Dynamic Modeling using Vector Space Decomposition

The vector Space decomposition theory has been introduced to transform the original six-dimensional space of the machine into three orthogonal subspaces or planes. Vector decomposition is based on the generalized two phase real component transformation of stator windings of n phase machine.

The generalized two-phase real component transformation is appropriate only for symmetrical n-phase machines in which each stator phase is separated from each adjacent stator phase by $360/n$ electrical degrees [10]. As a result, this transformation cannot be applied directly to the six-phase machine configuration with 30 degree separation. But, the generalized two-phase transformation of a symmetrical 12 phase machine can be used to derive transformation matrix for asymmetric six phase machine, see Figure 2-5.

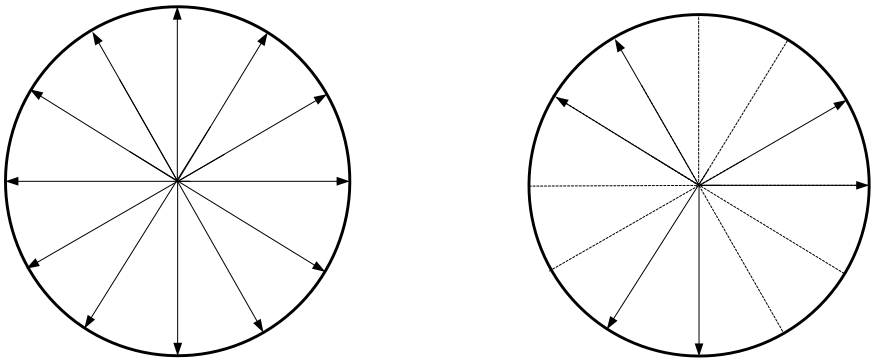

Figure 2-5 Winding axes for 12 phase and 6 phase windings.

For twelve phase machines, n=12, the transformation matrix [T12] is given in Appendix A1.

Then the twelve phase transformation matrix can be reduce to six phase transformation matrix as [T6], it is voltage invariant form.

$$[T_6] = \frac{1}{3}\begin{bmatrix} 1 & cos\,4\alpha & cos\,8\alpha & cos\,\alpha & cos\,5\alpha & cos\,9\alpha \\ 0 & sin\,4\alpha & sin\,8\alpha & sin\,\alpha & sin\,5\alpha & sin\,9\alpha \\ 1 & cos\,8\alpha & cos\,4\alpha & cos\,5\alpha & cos\,\alpha & cos\,9\alpha \\ 0 & sin\,8\alpha & sin\,4\alpha & sin\,5\alpha & sin\,\alpha & sin\,9\alpha \\ 1 & 1 & 1 & 0 & 0 & 0 \\ 0 & 0 & 0 & 1 & 1 & 1 \end{bmatrix} \quad (2.11)$$

$$[T_6]^{-1} = [T_6]^T$$

Rearranging the above equations the voltage equations are

$$V_\alpha = R_s I_\alpha + L_s \frac{dI_\alpha}{dt} - \lambda_{PM} sin\theta_r$$

$$V_\beta = R_s I_\beta + L_s \frac{dI_\beta}{dt} + \lambda_{PM} cos\theta_r$$

$$V_x = R_s I_x + L_s \frac{dI_x}{dt}$$

$$V_y = R_s I_y + L_s \frac{dI_y}{dt} \qquad (2.12)$$

$$V_{z1} = R_s I_{z1} + L_s \frac{dI_{z1}}{dt}$$

$$V_{z2} = R_s I_{z2} + L_s \frac{dI_{z2}}{dt}$$

Equation (2.12) is has rotor position dependent voltage equations. Appling the T_r voltage equations referred to rotating space vector decomposition.

$$V_d = R_s I_d + L_s \frac{dI_d}{dt} - \omega_r L_s I_q$$

$$V_q = R_s I_d + L_s \frac{dI_q}{dt} + \omega_r L_s I_d + \lambda_{PM} \omega_r \qquad (2.13)$$

Equation (2.13) is similar to mathematical model of three phase machine in rotor reference frame. It is used in vector control of six phase machine in similar approach to that of three phase machines. Therefore vector space decomposition method of modeling multiphase machines makes the control as ease as standard three phase machines.

Equivalent circuit in the three orthogonal planes can be derived using (2.12)-(2.13).

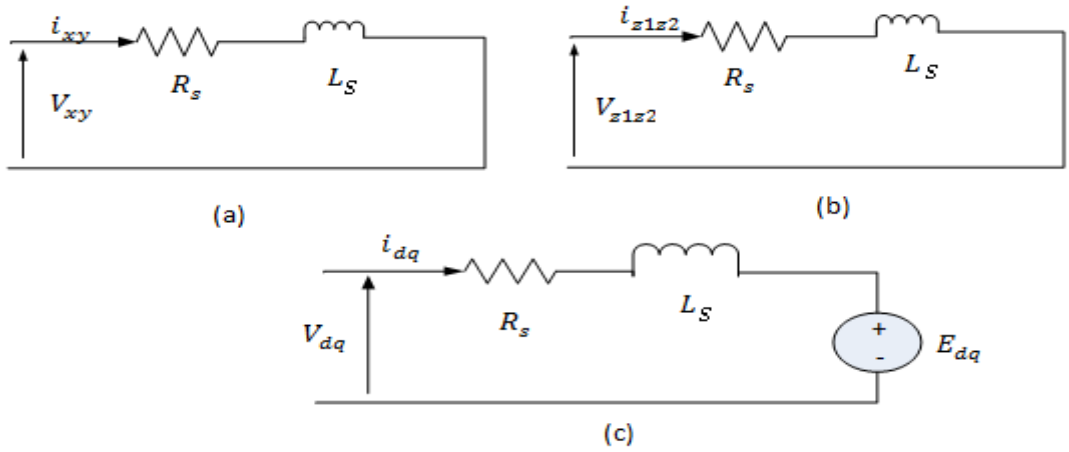

Figure 2-6 Equivalent Circuit of Six phase Generator in three subspaces (a) in x-y subspace, (b) in z1-z2 subspace, (c) in d-q subspace

As seen from (2.12)-(2.13), the current components in (x, y) and (z1, z2) are limited to stator resistor and stator inductance in the case of concentrated winding PMSG. These currents do not contribute to electromechanical energy conversion but losses. So, the electromechanical energy conversion variables are mapped in the only (d,q) subspace. This makes the control of the machine simpler and is equivalent to three phases PMSG.

Electromagnetic Torque

The electro-magnetic torque expression can be calculated from the air gap power. The air gap power is the part of input power which does not contribute to resistive loss or rate of change of stored energy in the inductances. The rate of change of stored magnetic energy could only be zero in steady state.

$$P_e = 3\begin{bmatrix} I_d \\ I_q \\ I_x \\ I_y \\ I_{z1} \\ I_{z2} \end{bmatrix}^T \cdot \begin{bmatrix} V_d \\ V_q \\ V_x \\ V_y \\ V_{z1} \\ V_{z2} \end{bmatrix} \textit{(only d-q component contribute for air gap power)} \qquad (2.14)$$

$$P_{ag} = P_e - P_{loss} - P_{rateChangeStoredMagnetic}$$

$$P_{ag} = 3\omega_r \lambda_M I_q$$

And if there are P poles, the electrical torque T_e is

$$M_e = \frac{P_{ag}}{\omega_m} = 3\,\frac{P}{2}\lambda_M I_q = K_t\, I_q \qquad (2.15)$$

$$K_t = 3\frac{\mathrm{P}}{2}\lambda_M = 2K_T$$

The toque expression given above is equivalent to that of DC machine or that of three phase AC machines in d-q plane.

Therefore, systems of six phase machine can be simplified to two phase windings systems which contribute for electromechanical energy conversion.

In general, multi phase machine modeling and control becomes easier using the vector decomposition technique. All those derivations of equations are to understand the behavior of multiphase machines which are used for control purpose. Before proceeding to control of six phase machine, the next chapter presents about the converters used to operate the machine.

3 Converters

In this chapter three phase converter operation with sinusoidal and space vector switching technique is discussed to pave the way for the analysis of six leg converters. The average model of three phase converter is depicted. The six leg converter topology is described with the extended space vector modulation technique, called the space vector decomposition technique, and is explained;

3.1 Wind Turbine Converter Topologies

Wind Turbines currently installed are either fixed speed or variable speed. In order to be able to operate wind turbine at its maximum power coefficient thereby obtaining larger wind energy capture over wide range of wind speed, variable speed wind turbine must be used in the wind energy system. Variable speed operation is achieved by controlling the generator speed by controlling the converter connected across the stator in fully rated converter configuration or by controlling the converters connected across the rotor windings in the case of doubly feed Induction generator. Fully rated converter based wind turbines may have different topologies based on the generator side converter configuration. These are diode rectifier based, thyristor based, and diode with boost converter based and IGBT based as shown in Figure below.

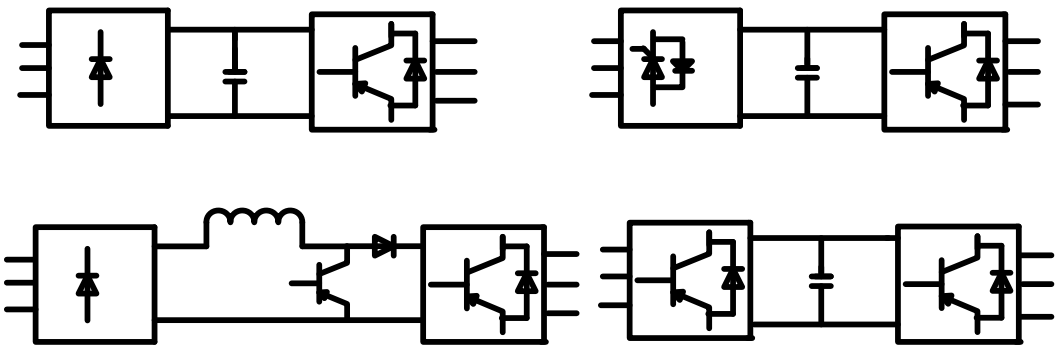

Figure 3-1 Fully Rated Converter based wind turbine converter topologies

IGBT rectifiers has enormous advantages, such as the current or voltage can be modulated generating less harmonic contamination; power factor can be controlled; they can be built as voltage source or current source rectifiers; the reversal of power can be achieved either by reversal of voltage or reversal of current[20]. The proposed converter topology is an IGBT based six-phase converter or cascaded converter having same dc link voltage. The six leg converter has advantages to increase the reliability of system and also

reduces ripple and or the harmonic distortion both in stator and dc link by creating smooth transition in switching states. The advent of fast processing and advanced DSP modules makes the real time control of complex algorithms easier and practical. So, it makes feasible to think of the application of multi leg converters as one, instead.

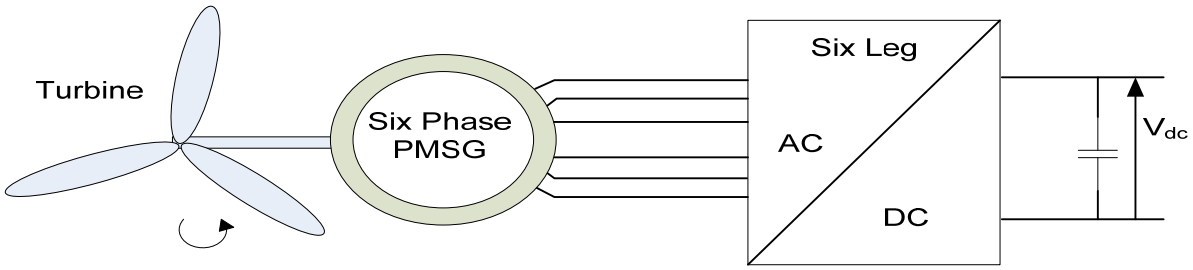

Figure 3-2 wind energy conversion six leg converter topology for six phase machines

As seen in Figure 3-2, the machine connected converters work in rectifier mode of operation most of the time. Therefore, the basic principles and switching of three phase rectifiers are discussed before jumping to six leg converters.

3.2 Operation of three phase rectifier

Three phase converter with fixed dc voltage polarity is called voltage source converter (VSC). VSC can make a smooth transition from the inverter mode to rectifier mode by reversing the direction of dc current; unlike current source rectifiers which reverse the dc voltage polarity. To elaboration the basic operation of VSC converter, a single leg of converter is depicted in below

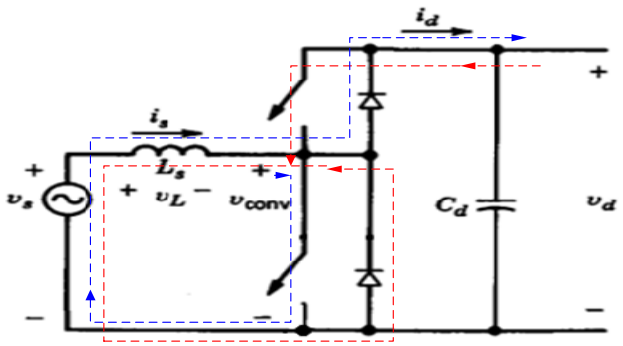

Figure 3-3 Single leg converter operation

Under Rectifier mode operation, the converter works like Boost converter. The upper switch and lower diode work complementarily, the blue line shows the direction of current flow. Under Inverter mode of operation, the converter works like Buck converter. The lower switch and the upper switch and lower diode work complementarily which is shown by red line in

Figure 3-3. The relationship between input voltage (assumed sinusoidal) and converter voltage, ignoring the harmonics, can be easily shown by a phasor

(3.1)

Figure 3-4 Rectifier mode (left) and Inverter mode (right) of operation at unity power factor

From Figure 3-4, the converter voltage is higher that the input voltage in both modes near unity power factor operation. Therefore, the dc link voltage should be sufficiently larger than diode rectification voltage otherwise the converter will behave like common diode bridge, . The active and reactive power flow is also well explained in [21]. When three separate single legs are connected together, they form three phase converter called voltage source converter.

There are many different switching techniques to control converters switching device. The sinusoidal PWM and Space Vector PWM are discussed here, since they are the one used in the implementation.

3.3 VSC-Sinusoidal Pulse Width Modulation

The Pulse Width Modulation is a technique of switching inverter power devices ON and OFF at a carrier frequency in order to generate sequence of pulses whose average value forms the reference signal. In another word, the reference signal is used to shape and control the magnitude and frequency of converter output voltage when the reference signal is sinusoidal waveform; the modulation is called sinusoidal PWM. In PWM, amplitude ratio or modulation index is defined as the ratio of the peak amplitude of the modulating signal and the amplitude of the triangular . The ratio of the frequency of carrier triangle and the frequency of fundamental component PWM pulse pattern is called frequency modulation ratio .

(3.2)

For $m_a \leq 1$, the modulation is called linear modulation in which the fundamental frequency component of the converter voltage linearly varies with m_a . For $m_a \geq 1$, the modulation becomes nonlinear and is called over modulation.

3.3.1. Switching model

In a three phase inverter only one of the switch in each leg is ON at a time; the upper three switches can represent the converter using a the switching function is defined

$$S_j = \begin{cases} 1, & ON(V_{control} > V_{tri}) \\ 0, & OFF(V_{control} < V_{tri}) \end{cases} \qquad j = A, B \text{ or } C \tag{3.3}$$

The converter leg output voltage is given by

$$V_{jN} = S_j V_{dc} \tag{3.4}$$

Using single carrier and three sinusoidal signals shifted by 120°, as shown in Figure 3-6(a), the sinusoidal PWM generated signal of phase and line voltage at the converter is shown Figure 3-6 (b); the converter leg voltage has a dc value of $\frac{\text{vd}}{2}$.

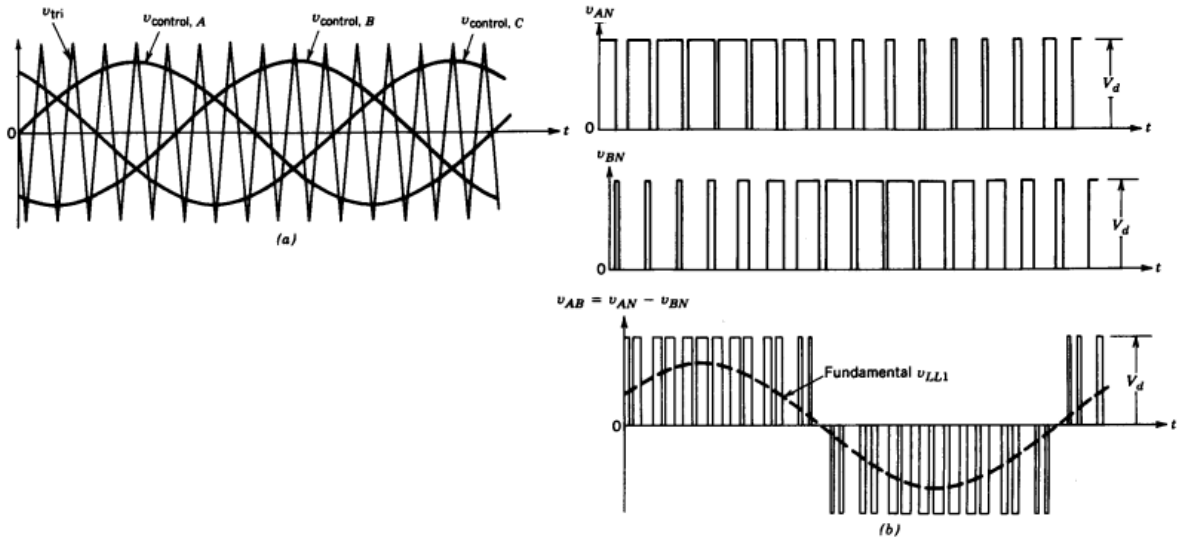

Figure 3-5 (a) Three phase PWM generation (b) phase and line voltages

3.3.2. Average value model of Converter leg

The average leg voltage at output can be obtained by integrating the switching voltage (3.4) over a switching period and dividing by Ts.

$$\overline{V_{jN}} = \frac{1}{Ts}\int_{to}^{to+Ts} V_{dc}\ dt = d_j V_{dc}, \quad j = A, B, C \tag{3.5}$$

The dependency of duty cycle with control signal and carrier signal can be given by

$$d_j = \frac{1}{2} + \frac{1}{2}\frac{v_{control,j}}{V_t} \tag{3.6}$$

For sinusoidal control signal, $v_{control,j} = V_c \sin(\omega t + \theta_j)$, the duty cycle can be written in terms of the modulation index,

$$\begin{aligned} d_j &= \tfrac{1}{2} + \tfrac{1}{2}\tfrac{V_c}{V_t} sin(\omega t + \theta_j) \\ d_j &= \tfrac{1}{2} + \tfrac{1}{2} m_a \, sin(\omega t + \theta_j) \end{aligned} \tag{3.7}$$

In the linear range the peak value of the fundamental frequency component in one of the inverter leg is given in (3.9), note that the dc off set is zero frequency components,

$$\widehat{\mathrm{V}}_{\mathrm{j1}} = \mathrm{m_a}\frac{\mathrm{V_{dc}}}{2} \tag{3.8}$$

The dc component the phase voltages cancel each other in the line to line voltages,

$$\begin{aligned} \overline{V_{jk}} &= d_{jk} V_d \\ d_{jk} &= d_j - d_k \end{aligned} \tag{3.9}$$

The amplitude of line to line voltage of fundamental frequency component across two legs of the converter is

$$\widehat{\mathrm{V}}_{\mathrm{jLL}} = \sqrt{\frac{3}{2}}\mathrm{m_a}\frac{\mathrm{V_{dc}}}{2} \tag{3.10}$$

Equation (3.10) shows that only 61.2% of the dc link voltage can be utilized in the linear range. There are other modulation techniques such as the space vector PWM which will be discussed later and third harmonic injection sinusoidal PWM. Both the modulation techniques allow dc link voltage utilization up to 70.7% in the linear range [22], [23].

The total currents in the three legs sum up to give the dc link current.

$$I_{dc} = \sum_j d_j \bar{I}_j \ , \quad j = A, B \ \& \ C \ . \qquad (3.11)$$

where $\bar{I}_j$ is the average line current and

Combining (3.9) - (3.11), the average model of three phase converter is Figure 3-7. Average models make simulation fast though losing some degree of accuracy.

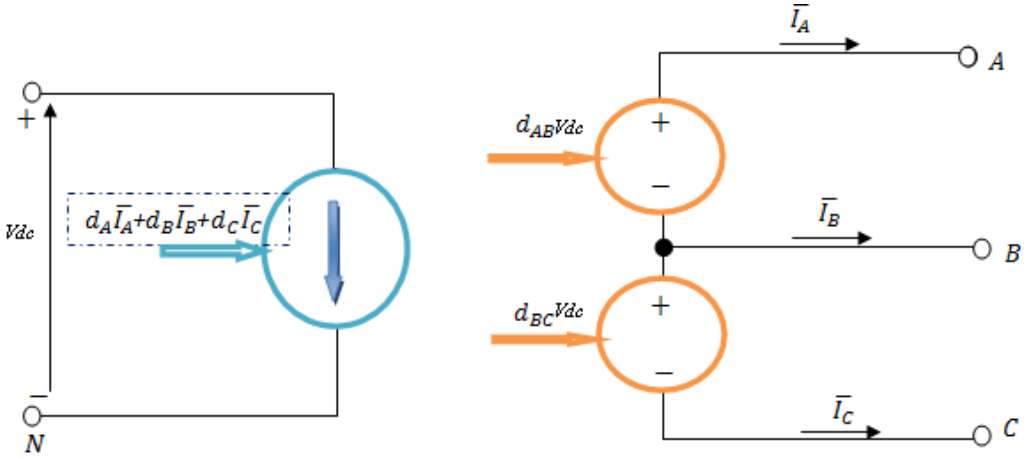

Figure 3-6 Three phase VSC average model

3.4 VSC-Space Vector Pulse Width Modulation

Space vector Pulse Width Modulation (SVPWM) has interesting characteristics over sinusoidal PWM. It improves the DC link voltage utilization and also reduces harmonics in the voltages and currents. At any instant of time the vector sum of phase voltages in space gives one vector –space vector. The use of the magnitude and frequency of this vector to control switching states of the converter is named space vector modulation.

The switch mode converter connected to Machine is shown below

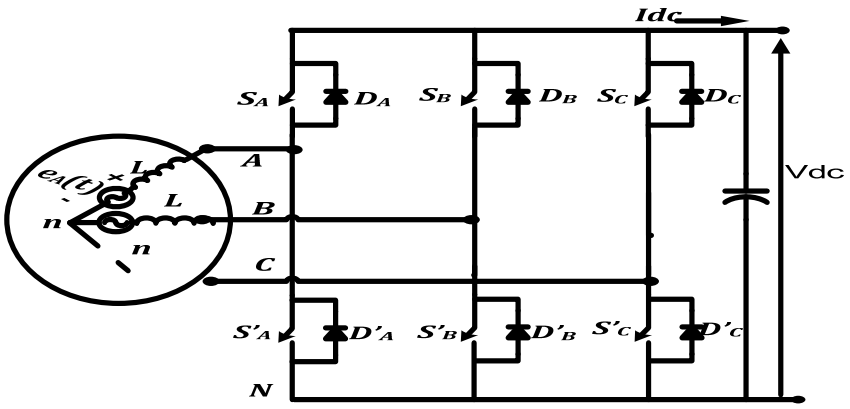

Figure 3-7 Three phase converter connected to machine

As it is discussed before, the upper three switches can represent the converter state since the lower switches are complementary to the upper switches. Therefore, there are only eight possible states of which six are active states and two are zero states.

The switching model of the converter leg voltage is shown in (3.4),$V_{jN} = S_j V_{dc}$. The generator phase is sum of leg voltage and neutral point voltageV_{Nn}

$$\begin{aligned} V_{as} &= V_{aN} + V_{Nn} = S_a V_d + V_{Nn} \\ V_{bs} &= V_{bN} + V_{Nn} = S_b V_d + V_{Nn} \\ V_{cs} &= V_{cN} + V_{Nn} = S_c V_d + V_{Nn} \end{aligned} \tag{3.12}$$

For a balanced system the sum of stator phase voltages is zero. This makes the voltage between the neutral equal to one third of the sum of the converter leg voltages. Mathematically,

$$\begin{aligned} V_{Nn} &= \frac{1}{3}(V_{aN} + V_{bN} + V_{cN}) \\ V_{Nn} &= \frac{1}{3}(S_a V_{dc} + S_b V_d + S_c V_{dc}) \end{aligned} \tag{3.13}$$

Then the phase voltages in terms the switching states is calculated from the above two equations as

$$\begin{bmatrix} V_{as} \\ V_{bs} \\ V_{cs} \end{bmatrix} = \frac{1}{3}\begin{bmatrix} 2 & -1 & -1 \\ -1 & 2 & -1 \\ -1 & -1 & 2 \end{bmatrix}\begin{bmatrix} V_{aN} \\ V_{bN} \\ V_{cN} \end{bmatrix} = \frac{V_{dc}}{3}\begin{bmatrix} 2 & -1 & -1 \\ -1 & 2 & -1 \\ -1 & -1 & 2 \end{bmatrix}\begin{bmatrix} S_a \\ S_b \\ S_c \end{bmatrix} \tag{3.14}$$

The line to line and phase voltages of the generator as all the states is shown in Table 3-1;

Table 3-1 Switching states and generator line and phase voltages normalized to Vdc

Voltage Vector	Switching vectors			Line to Neutral voltages			Line to Line voltages		
	a	b	c	V_{an}	V_{an}	V_{an}	V_{ab}	V_{bc}	V_{ca}
V_0	0	0	0	0	0	0	0	0	0

V_1	1	0	0	$\frac{2}{3}V_d$	$-\frac{1}{3}V_d$	$-\frac{1}{3}V_d$	V_d	0	$-V_d$
V_2	1	1	0	$\frac{1}{3}V_d$	$\frac{1}{3}V_d$	$-\frac{2}{3}V_d$	0	V_d	$-V_d$
V_3	0	1	0	$-\frac{1}{3}V_d$	$\frac{2}{3}V_d$	$-\frac{1}{3}V_d$	$-V_d$	V_d	0
V_4	0	1	1	$-\frac{2}{3}V_d$	$\frac{1}{3}V_d$	$\frac{1}{3}V_d$	$-V_d$	0	V_d
V_5	0	0	1	$-\frac{1}{3}V_d$	$-\frac{1}{3}V_d$	$\frac{2}{3}V_d$	0	$-V_d$	V_d
V_6	1	0	1	$\frac{1}{3}V_d$	$-\frac{2}{3}V_d$	$\frac{1}{3}V_d$	V_d	$-V_d$	0
V_7	1	1	1	0	0	0	0	0	0

The analysis of calculation of the space vector is easy in stationary reference frame rather than adding the complex phase variables. Applying Clark's transformation to (3.14),

$$\begin{bmatrix} V_\alpha \\ V_\beta \\ V_o \end{bmatrix} = \frac{2}{3} V_d \begin{bmatrix} 1 & -0.5 & -0.5 \\ 0 & \frac{\sqrt{3}}{2} & -\frac{\sqrt{3}}{2} \\ 0 & 0 & 0 \end{bmatrix} \begin{bmatrix} S_a \\ S_b \\ S_c \end{bmatrix} \qquad (3.15)$$

V_α and V_β gives the magnitude of the reference space vector-radius of circle as shown in Fig3.10b.

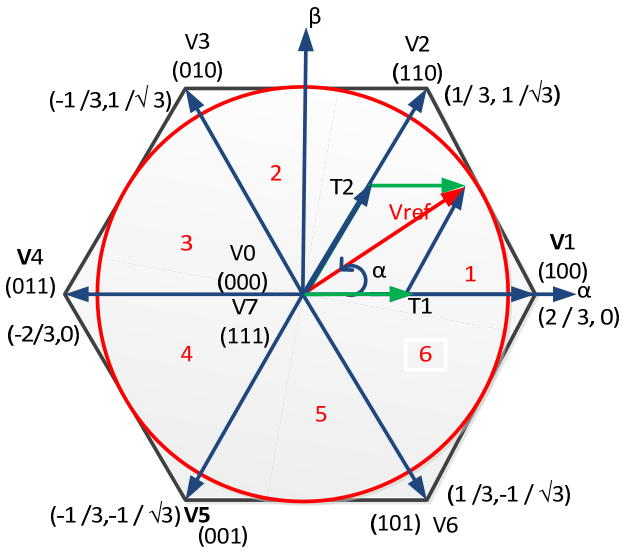

Figure 3-8 switching vectors position and sector on stationary reference axis

The maximum value of the average reference that can be used without distortion $\overline{V}_{ref}$ is when it is equal to the radius the circle inscribed hexagon. Then the peak value of the phase and its root mean square can be calculated as

$$\overline{V}_{refMax} = V_1 \cos(30) = \frac{\sqrt{3}}{2} V_d$$

$$V_{phaseMax} = \frac{2}{3} \bar{V}_{refMax} = \frac{1}{\sqrt{3}} V_d \qquad (3.16)$$

$$V_{LL,Max(rms)} = \sqrt{\frac{3}{2}} V_{phaseMax} = \frac{1}{\sqrt{2}} V_d = 0.707\, V_d$$

This shows that using space vector modulation has 15 percent higher dc link voltage utilization than that of sinusoidal modulation, compare with (3.10).

Next stage on SVPWM is identifying the sector where the reference voltage is laid. Then calculate the time that the adjacent vectors inscribing the reference so as to keep the voltage-second balance.

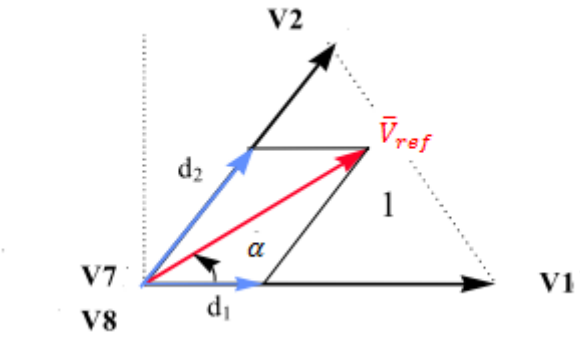

Figure 3-9 synthesis of required voltage in sector 1

Depending on the criteria required zero vectors has to be selected to make the switching frequency constant. When reference vector is in sector 1, see Fig.3.11, the duty cycle for the adjacent vector V1 and V2, and zero vectors can be calculated as

$$d_2 = \frac{2}{\sqrt{3}} \overline{V}_{ref} \sin\, \alpha$$

$$d_1 = \frac{2}{3} \overline{V}_{refMax} = \frac{1}{\sqrt{3}} \overline{V}_{ref} (\sqrt{3} \cos\alpha - \sin\alpha) \qquad (3.17)$$

$$d_o = 1 - d_1 - d_2$$

The above formula can be used as general formula for the other sectors by adjusting the angle the respective vectors. The detailed analysis for selection of zero vectors and the different space vector algorithms are covered in [24]-[25].

Space vector source code is included in Appendix F.

3.5 Six Leg Converters

3.5.1. Model

Sig leg converter can be built, in similar fashion to that of three phases, by connecting six bridge legs; or simply by connecting two VSC with common dc link voltage.

In this project, two identical three phase converters modules are used Figure 3.10(right side).

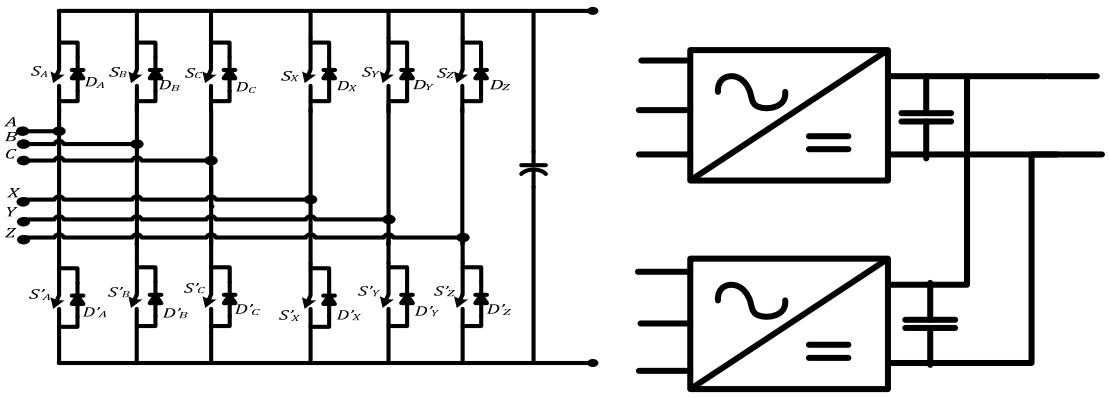

Figure 3-10 Six leg converter

The six-phase voltage source converter contains a switching network of 12 power switches arranged to form 6 legs, each leg connected to one phase of the generator. Only one of the power switches of the same leg can operate in the ON state to avoid the short circuit of the dc link so that the upper six switches determine the switching state of the converter. Thus, 64 possible states are available and having many switches states gives freedom in the control of the converter and also it reduces the harmonics in voltage and current that would have been introduced by having less number of switching states.

The neutrals of the generator are isolated from each other and from the converter. For a balanced system, the voltage between the converter and machine for each set of three phase windings becomes one third of the sum of the respective leg voltages, as shown in (3. 14) for three phase machine

Therefore, using similar analysis the phase voltages can be written as

$$\begin{bmatrix} V_{as} \\ V_{bs} \\ V_{cs} \\ V_{xs} \\ V_{ys} \\ V_{zs} \end{bmatrix} = \frac{1}{3} \begin{bmatrix} \begin{bmatrix} 2 & -1 & -1 \\ -1 & 2 & -1 \\ -1 & -1 & 2 \end{bmatrix} & \emptyset \\ \emptyset & \begin{bmatrix} 2 & -1 & -1 \\ -1 & 2 & -1 \\ -1 & -1 & 2 \end{bmatrix} \end{bmatrix} \begin{bmatrix} V_{aN} \\ V_{bN} \\ V_{cN} \\ V_{xN} \\ V_{yN} \\ V_{zN} \end{bmatrix} = [C] \begin{bmatrix} V_{aN} \\ V_{bN} \\ V_{cN} \\ V_{xN} \\ V_{yN} \\ V_{zN} \end{bmatrix} \quad (3.18)$$

$$[V_{js}] = [C][V_{jN}]$$

The converter leg voltage is product of the dc link voltage V_d and the switching state of the respective leg. For the six legs the converter voltages in matrix form can be written as

$$[V_{jN}] = V_d[\, S_a\ S_b\ S_c\ S_x\ S_y\ S_z\,] = V_{dc}[S_j\,] \quad (3.19)$$

Finally, substituting (3.19) to (3.18), the stator voltages of the generator in terms of the switching states of the converter are

$$[V_{js}] = V_d[C][S_j\,], \quad j = a, b, c, x, y, z \quad (3.20)$$

As shown in (3.21), by changing the switches states of the converter the stator voltages can be controlled, or vice verse. The generation of control signal to the converter varies with modulation scheme used. To take advantage of the higher number of switching states of the vector decomposition space vector PWM is used.

3.5.2. Sinusoidal Modulation

The six leg converter can be treated as two independent three phase system. For a balanced load, the two converters will have similar reference signal which are separated by the phase difference angle of the phase groups. DC link voltage utilization is as same as to that of three phase converter. This modulation is very simple, in this project it is used in the initial stage of the development of drive controller.

3.5.3. Space Vector Modulation-Vector Classification

Similarly, standard three phase space vector modulation can be use for the two converters. First case is, using separate reference signals for each converter but the same switching states. The same space vector modulation can be used, only by changing the input signal to the function. This modulation strategy is implemented in this project.

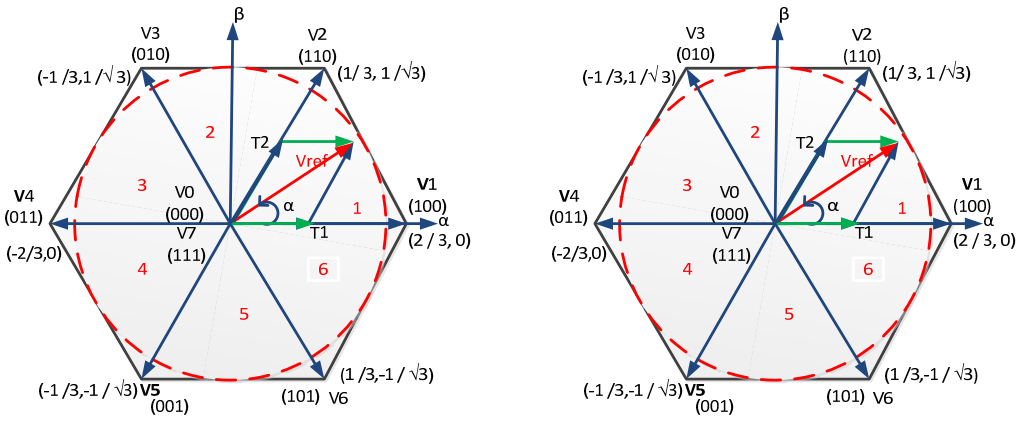

Figure 3-11 space vector modulation with different reference and same state vector position

The second case, is using the same reference signal but different position of switching states, the switching states of one of the converter are uniformly displaced by the angle which is equal to the phase difference of the two groups of three phase winding of the generator.

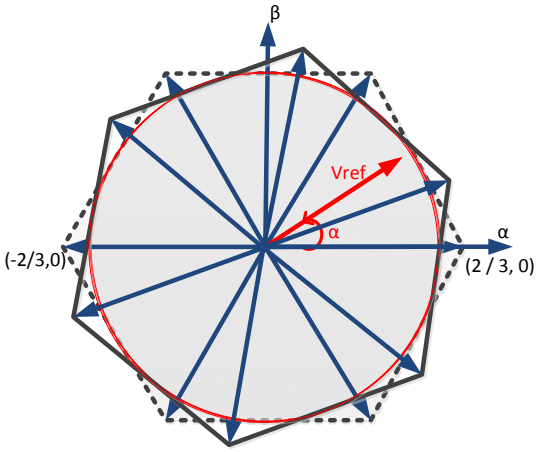

Figure 3-12 space vector modulation with single reference and different vector position

3.5.4. Modulation - Vector Space Decomposition Space Vector PWM

As introduced earlier, for three phase converter modulation, space vector modulation is based on the projection of the stator space vector in to stationary reference frame(s). From the general two phase real component transformation, six space phase voltages can equally be represented by vectors of three orthogonal stationary reference frames.

The stator voltages on three orthogonal planes can be found by multiplying (3.20) using six phase transformation, Appendix A.

$$[V_{svd}] = V_d[T_6][C][S_j] \qquad (3.21)$$

$$\begin{bmatrix} V_\alpha \\ V_\beta \\ V_x \\ V_y \\ V_{z1} \\ V_{z2} \end{bmatrix} = \frac{V_d}{\sqrt{3}} \begin{bmatrix} 1 & -\frac{1}{2} & -\frac{1}{2} & \frac{\sqrt{3}}{2} & \frac{-\sqrt{3}}{2} & 0 \\ 0 & \frac{\sqrt{3}}{2} & \frac{-\sqrt{3}}{2} & \frac{1}{2} & \frac{1}{2} & -1 \\ 1 & -\frac{1}{2} & -\frac{1}{2} & -\frac{\sqrt{3}}{2} & \frac{\sqrt{3}}{2} & 0 \\ 0 & -\frac{\sqrt{3}}{2} & \frac{\sqrt{3}}{2} & \frac{1}{2} & \frac{1}{2} & -1 \\ 0 & 0 & 0 & 0 & 0 & 0 \\ 0 & 0 & 0 & 0 & 0 & 0 \end{bmatrix} \begin{bmatrix} S_a \\ S_b \\ S_c \\ S_x \\ S_y \\ S_z \end{bmatrix}$$

Where: $V_{vsd} = [V_\alpha \; V_\beta \; V_x \; V_y \; V_{z1} \; V_{z2}]^T$

As it is seen, (3.21), no voltage components are generated in the (z1-z2) subspace; this is because of the two neutral of the machine are separated and system is assumed balanced.

There are 64 switching modes in each (α, β) and $(x, y$ .The vector space diagram of the switching states normalized with Vdc are shown below.

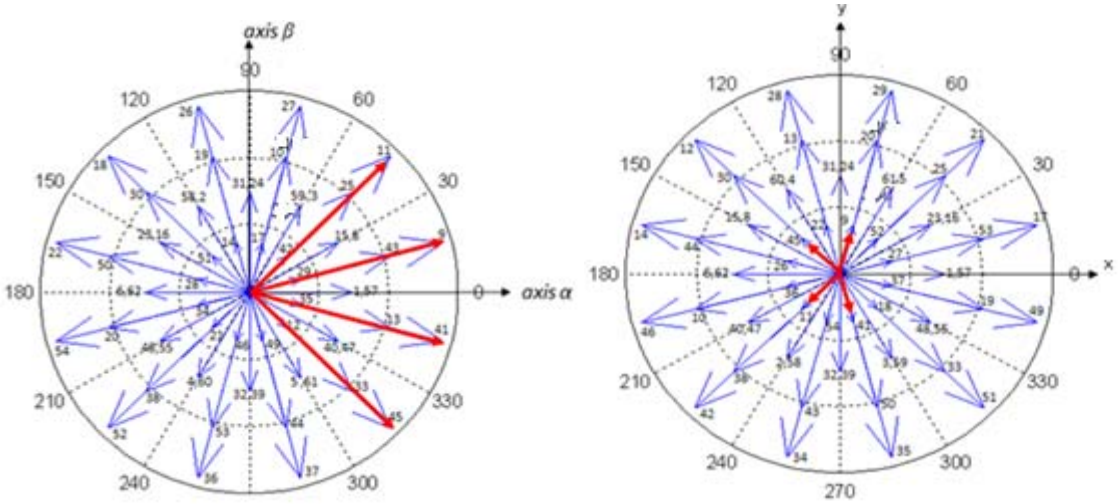

(a) (b)

Figure 3-13 (a) projection of stator voltage (a,b) plane , (b)projection of stator voltage (x,y) plane, null voltage vectors: 0, 63,7,56

Looking at the magnitude of the voltage vectors of above Figure 3-13, there are five vector groups; the zero voltage group has 4 states Uo=0, the smallest voltage U1=0.299Vd group(12 states), the small-medium vector group has 12 states U2=0.577Vd, the medium voltage group has 24 states U3=0.816Vd , and the largest voltage group has 12 states U4=1.115Vd;

From the two projection planes voltage diagrams, it is evident that the largest vectors (U4) in(α, β) plane are mapped to the smallest vectors in (x,y) plane. While the others two medium voltages are same in both planes. So, does all the 128 vectors participated in modulation/controlling of converter? As it is discussed in chapter 2, the space vector

decomposition modeling of generator shows only (α, β) planes contribute for electromechanical energy conversion while (x, y) corresponds to stator losses. That means, it is wise to choose vectors which have largest projection on the (α, β) and at the same time smallest in (x, y). As a result, the vector diagram is simplified to 12 vectors-U4 group in(α, β) and their 12 projection vectors-U1 group in (x, y) as shown in Figure 3-14.

There are two 12 sectors each separated by 30^o. SVPWM technique of three phase converters with 6 sectors can be extended to that of six phase converters-two 12 sectors.

Since the control of(α, β) and(x, y) orthogonal planes of one another, this gives additional degree of freedom in the control of machine- converter system, so that the losses in(x, y) plane is intended to be as low as possible, by selecting four active vectors to generate reference space vector in (α, β) and zero volt-second in (x, y).

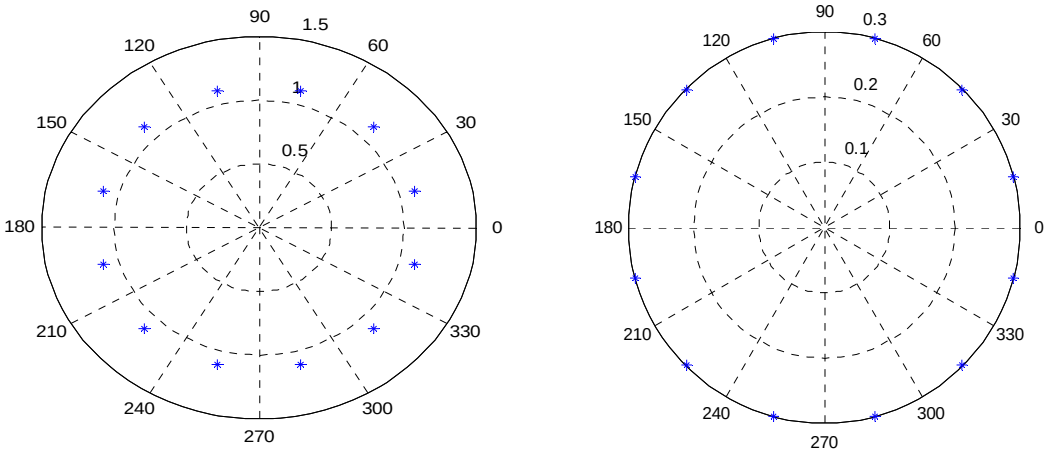

(a) (b)

Figure 3-14 vector-U4 group, of stator voltage (a,b) plane(x,y) plane

Supposing the reference vector is sector 1, the four adjacent vectors 45, 41, 9 and 11 are used. The important features of these four adjacent voltages is that they lie in different quadrants of(x, y) plane which helps cancellation.

There are four zero vectors for each sector to choose from. Here, only one zero vector for each sector is used and is selected to minimize the number of state changes of switch in each leg. Table shows switching table for sector 1,

Table 3-2 Switching table of sector 1

Sector 1	S_z	S_y	S_x	S_c	S_b	S_a

V0	63	1	1	1	1	1	1
V1	45	1	0	1	1	0	1
V2	41	1	0	1	0	0	1
V3	9	0	0	1	0	0	1
V4	11	0	0	1	0	1	1

As shown in Table 3.1, the all switch legs change state once in sampling time except leg b which switches twice, and it is inevitable to have at least two state changes in sampling rate in any combination. Therefore, it is possible to have different ways of choosing zero vectors and thorough study can be done on the different combinations. The switching table for the other sectors is included in Appendix C.

The dwelling time of these five vectors is calculated in such way that the voltage-second is balanced [26],[27].Let T_0, T_1, T_2, T_3 and T_4 be the dwelling time of the vectors V_0, V_1, V_2, V_3 and V_4 respectively. The voltage-second balance is

$$\begin{aligned} V_0T_0 + V_1T_1 + V_2T_2 + V_3T_3 + V_4T_4 &= V_{ref}T_s \\ T_0 + T_1 + T_2 + T_3 + T_4 &= T_s \end{aligned} \tag{3.22}$$

Further decomposing the vectors in to the subspaces which we have the information that the voltage-second balance must be zero to minimize losses and is given by

$$\begin{bmatrix} V_\alpha{}^0 & V_\alpha{}^1 & V_\alpha{}^2 & V_\alpha{}^3 & V_\alpha{}^4 \\ V_\beta{}^0 & V_\beta{}^1 & V_\beta{}^2 & V_\beta{}^3 & V_\beta{}^4 \\ V_\alpha{}^0 & V_x{}^1 & V_x{}^2 & V_x{}^3 & V_x{}^4 \\ V_\beta{}^0 & V_y{}^1 & V_y{}^2 & V_y{}^3 & V_y{}^4 \\ 1 & 1 & 1 & 1 & 1 \end{bmatrix} \begin{bmatrix} T_0 \\ T_1 \\ T_2 \\ T_3 \\ T_4 \end{bmatrix} = \begin{bmatrix} T_s V_\alpha{}^* \\ T_s V_\beta{}^* \\ 0 \\ 0 \\ T_s \end{bmatrix} \tag{3.23}$$

where, $V_k{}^i$ is the projection of the i^{th} voltage on the k-plane and T_i is the dwelling time of the vector $V_k{}^i$ over a sampling period T_s; $V_\alpha{}^*$ and $V_\beta{}^*$ are the projection of reference space vector on (α, β) plane .

Now, the timing signals of the legs or phases of the converter can be calculated by adding the dwelling times according to switching states of the five vectors for the given sector. Table 3.3 shows the switching table for sector I.

Table 3-3 switching table time and dwelling time of sector 1

Sector 1		S_z	S_y	S_x	S_c	S_b	S_a
V_0	63	1	1	1	1	1	1
		T_0	T_0	T_0	T_0	T_0	T_0
V1	45	1	0	1	1	0	1
		T_1	0	T_1	T_1	0	T_1
V_2	41	1	0	1	0	0	1
		T_2	0	T_2	0	0	T_2
V3	9	0	0	1	0	0	1
		0	0	T_3	0	0	T_3
V4	11	0	0	1	0	1	1
		0	0	T_4	0	T_4	T_4
$\sum T_{on}$		$T_0 + T_1 + T_2$	T_0	T_s	$T_0 + T_1$	$T_0 + T_4$	T_s

Note that: T_s is the sampling time which has to be smaller than the switching time.

The ratio of the dwelling time to the sampling time can be defined as the duty cycle on that sampling period,

$$d_i = \frac{T_i}{T_s},\ i = 0, 1, 2, 3, 4 \qquad (3.24)$$

The normalized switching gate signals then can be shown as

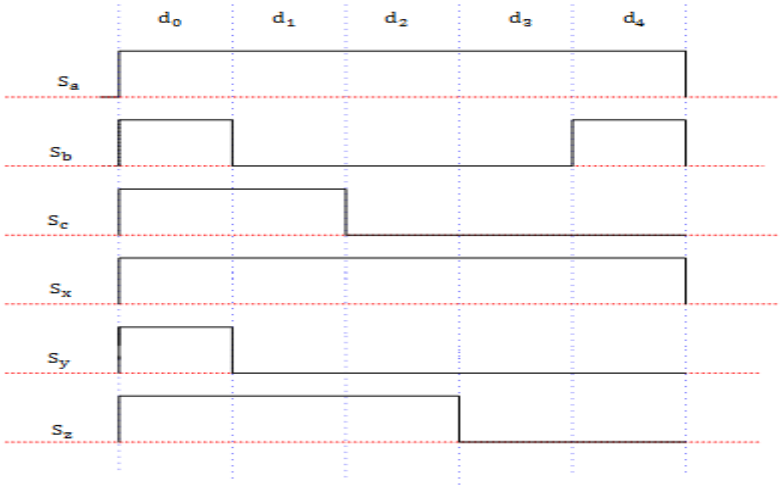

Figure 3-15 switching gate signals

The sum normalized dwelling time of each vector gives the duty cycle of the switch or leg. For this particular case, reference vector is in sector 1, the duty cycles of the six phases are as follows.

$$\begin{aligned} d_a &= 1 \\ d_b &= d_1 + d_4 \\ d_c &= d_1 + d_2 \\ d_x &= 1 \\ d_y &= d_1 \\ d_z &= d_1 + d_2 + d_3 \end{aligned} \qquad (3.25)$$

The generation of switching signals must be handled carefully. The switching signals generation should be handled in different way for the leg which changes state twice in a sampling period.

The average model of six phase converter can be developed from the duty cycles of each phase. The phase voltage is given by

$$\bar{V}_{js} = d_j \; V_d \,, \; j = a, b, c, x, y, z \qquad (3.26)$$

Ignoring the witching losses the input and output are assumed to be equal, the DC link current becomes as

$$\begin{aligned} I_d V_d &= \sum_j \bar{V}_{js} \, \bar{I}_j \quad , \quad j = a, b, c, x, y, z \\ I_d &= \sum_j d_j \, \bar{I}_j \,, \end{aligned} \qquad (3.27)$$

From (3.27) and (3.28), the average value model is composed of one controlled current source on DC side and six controlled voltage sources from the AC side, see below

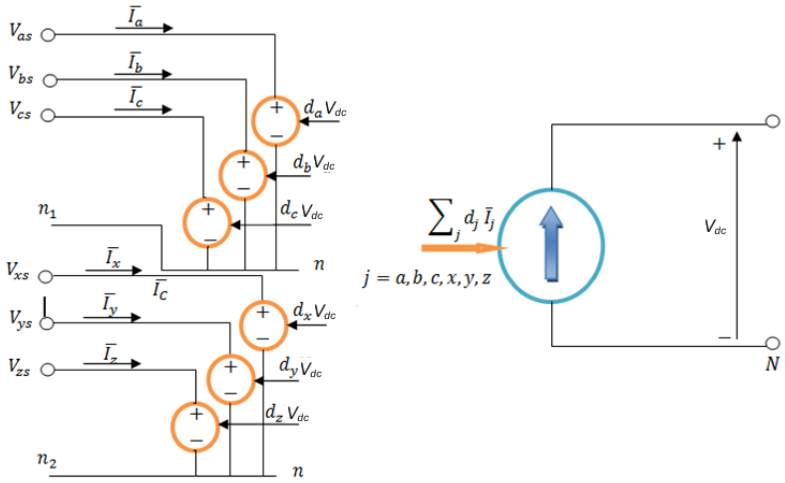

Figure 3-16 Average value model of six leg converter

Using average value model, it is possible to do away with the gate signal generation process and at same time reducing the simulation time of the system.

To wrap up, the SVPWM has three main steps which have been discussed earlier: vector selection, switching time calculation and gate signal generation. The Matlab codes for selection of vector and switching time calculation are included in Appendix C.

4 Control of Six Phase PMSG

In this chapter the Field Oriented Control or Vector control Method of six phases PMSG is introduced. The detailed analysis of the generation of control signals for independent control of torque and speed of the generator is discussed. Both single synchronous rotating current control and dual synchronous rotating frame current control are included.

4.1 Introduction

In general Control of AC machines can be divided into Scalar control and Vector Control. In Scalar control only the magnitude and frequency of control variables can be controlled where as in vector control not only the magnitude and frequency but also phase of the control variables can be controlled. The main idea of vector control is in order to be able to control the flux and toque of the machine independently which is not so easy in AC machines because of the interactions between the stator and rotor fields. In other word, vector controlled AC machine emulates DC machine which the field current controls the machine flux and the armature current controls the torque independently of the flux.

The construction of a DC machine is such that by mechanical means the field flux is perpendicular to the armature flux. DC machine-like performance can be obtained by orienting the stator current in such a way that it will be decoupled in to flux producing and torque producing components.

Vector control came into the field of AC drives research in the late 1960s and was developed prominently in the 1980s to meet the challenges of oscillating flux and torque responses in inverter fed induction and synchronous motor drives.

Vector control of PMSM drives, is intended to control the speed and torque of the machine independently. Not only this, there are different control strategies or objectives which come along with the vector control. Some of them are constant torque angle, unity power factor (UPF), control of angle between flux and current phasors, optimum torque per unit current, constant power loss, and maximum efficiency,[28].

In constant torque angle control the torque angle is maintained at 90 deg. It is also called zero d axis current control. Since Id=0, field weakening cannot be achieved. In this control strategy per unit torque is equal to per unit stator peak current. This makes the implementation simple.

This control strategy also gives the optimal torque for surface mounted PM machines. The field weakening operation is not of interest for wind generator drives application. Therefore, zero d axis current control strategy is chosen as the part of vector control in this thesis.

Six phase machine control is based on the machine model. Six phase machines can modeled as one six phase system or simply as two three phase systems As it is explained in chapter 2 , machine modeling becomes simpler on synchronous rotating frames on which the inductance terms become independent of rotor position and stator variables(V,I and flux) are constant at steady state. Therefore, six phase machine control is done on synchronous rotating frame using one full six phase machine model or using two-three phase machine models. The former is called single synchronous rotating frame current control, while the latter is called dual synchronous rotating frame current control. These control schemes are the heart of this chapter.

The different topologies of converters in a wind energy system are shown in chapter 3. The fully rated converter topology is preferable to other types for PMSG based Wind Energy System. Back to Back connected fully rated VSCs can be controlled in two ways in Wind energy system turbine control. First method, when VSC-1 (machine side converter), controls the generator power and VSC-2 maintains the DC link voltage at required value, Figure 4-1.

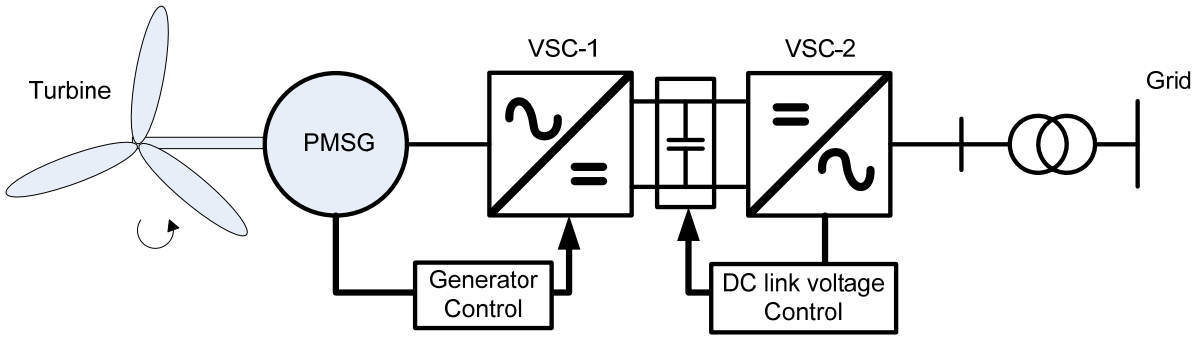

Figure 4-1 Fully rated converter control strategy 1

In section 4.2 and 4.3 presents the design of generator control for this strategy, assuming that VSC-2 is an ideal constant voltage source.

Second arrangement is shown in Figure 4-2, when VSC-1 maintains the DC link voltage, while VSC-2 controls the generator power.

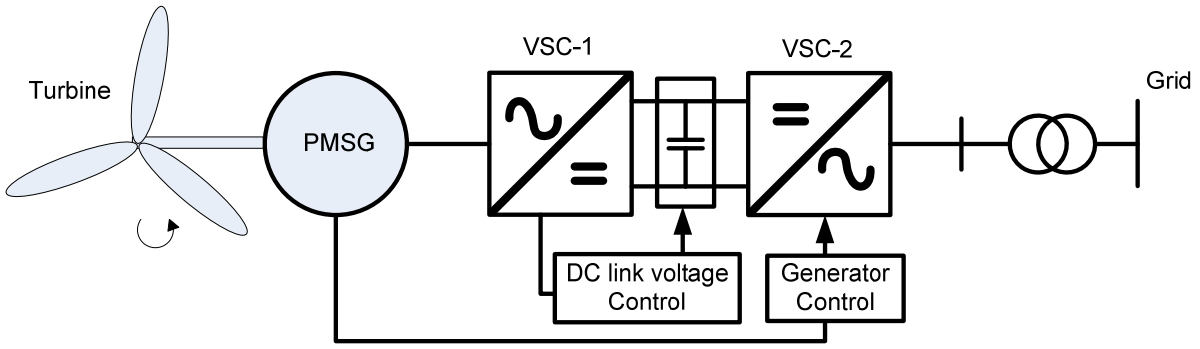

Figure 4-2 Fully rated converter control strategy 2

The design of DC link voltage control is presented in section 4.4.

4.2 Single Synchronous Rotating Frame Current Control

In the previous chapters the modeling of generator –converter system is simplified by using six phase transformation. The electromechanical energy conversion takes place in only one of the sub spaces, namely the (d, q) subspace. Therefore, by controlling this subspace the machine operation can be controlled.

Further the machine operation can be optimized by maintaining the (x,y) subspace currents to minimum in order to reduce the losses. These losses can also be reduced by having larger inductance. For concentrated winding machines this inductance term is equal to the main inductance where as for distributed winding machines the inductance term is leakage inductance. Therefore, since the machine in use is concentrated winding machine, it experiences smaller (x,y) plane current thereby smaller current.

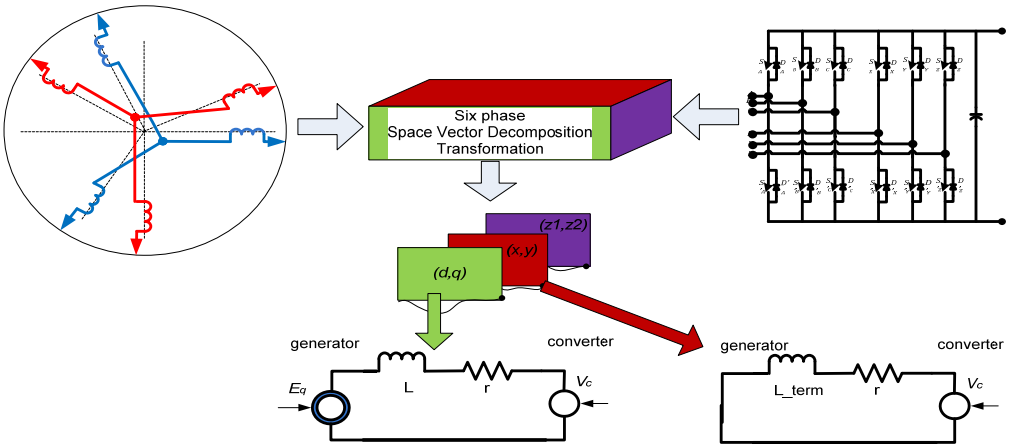

Figure 4-3 General schematics of Transformation of Generator and Converter, L_term=linkage inductance for concentrated winding, L_term=Leakage term

The equivalent circuit of six phase machine in (d, q) subspace can be explicitly shown in Figure 4-4 which is exactly similar to three phase generator converter system.

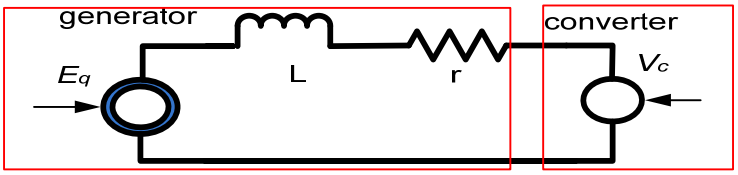

Figure 4-4 Equivalent circuit of six phase machine-converter system in (d, q)

Therefore, control of six phase machine –converter system is designed in a similar manner as that of three phase machine-converter system.

Generally, Drive system is operated in torque control mode, speed control mode or position control mode. The position control mode is not of interest of this work.

Torque control mode-torque is set to a desired reference value and the speed varies depending on the load. Since torque is a constant multiple of q axis current (even torque is equal Iq in per unit), the torque is controlled by regulating the current using a current feedback loop. The Generalized FOC control of six phases PMSG is in Torque control mode is shown below

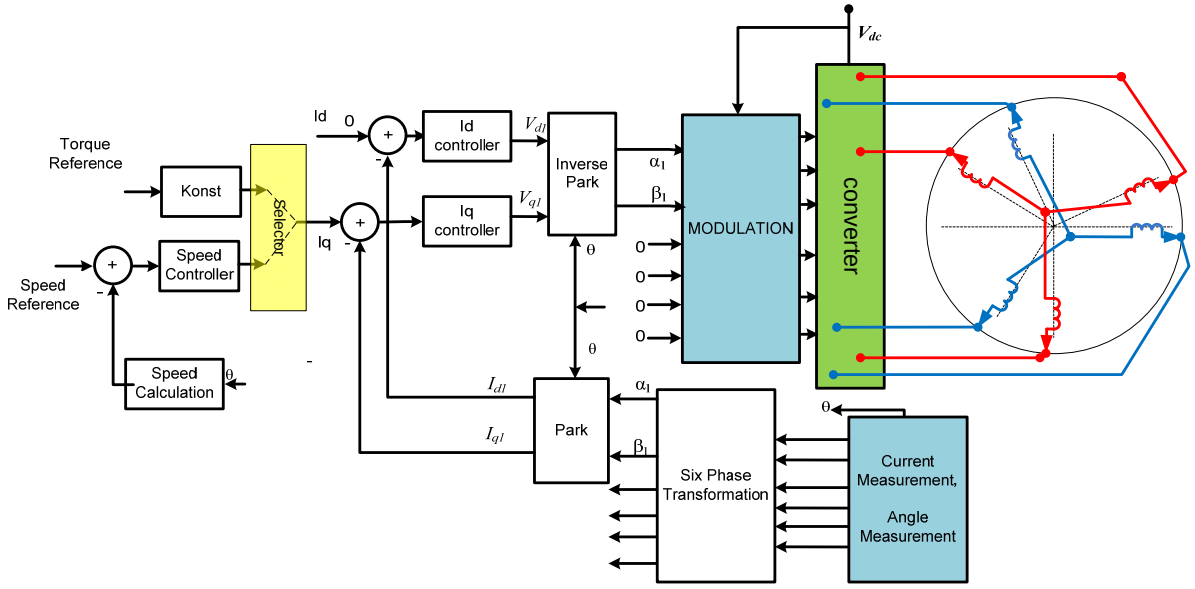

Figure 4-5 FOC block diagram on a single synchronous rotating frame

Speed Control Mode-speed is set to a reference value and the torque varies based on the loading of the system. Speed control mode is obtained by adding an outer speed control feedback loop to the torque controlled drive, as shown in Figure 4-5. Both speed and Torque

control mode operations have same inner control loop. First the current control loop design is presented and latter the outer control loop.

4.2.1. Design of inner control loop

The output of inner control loops are inputs to PWM modulator which shapes the magnitude, frequency and phase angle of the converter voltage. The converter currents change according to the generator behavior and required loading. Therefore, current control loops design base on the basic relationship of the generator and converter model. Since the generator is directly connected to the converter, its terminal voltage is equal converter voltage. The converter voltages the become, the per unit system is chosen for controller design

$$v_{cd} = v_d$$
$$v_{cq} = v_q \tag{4.1}$$

$$v_d = r_s i_d + l_s \frac{di_d}{dt} - n \cdot x_q \cdot i_q$$
$$v_q = r_s i_q + l_s \frac{di_q}{dt} + n \cdot x_d \cdot i_d + e_q \tag{4.2}$$
$$e_q = n \cdot \psi_m$$

Converter voltages without v'_{cd} and v'_{cq} cab be written as

$$v'_{cd}(s) = r_s i_d(s) + s l_d i_d(s)$$
$$v'_{cq}(s) = r_s i_q(s) + s l_q i_q(s) \tag{4.3}$$

$$\frac{i_d(s)}{v'_{cd}(s)} = \frac{i_q(s)}{v'_{cq}(s)} = \frac{1}{r_s}\frac{1}{1+s} \tag{4.4}$$
$$\tau_a = \frac{l_q}{r_s} = \frac{l_d}{r_s}, for\ SPMSG$$

Putting the above equations together, the current control block diagram is given in Figure 4-6

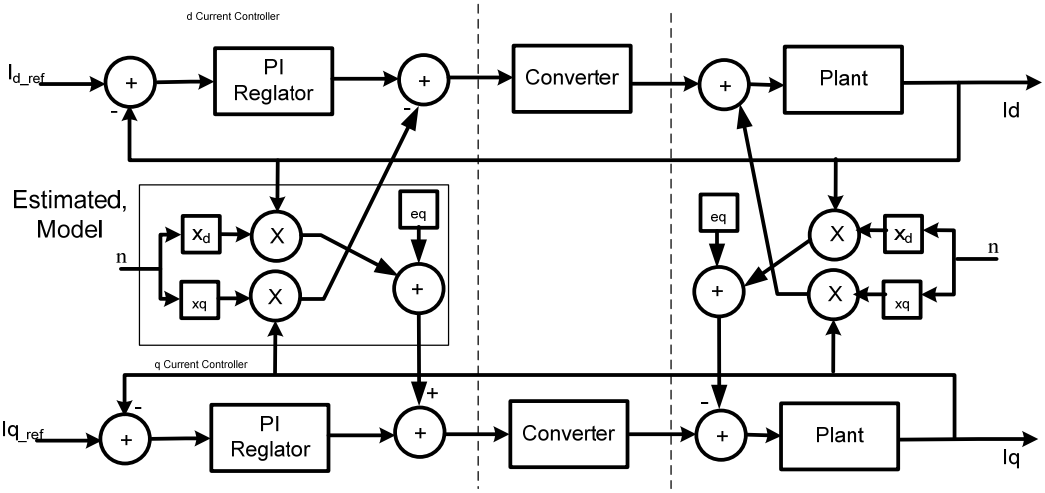

Figure 4-6 general block diagram of current controllers

For physical implementation of the control, the delay introduced by the filters, delay introduced by digital to analog converter of current reading and delay introduced by the digital signal processor has to be taken into account. The d axis and q axis current loops are similar except their feed terms. Considering the feed terms as a disturbance the d axis and q axis current control loop can be simplified as shown in figure below.

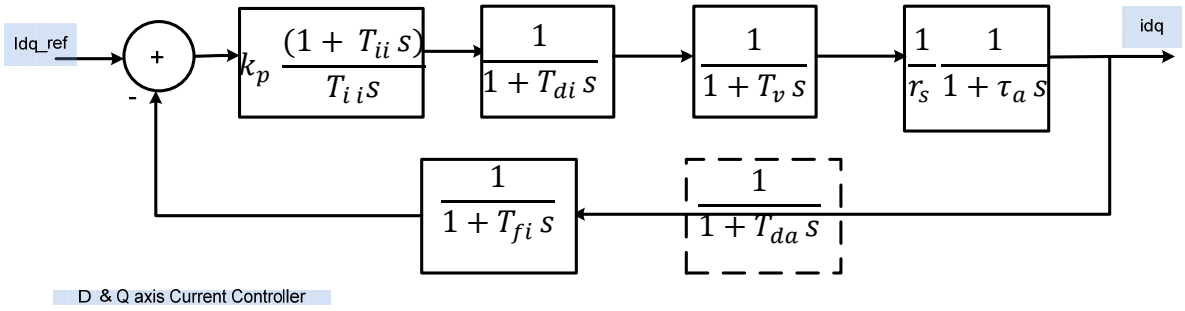

Figure 4-7 current control loop (for both d & q axis)

The Proportional Integrator (PI) regulator is represented transfer function as

$$G_c(s) = k_{pi} + k_{ii}\frac{1}{s} = k_{pi}\frac{(1+T_{ii}s)}{T_{ii}s} \qquad (4.5)$$

Where $k_{pi}$and K_i are proportional and integral constants, $T_{ii} = \frac{K_{pi}}{K_{ii}}$ is integral time constant;

The converters are modeled as first order function with time delay as

$$C(s) = \frac{1}{1+T_v s}$$

$$T_v = 0.5T_{sw} \qquad (4.6)$$

Where T_v delay introduced by the converter, and T_{sw} is the switching period.

The delay introduced by digital calculation of the current control loop is represented by first order transfer function which has time constantT_{di} . This time delay is has to be checked from real time implementation.

The current feedback has also a delay because of the analog to digital converter (ADC) which is approximated by first order function with time constant equal toT_{da} . This time constant is very small since it is taken care by the FPGA. It can be ignored.

The measured current is passed through a low pass filter. The filter introduces delay of which is equal to its time constant T_{fi}

Therefore, the open loop transfer function of the current control loop becomes

$$G_{OL_i} = k_{pi}\frac{(1+\ T_{ii}\,s)}{T_{ii}\,s}\frac{1}{1+T_{di}\,s}\frac{1}{1+T_v\,s}\frac{1}{1+\tau_a\,s}\frac{1}{1+T_{fi}\,s} \tag{4.7}$$

$G_{O\,L_i}$ can be arranged to have one large and one small non zero poles,

$$G_{OL_i} = k_{pi}\frac{(1+\ T_{ii}\,s)}{T_{ii}\,s}\frac{1}{1+T_{isum}\,s}\frac{1}{r_s}\frac{1}{1+\tau_a\,s} \tag{4.8}$$

$$T_{isum} = T_{di}\ + T_v\ + T_{fi}$$

Modulus optimum criterion is base on the design objective of having the magnitude of closed loop response as flat as close to unity for as large frequency range as possible[29].

$$T_{ii}\ = \tau_a\ \ ,\ \tau_a\ = \frac{L_d}{R_s} \tag{4.9}$$

$$k_{pi}\ =\ \frac{\tau_a\ * r_s}{2T_{isum}}$$

4.2.2. Outer controller Design

The outer controller can be either torque constant in the torque control mode or speed regulator loop in case of speed control mode. In both cases the d axis current reference is set to zero and the output of the regulators become reference current along q axis.

Torque control

The electrical torque of six phase PMSG in (d, q) subspace is shown (2.15)

$$m_e = \psi_{PM} i_q = k_t i_q \tag{4.10}$$

Speed Control

The speed control loop is shown in below,

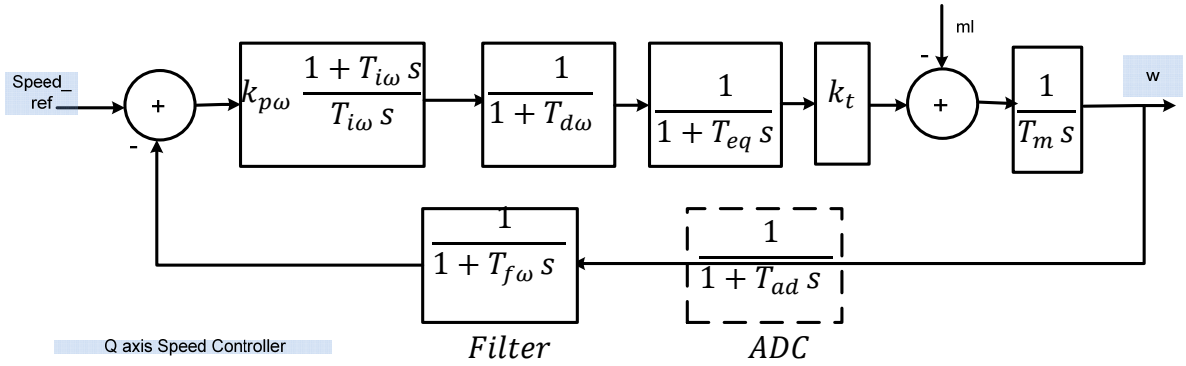

Figure 4-8 Speed control loop

Where, m_L is mechanical Load torque, k_t is Torque constant, and T_m is mechanical time constant.

The speed controller is a PI regulator with

$$G_w(s) = k_{p\omega}\,\frac{1+T_{i\omega}\,s}{s} \tag{4.11}$$

Where k_{pw} and $T_{i\omega}$ are the proportional gain and time integral of speed controller which are design parameters.

The current control is approximated by the by first order function with time delay, T_{eq}

$$G_{iq}(s) = \frac{1}{1+T_{eq}\,s},\ T_{eq} = 2T_{isum} \tag{4.12}$$

The delay introduced by calculation of speed control loop is represented by first order transfer function which has time constant $T_{d\omega}$ it is found out that, the processor uses 1/100 of the speed loop sampling time, this may vary from program to program depending the number of instructions inside the speed interrupt;

The speed is measured with an Encoder. The measured speed is passed through a digital low pass filter with time filter time constant$T_{f\omega}$. The filter is designed with cut off frequency of 70Hz; $T_{f\omega} = \frac{1}{2\pi 70} = 2.274\ ms$

From Figure 4-8, taking for disturbancem_L, the speed control looks like

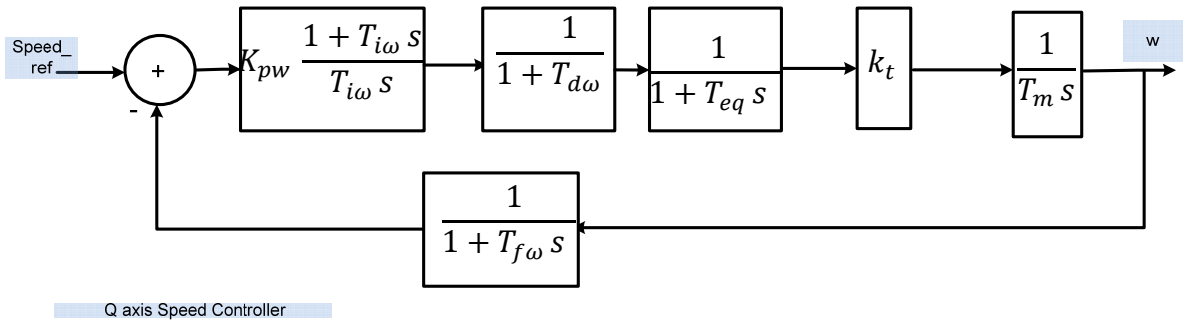

Figure 4-9 current control loop simplified

The open loop Transfer function

$$G_{OL\omega}(s) = \left(k_{p\omega}\ \frac{1+T_{i\omega}\,s}{T_{i\omega}\,s}\right)\left(\frac{k_t}{1+T_{eq}\,s}\right)\left(\frac{1}{T_m\,s}\right)\frac{1}{1+T_{d\omega}\,s}\ \frac{1}{1+T_{f\omega}\,s} \qquad (4.13)$$

Since the disturbance is not located at the reference input and the presence of free integrator in the plant, the symmetric optimum criterion is used to design the PI regulator rather than the modulus optimum which only optimizes the closed loop transfer function between the reference input and the variable to be controlled [29]. The open loop transfer function can be tailored so as to use symmetrical optimum criterion.

$$G_{ol\omega}(s) = \left(k_{pw}\ \frac{1+T_{i\omega}\,s}{T_{i\omega}\,s}\right)\left(\frac{k_T}{1+T_{\omega sum}\,s}\right)\left(\frac{1}{T_m s}\right) \qquad (4.14)$$

$$T_{\omega sum} = T_{eq} + T_{d\omega}\ + T_{f\omega}$$

By using symmetrical optimum criteria $k_{p\omega}$ and $T_{i\omega}$ can be calculated for the given system

$$k_{p\omega} = \frac{T_m}{2k_T T_{\omega sum}} \qquad (4.15)$$

$$T_{i\omega} = 4T_{\omega sum}$$

4.3 Dual Synchronous Rotating Frame Current Control

As name indicates, in this control strategy separate controller is used for each three phase groups.The six phase machine is considered as independent three phase machines connected to same shaft. It is based on individual transformations matrices.

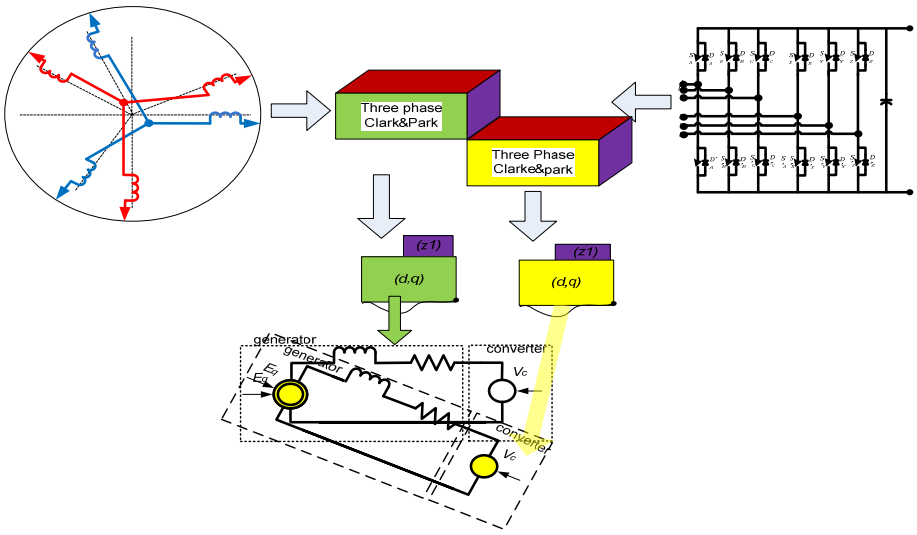

Figure 4-10 General schematic of Generator converter system in two independent system

The generator model is similar to ordinary three phase model. The two stator coils share same air gap flux which induces equivalent back emf on them. That means, the generator can be considered as a controllable voltage source connected across two RL elements connected in parallel, see Figure 4-10.

Similar to the previous discussion, the Field oriented control strategy can be studied separately for torque control Mode and speed control mode.

In Torque control mode, the speed of generator is load dependent and is free variable. The speed is directly governed by the inertia formula of the system. The Torque control mode is shown below in Figure 4-11 when the selector connects the upper leg.

In Speed control mode, the speed is set by the input reference. The electrical torque is a free variable and is equal to the load of the system at steady state. The toque is the inner loop of the speed control mode. The block diagram of the speed control mode of FOC is shown in Figure 4-11 when the selector connects to lower leg

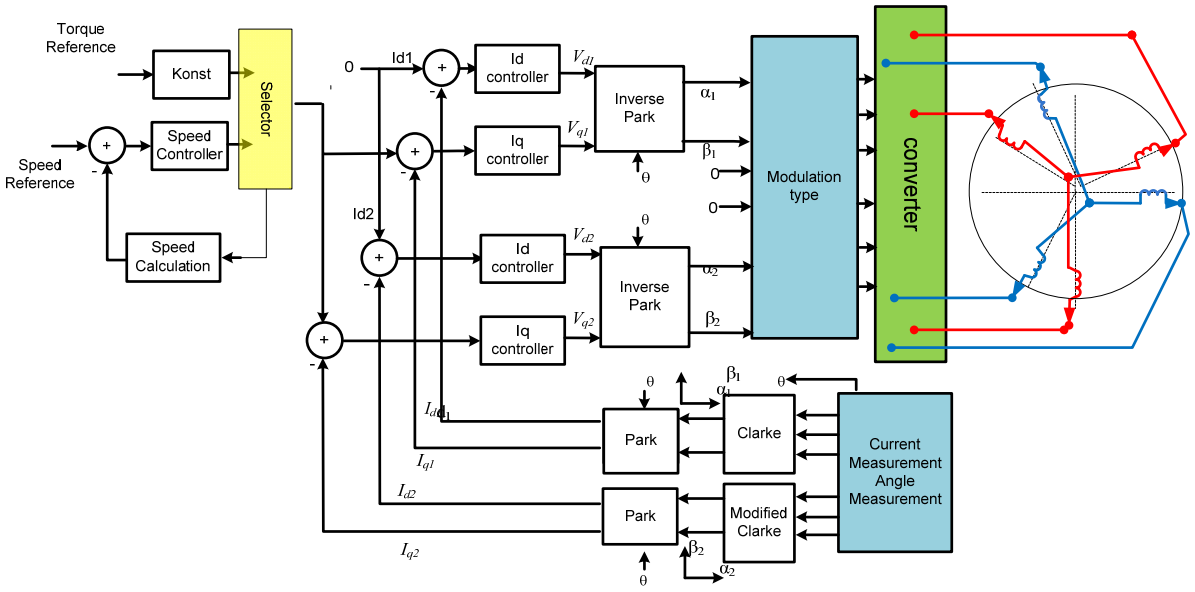

Figure 4-11 Speed control and Torque control, FOC

All four PI controller are identical since the generator is surface mounted machine with Ld=Lq, which results in same time constants. Also both speed control mode and Torque control mode operations have similar inner control loop. Therefore, only one current control design is enough to show.

The outer control is simple proportional controller in the case of control mode. On the other hand the outer controller of speed control mode is PI controller.

4.3.1. Design of inner control loop

Since the generator is directly connected to the converter, its terminal voltage is converter voltage. The converter voltages the become

$$v_d = r_s i_d + l_s \frac{di_d}{dt} - n \cdot x_q \cdot i_q$$

$$v_q = r_s i_q + l_s \frac{di_q}{dt} + n \cdot x_d \cdot i_d + e_q \qquad (4.16)$$

$$e_q = n \cdot \psi_m$$

Equation 4.17 is exactly similar to Equation (4.2), and the inductance values of the three phase system are equal to six phase system. This is the case that the machine model is for concentrating winding in which there is little coupling intra phase group and inter phase groups. But this is not true in the case of distributed winding stators coils. Therefore, we can do away with the recalculation of current controllers.

Therefore, Both d axis d1 & d2 current, and q axis q1 & q2 controller from the inside looks like

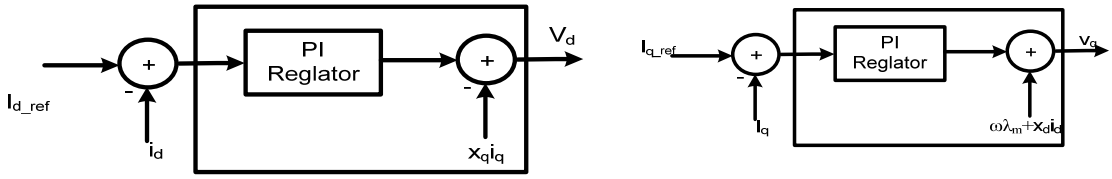

Figure 4-12 Current controller block diagram of Figure 4-11

In order to be complete, the PI parameters become, similar to equation (4.9)

$$G_c(s) = k_{pi}\frac{(1 + T_{ii}\,s)}{T_{ii}\,s}$$
$$T_{ii} = \tau_a \qquad (4.17)$$
$$k_{pi} = \frac{\tau_a * r_s}{2T_{isum}}$$

4.3.2. Outer controller Design

The outer controller can be torque controller or speed controller based on the required operating mode. In both cases the d axis current reference is set to zero for constant load angle at maximum torque operation is chosen. For wind energy systems the generator does not operate over the rated speed, so field weakening operation is not considered and therefore the magnet flux is at its rated value.

Torque control

The electrical torque of six phase PMSG in created in (d,q) subspace is shown torque equation (2.9)

$$\mathrm{m_e} = \frac{1}{2}\psi_m\left(i_{q1} + i_{q2}\right)$$
$$\mathrm{m_e} = \psi_m i_{q1},\ i_{q1} = i_{q1} \qquad (4.18)$$

Speed Control Mode

The speed control loop is similar to Figure 4-9. Following similar procedure, the PI parameters of the speed controller $G_{cw}(s)$ is equal to that of equation (4.15). It is rewritten

$$G_{cw}(s) = k_{p\omega}\frac{1 + T_{i\omega}\,s}{T_{i\omega}\,s}$$

$$k_{p\omega} = \frac{T_m}{2k_T T_{\omega sum}} \qquad (4.19)$$

$$T_{i\omega} = 4T_{\omega sum}$$

4.4 Dc LINK Voltage control

4.4.1. DC link Model

The DC link model is shown

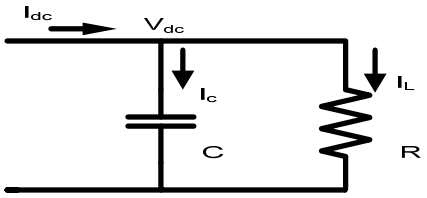

$$I_c = I_{dc} - I_L$$

$$I_c = C\frac{dV_{dc}}{dt} \qquad (4.20)$$

$$I_L = \frac{V_{dc}}{R}$$

From power balance equation (the active power component of the ac side is equal to the dc side power) and $I_d = 0$ Control, the dc link current of the six phase system is

$$I_{DC} = 3\left(\frac{V_q}{V_{DC}}\right)I_q$$

$$I_{DC1} = \frac{3}{2}\left(\frac{V_q}{V_{DC}}\right)I_q, for\ one\ of\ converter \qquad (4.21)$$

Per unit DC link Model is shown in Appendix B.

4.4.2. DC link controller design

Dual synchronous current control is used for current control. The dc link control block diagram is shown in figure below

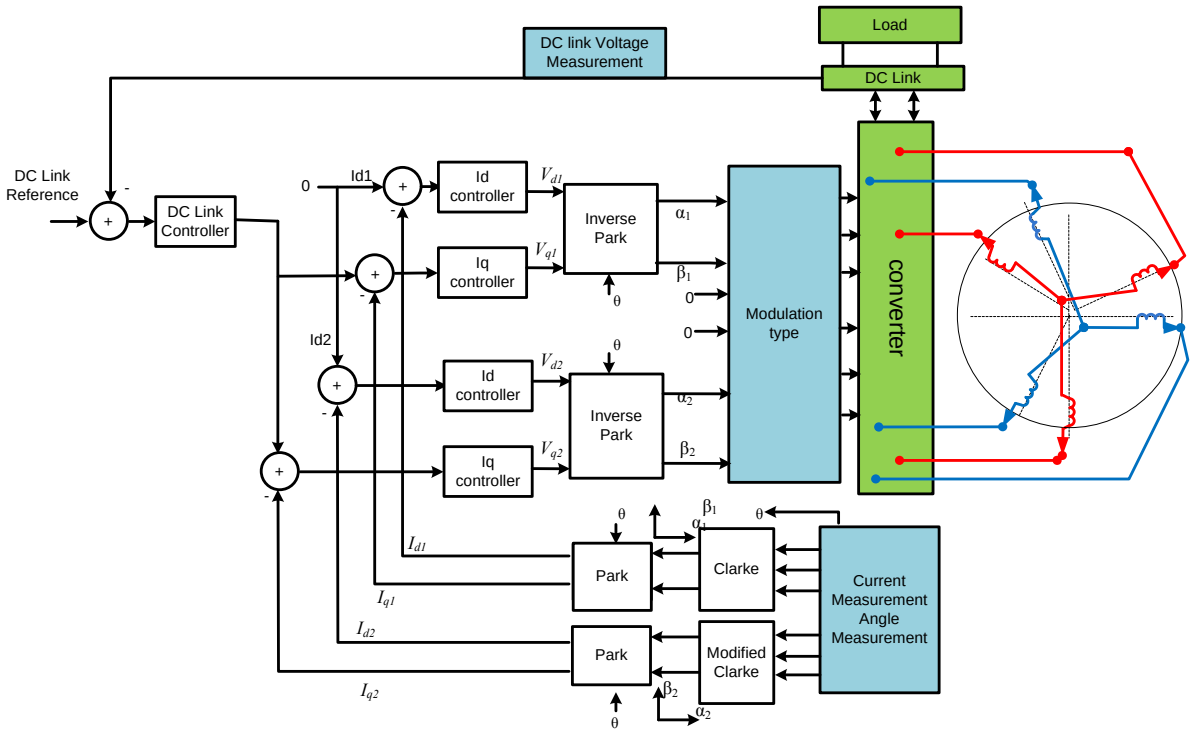

Figure 4-13 DC link control structure

The DC link controller is an outer controller. The structure of DC link Control is similar speed control except the speed is replace by dc link voltage. The general block diagram of the dc link controller is shown,

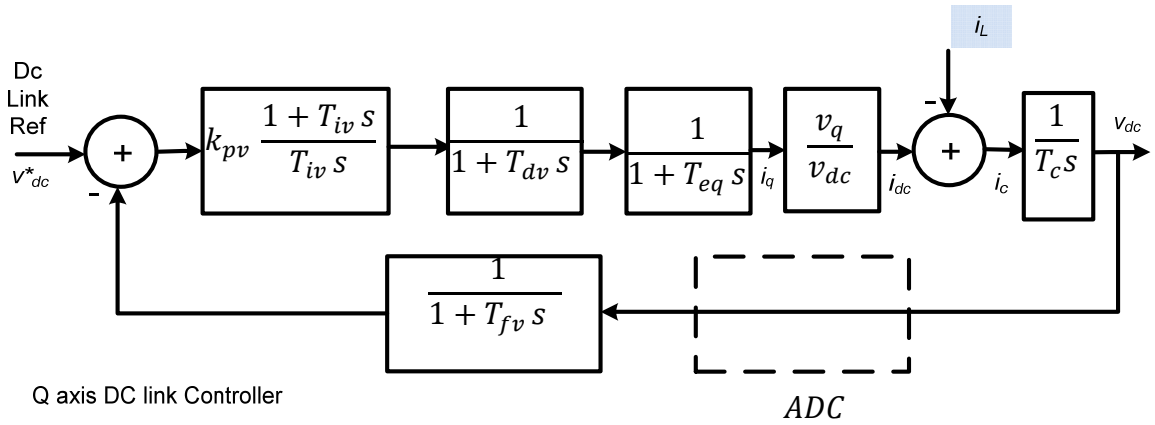

The current controller is simplified to first order system with time delay of twice the sum of small time constants, $T_{eq} = 2T_{isum}$

Sampling time of the outer control is taken 10 times the inner control loop sampling time.

The delay introduced by the processor is T_{dv} .

The ratio $\frac{v_q}{v_{dc}}$ can be taken 1 to make the analysis simpler and the PI regulator adjusts the error introduced by it.

The filter for the dc link measurement has a filter time constant $T_{fv} = 0.02\text{ms}$;

The analog and digital conversion process is done by the FPGA, and takes literally no time compared to speed sampling time. It is not included in the feedback loop transfer function calculation.

The time constant T_c is equal to capacitor value in per unit.

The open loop transfer function of the dc link control loop becomes

$$G_{ol}(s) = \left(k_{pv}\,\frac{1 + T_{iv}\,s}{T_{iv}\,s}\right)\left(\frac{\frac{v_q}{v_{dc}}}{1 + T_{vsum}\,s}\right)\left(\frac{1}{T_c s}\right) \tag{4.22}$$

$$T_{vsum} = T_{dv} + T_{eq} + T_{fv}$$

The open loop transfer function G_{ol} consists of double pole at origin. The system cannot be designed by cancelling the pole and zero, because it will result in two poles at origin and the system becomes unstable (with zero phase margins).

Therefore, the dc link voltage PI regulator parameters are calculated using the symmetric optimum technique. The load current is disturbance to system.

$$T_{vsum} = T_{eq} + T_{dv} + T_{fv}$$

$$T_{iv} = 4T_{vsum} \tag{4.23}$$

$$k_{pv} = \frac{T_c}{2kT_{vsum}}$$

So far, the controller parameters for current, speed and voltage control loops are designed and in chapters 6 the calculation of controller parameters values and tuning is presented.

5 Experimental Setup

In this chapter the high level schematic of the laboratory set up is shown. The main components in the setup are further discussed. The software development and real time interaction tool are included.

5.1 Setup

The laboratory set up consists two machines (six phase PMSG and DC motor that are mounted on the same shaft with a torque Encoder in between), FPGA processor board, two inverters, three rectifiers, three Variacs, variable resistors, Encoder and many measurement instruments. The lab bench is equipped with both AC and DC power supply with full protection as well as voltage and current measurements.

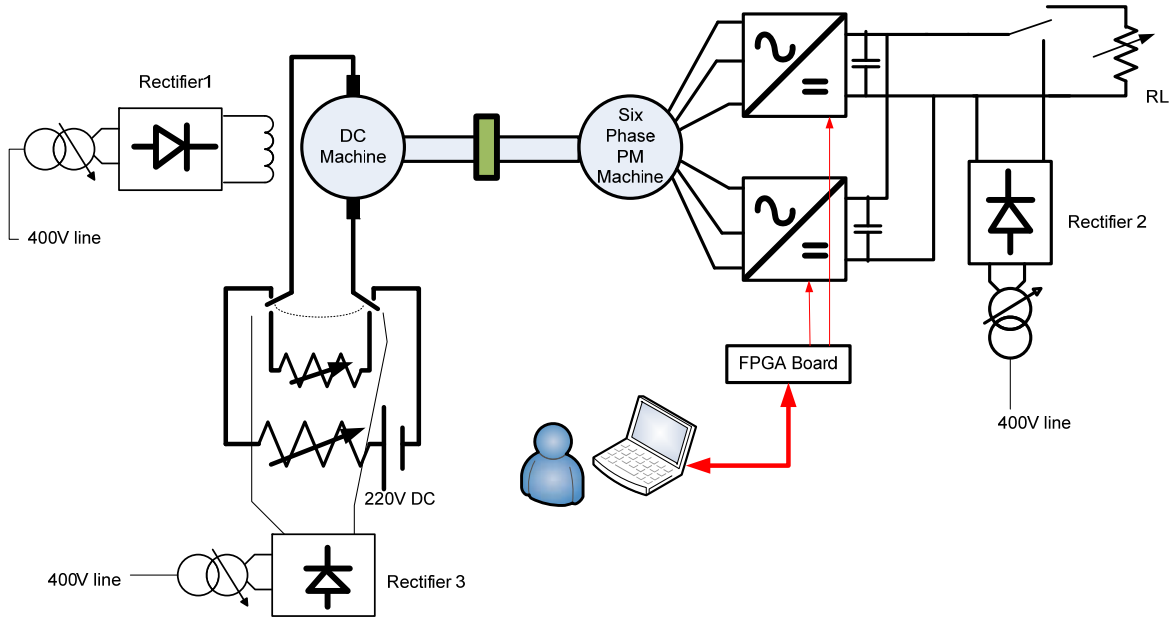

Figure 5-1 overview of laboratory setup schematics

The objective of the laboratory work is to control the six phase permanent magnet synchronous machine as a motor and as a generator. The DC machine acts as motor when permanent magnets synchronous machine is Generator mode operation, and DC machine becomes a load or generator when the permanent magnets synchronous machine is Motor mode operation. In order to achieve these modes of operation the arrangement of the source and load of the DC machine has to be taken care of by the user.

Setup can be described as follow for two modes of operation.

PM machine as a Motor -Motor Mode operation

The dc machine acts as a generator, the armature terminals of the dc machine either can be open for load operation or can be connected to variable resistance. And the six phase converter has to be supplied by the Rectifier 2. The loading dc generator can also be varied by continuously varying the excitation voltage at the output of Rectifier 1.

The Load resistor RL is always disconnected.

PM machine as Generator-Generator mode operation

The dc machine run as a motor, the armature terminals has to be connected to dc power supply. The speed of PM generator (177 rpm) is very small compared to the rated speed of the dc machine (1500 rpm), the back emf of the dc motor is very small (the range of 20V). Taking this into account armature supply voltage is connected in two ways

- The armature terminals are connected to 220 V DC power source from the board though a 50 Ohm resistor. This makes the dc motor as a constant current source or constant torque for a fixed excitation when it is seen from PM machine side. That means the power transfer is directly proportional to speed. Therefore, dc motor emulates wind turbine in the linear region of the power curve by which torque variation is done by the excitation control.
- The armature terminals are directly connected across a variable voltage source at the output of Rectifier 3. Since the armature resistance is very small 1 Ohm, an increase in back emf has pronounced effect on loading. The dc machine act as a constant power source.

From the PM generator side, the generator is connected to dc link by the two converters. The Load resistor has to be connected all the time in order to damp to power delivered by the PM generator. When constant dc link operation is need, Rectifier 1 maintains it. Dc link voltage control is done by disconnecting Rectifier 1 or by keeping its output voltage below the required range of dc link voltage control.

5.2 Components

5.2.1. The FPGA based processor board

The processor board is designed by SINTEF Energy research for use in converter control system based on a Xilinx Virtex5 30 FXT FPGA. In order to use this board dedicated hardware IP circuitry inside the FPGA are required. These IP modules are interface modules, signal processing modules or miscellaneous m IP modules are available in [31]

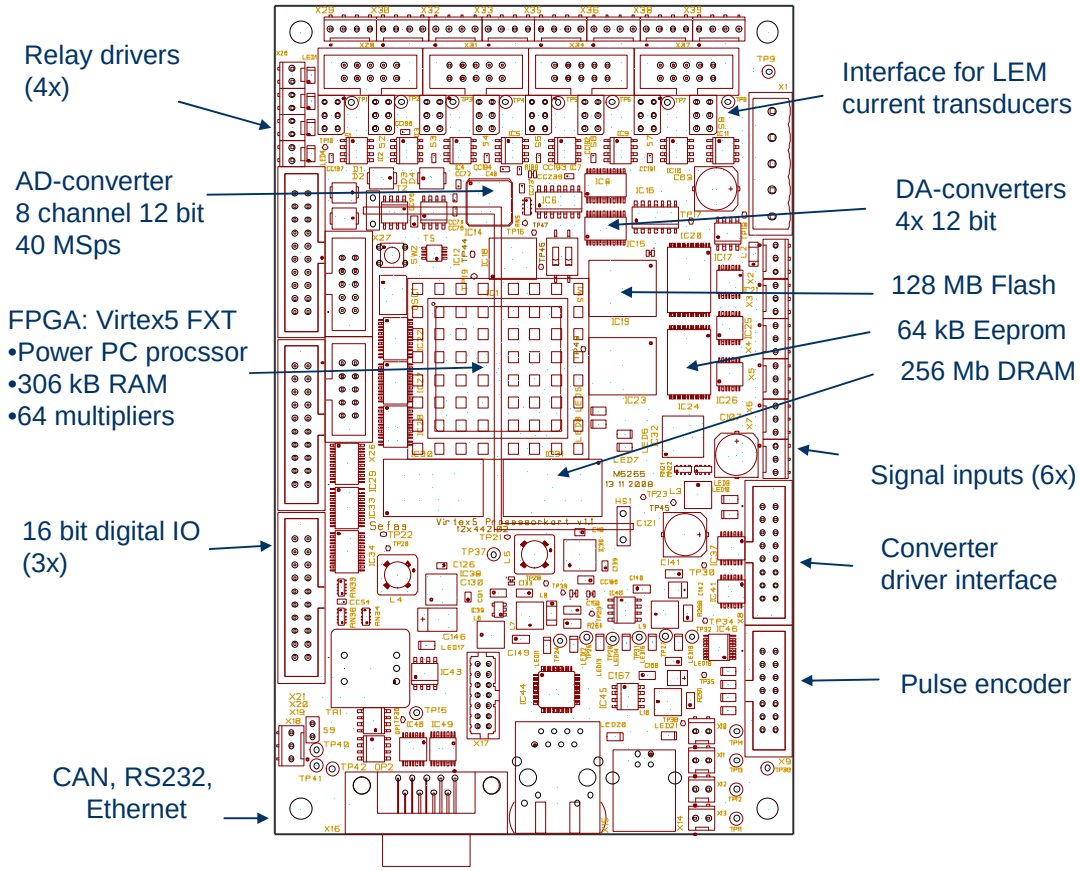

Figure 5-2 Main parts of FPGA based processor board [31]

5.2.2. Machines

There are two machines, the six phase permanent magnet machine and dc machine as in Figure 5-2b.

Six-Phase PMSG

The PMSG is model of wind turbine generator with high torque and low speed operation. The machine has surface mounted rotor with 34 poles and 36 stator slots. The machine has concentrated stator coils with single layer winding configuration. That means there are only 18 stator coils.

Originally these 18 stators coils are arranged in such a way that the stator flux axis of the six phases are 60 degree separated. Since the interest of the work is to have 30 degree separation between the two three phase groups, reconnection of the stator windings has been done. 30 degree separation can be obtained if and only if the number stator coils are an integer multiple of 12. In this case, it is not possible to obtain exact 30 degree separation. But by systematic selection of the stator coils connection 33.2725 degree separation between the two groups is

achieved. Figure 5-3a below shows the axial view from one side when it was opened for reconnection.

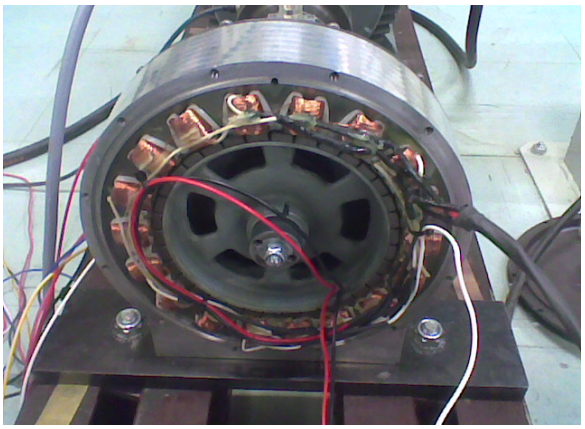

(a)

(b)

Figure 5-3 (a) Six phase PMSG opened for reconnection of stator coils, (b) PM machine assemble with the dc machine

DC machine is a separately excited 220 V, 7.5 kW, 50 Hz, 4 pole machines. It has 1 Ohm armature resistance. And 220 V and 2 A are rated parameters for the field winding.

5.2.3. Six leg Converter

Two identical converters modules are connected in parallel to a common dc link voltage to form the six leg arrangement.

The inverter and rectifier used in the experimental work are developed in the Power Electronics group at NTNU and at SINTEF Energy AS. The inverter ratings are 20 kW, DC-voltage 0- 650V, 3300uF Capacitor bank, 70 A maximum continuous current at 300 V DC and recommended switching frequency in the range 0 – 25 kHz. The converter module has gate drivers, hardware dead time generation, over load protection, over current and current limitations, and dc link voltage protections [32].

(a)

(b)

Figure 5-4 inverter module (a) ac output side, (b) driver card side

5.2.4. Current and Voltage Measurement, angle measurement

LEM Current Transducer LA 205-S is used for current measurement. It has primary nominal current of 200A, and current transformation ration 1 to 2000. The detail data sheet is given in [33] Figure 5-5 (a) shows LEM current sensors mounted on the assembly plate.

The rated current of the PMSG is 1.15 A. in order to increase the accuracy of this small current compared to the rated current of the sensor, all the six phase currents are wound in 10 turns around the their respective sensor. For one of the three phase-groups current sensors are shown in Figure 5-5 (b)

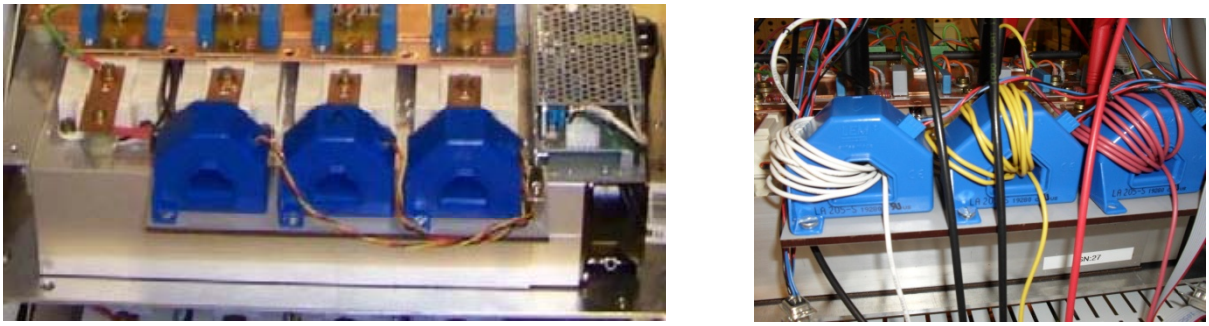

(a) (b)

Figure 5-5 LEM Current sensors (a) without current loop (b) with 10 current conductor loop

DC link voltage is measured using LEM voltage measurement cards, voltage transducer LV 25-600, which has primary nominal RMS voltage of 600 V and a conversion ratio of 600 V/ 25 mA, given in[34] .

Angle Measurement

The relative position of the rotor is measured using incremental encoder mounted on the shaft. In order to find the absolute position initial angle detection has to be done. Speed of the shaft is simply the rate of change of the rotor position.

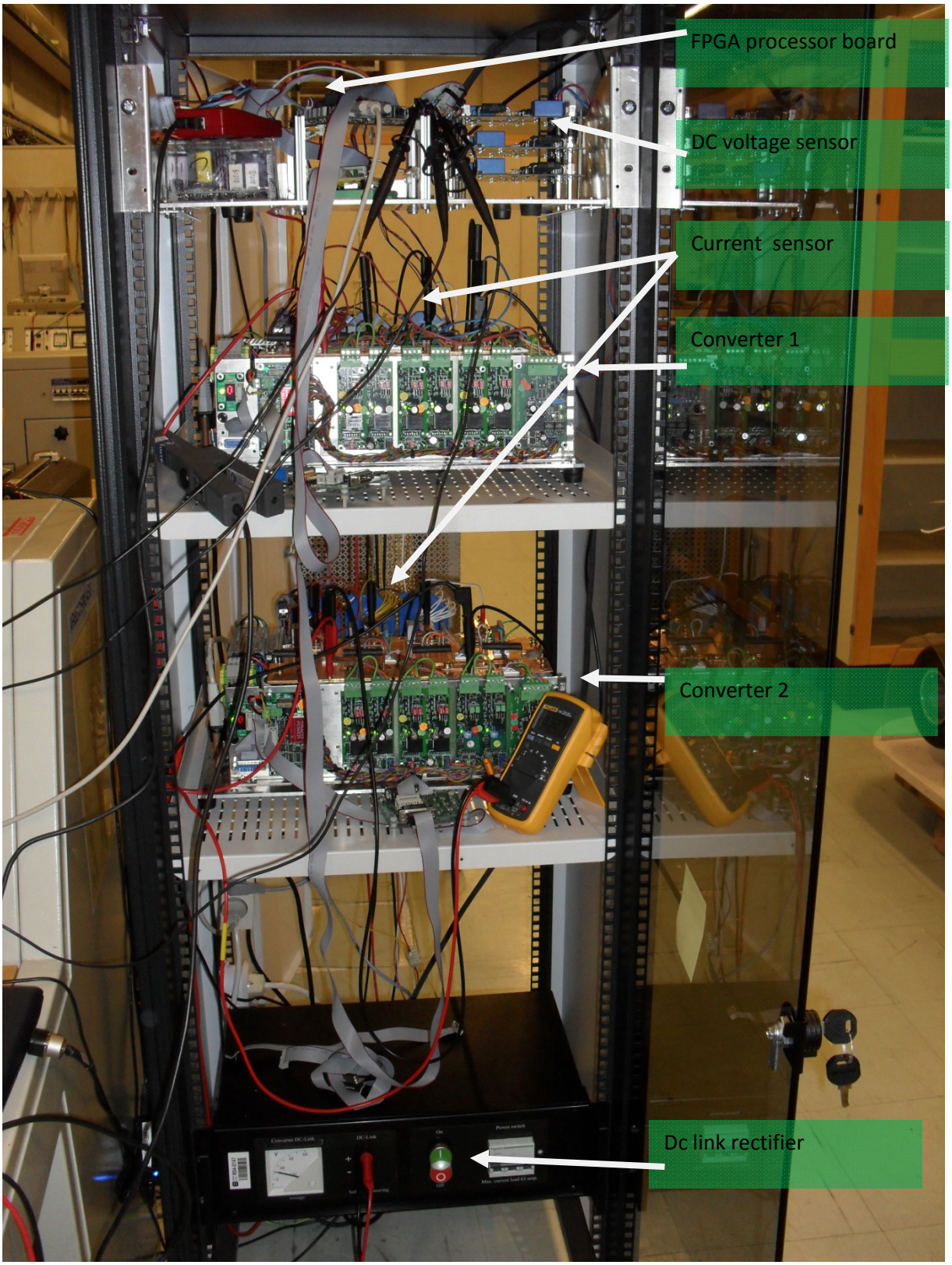

Figure 5-6 drive system assembly

5.3 Drives development

The software development part is done Xilinx C/C++ Software Development Kit. The different tasks in drive control are grouped in two, tasks which as to be done as fast as possible and tasks which gives time. To suit this, two interrupt routines are used, one is called fast interrupt routine and the other slow interrupt routine.

The fast routine interrupt interrupts every PWM switching frequency, 5 kHz. All protection and measurement, inner current control loops and modulation is takes place in here. Therefore, the processor has to finish all the fast routine faster than the sampling time (200 us). Both sinusoidal and SVPWM modulations running, the fast subroutine took 150 us. This time can be minimized by using fixed point arithmetic and optimizing the code.

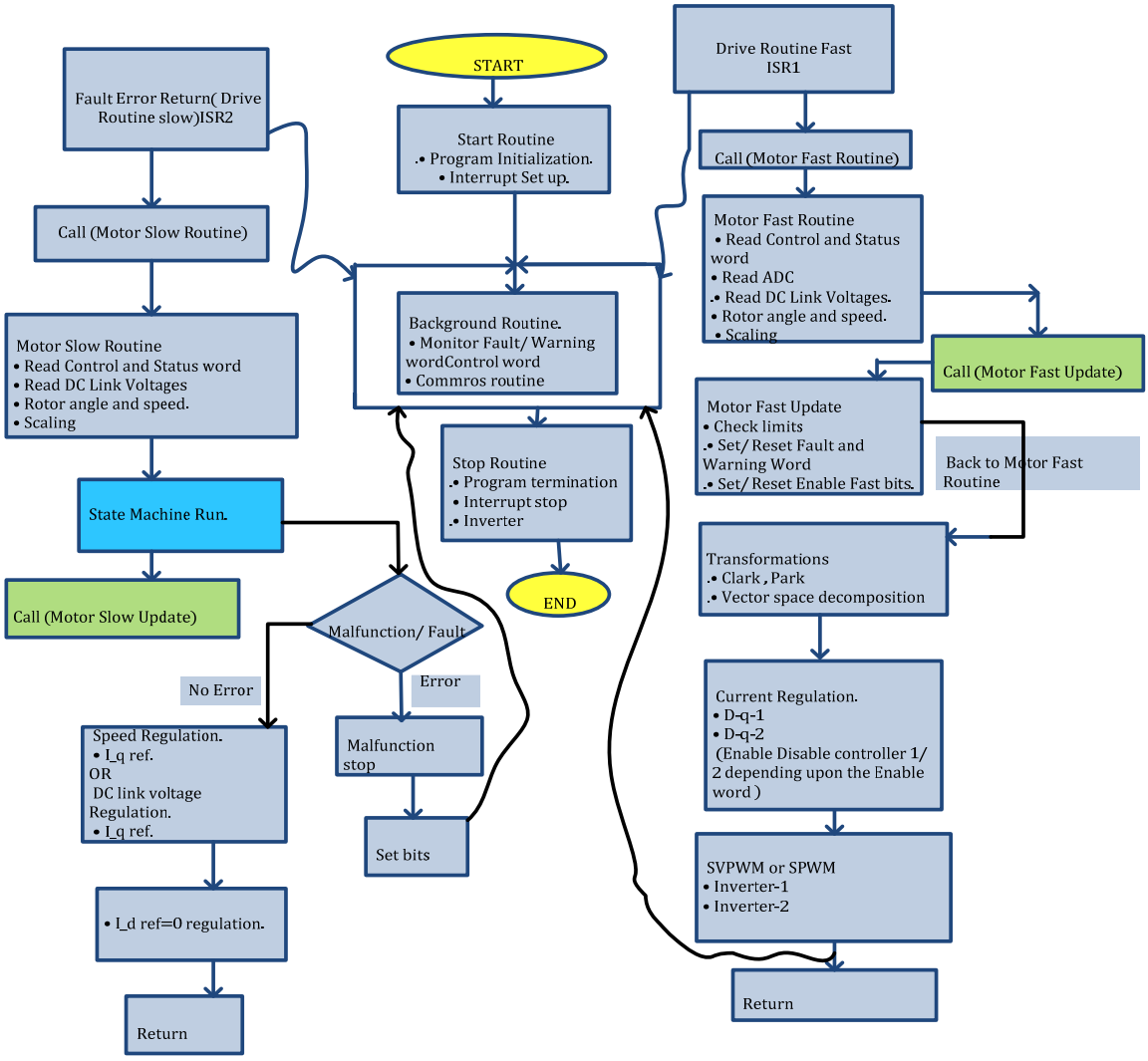

Figure 5-7 interrupts and program flow

Those routines which are not time critical, like outer control loop which is either speed control or dc link voltage control are place inside slow interrupt. The slow interrupt time is taken as 10 times of the fast interrupt time, 2000 us. Since there is no much process in this interrupt routine, it takes only 17 us to end the computation.

5.3.1. State machine

A state represents a specific internal and external behavior. It can only be terminated by means of defined events. Corresponding state transitions are assigned to events. Actions can be executed at a transition. The state's response is altered at the transition. When the transition is ended, the current state is changed to the follow-up state.

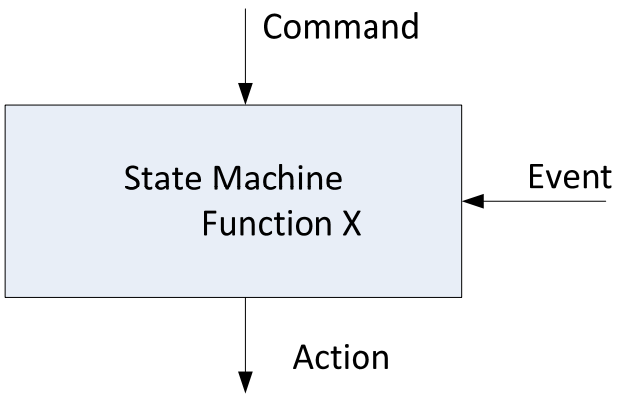

Figure 5-8 Function X state machine

The state machine .for the drive system is done according to DRIVECOM standard [35].it is shown in Figure below

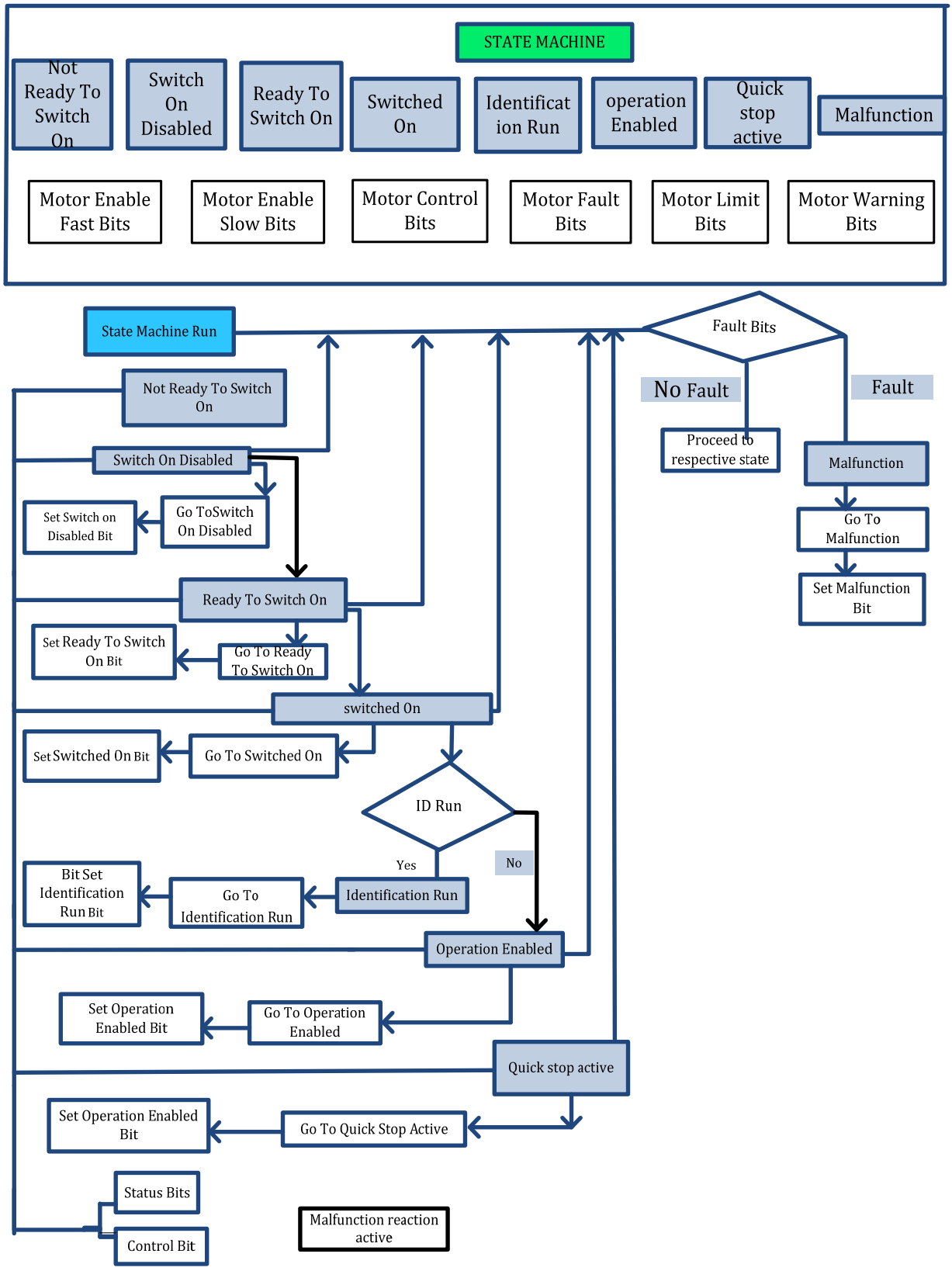

Figure 5-9 State Diagram

5.3.2. Real time interface---active DSP

For real time interaction with the FPGA processor PowerPC 440, Active DSP V 1.507 is used. The application tool helps real time debugging, controlling and monitoring of variables and real time logging of variables [36],

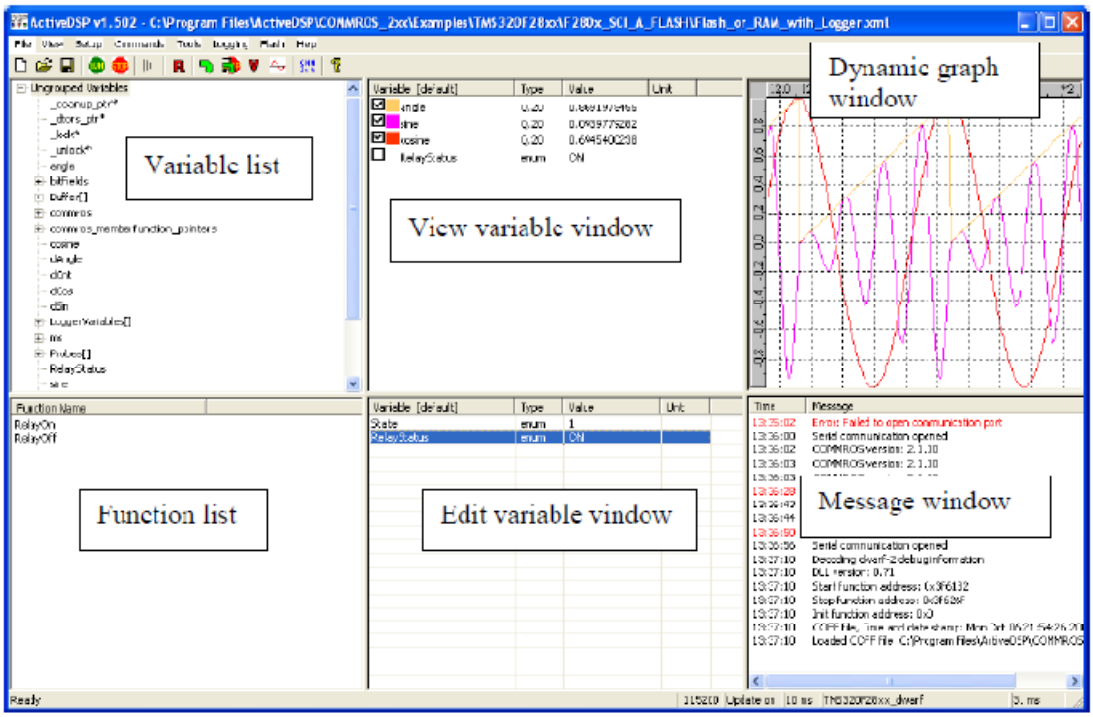

Figure 5-10 Active DSP interface window

6 Simulation and Experimental Results

6.1 Six phase PMSG testing

Originally, the six- phase PMSG has two groups of three phases which are separated by 60 deg. As it is explained before, it is not possible to obtain 30 deg separations between the two groups of the three phases. However, it found that 33.2725 deg is the nearest angle to 30 deg.

No-load test

The following three major tasks are performed.

First the phase sequence of each phase groups, that is (a, b, c) and (x, y, z), are identified; phase sequence is important for control and reference transformation. Once the phase sequence is identified each coils are tagged for future use. The two phase groups are totally symmetrical.

Second, Phase difference between the two groups of three phases is calculated. This is done by comparing waveforms on scope. The group (a, b, c) is marked as the leading phase group.

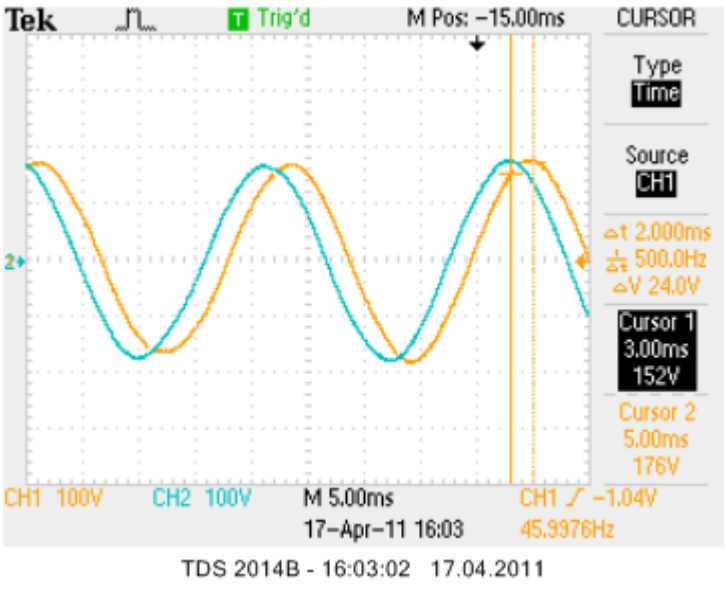

Figure 6-1 No Load Line voltages Vab (blue)and Vxy(yellow) six phase PMSG after rewinding

The no load voltages of the six PM machine Vab and Vxy is shown above, the time difference Δt between them is 2 ms. The phase difference is measured by comparing the difference time with their frequency 46 Hz.

$$\Delta\theta = 2\pi f \Delta t \; rad$$
$$\Delta\theta = 0.578 \, rad, or \; 33.12 \; deg \qquad (6.1)$$

The angle difference found by analytical calculation is 33.2725 deg, which perfectly matches with the measurement.

Third, the No Load test is also used to estimate the PM flux linkage

$$\lambda_{PM} = \frac{\sqrt{2}V_{0line}}{\sqrt{3}\omega_e} \qquad (6.2)$$

V_{0line} is line to line no load voltage(*RMS*)

The No load line voltage is measured at different operating frequencies and the PM flux linkage is calculated is as seen in the Table below

Table 6-1measured No Load Line voltage and Calculated PM flux linkage a different frequency

Frequency per unit	Electrical Angular speed(rad/s)	Line to Line Voltage(V)	Calculatedλ_{PM} (Wb)
0.2	62.832	26.5	0.344365
0.3	94.248	39.4	0.341333
0.4	125.664	52.2	0.339167
0.5	157.08	65.5	0.340467
0.6	188.496	78.5	0.340034
0.7	219.912	91.5	0.339724
0.8	251.328	105	0.341117
0.9	282.744	117.8	0.340178
1.0	314.16	131	0.340467

From the table above, the permanent flux linkage is constant around 0.34.

The phase inductance and dc resistance of the PM machine are measured, and found 140 mH and 17 Ohm.

The generator parameters are given as follows

Table 6-2 Six-Phase PMSG parameters

Parameter	Value
Nominal current	1.15 A
Nominal Back emf	131 V
Frequency	50 Hz
Torque	24 Nm
Pole Pair	17
Inductance	140 mH
Resistance	17 Ohm
PM flux linkage	0.344 Wb
Efficiency	0.32

These parameters are used for the calculation of base values of per unit system. The PM machine is recommended to run below 0.3 pu (15 Hz) speed since it is designed typically for low speed application.

6.2 Parameter Tuning

6.2.1. Current controller Test

Open loop transfer function of the current control loop is given by equation (4.8) chapter 4.2.1; its second order approximation, which has one small and one large time constants, is also given by

$$G_{OL_i} = k_{pi}\,\frac{(1 + T_{ii}\,s)}{T_{ii}\,s}\,\frac{1}{1 + T_{isum}\,s}\,\frac{1}{r_s}\,\frac{1}{1 + \tau_a\,s} \qquad (6.3)$$

Controller transfer is tuned using modulus optimum criteria

$$G_c(s) = k_{pi} + k_{ii}\frac{1}{s} = k_{pi}\frac{(1 + T_{ii}\,s)}{T_{ii}\,s}$$

$$f_s = 5\ kHz, T_s = 0.2\ ms$$

$$T_{di} = 0.5T_s = 0.1\ ms$$

$$T_v = 0.5T_s = 0.1\ ms$$

$$T_{fi} = 1\ mse, \qquad (6.4)$$

$$\tau_a = \frac{L_d}{R_s} = \frac{l_d}{r_s} = \frac{l_d}{r_s}$$

$$T_{ii} = \tau_a\ ,\ , k_{pi} = \frac{\tau_a\, r_s}{2T_{isum}}$$

$$T_{isum} = T_{di} + T_v + T_{fi}$$

The switching frequency of the converters is 5 kHz. The interrupt of the current control loop has the same frequency of the switching frequency. That means, currents are sampled every PWM period. The time delay introduced by the converters is half of the sampling frequency and the processor delay is taken

$$\tau_a = \frac{0.14}{17} = 8.235\ ms \qquad (6.5)$$

$$T_{isum} = T_{di} + T_v + T_{fi} = (0.1 + 0.1 + 1.0)ms = 1.3\ ms$$

Using Modulus optimum criteria,

$$G_c(s) = k_{pi} + k_{ii}\frac{1}{s} = k_{pi}\frac{(1 + T_{ii}\,s)}{T_{ii}\,s}$$

$$T_{ii} = \tau_a = 0.008235sec = 8.235msec \qquad (6.6)$$

$$k_{pi} = \frac{\tau_a * r_s}{2T_{isum}} = 0.88935$$

The open loop transfer function is then becomes

$$G_{OL_i} = 3.4313\ \frac{1}{0.008235s}\ \frac{1}{1+0.0001s}\frac{1}{1+0.0001s}\frac{1}{1+0.001s}\frac{1}{1+0.008235s}, original$$

$$G_{OL_i} = 3.4313\ \frac{1}{0.008235s}\ \frac{1}{1+0.0012}, second\ order\ approximated\ equivalent\ sytem$$

The bode plots of the original and its second order approximation is shown in Figure 6-2,

As it can be seen from Figure 6-2 below, the minimum stability margins are 22.4 dB (Gain Margin) and 65.5 deg. (Phase Margin). The second order approximation of open loop current transfer function has same phase margin but its phase margin is over estimated, which is infinity.

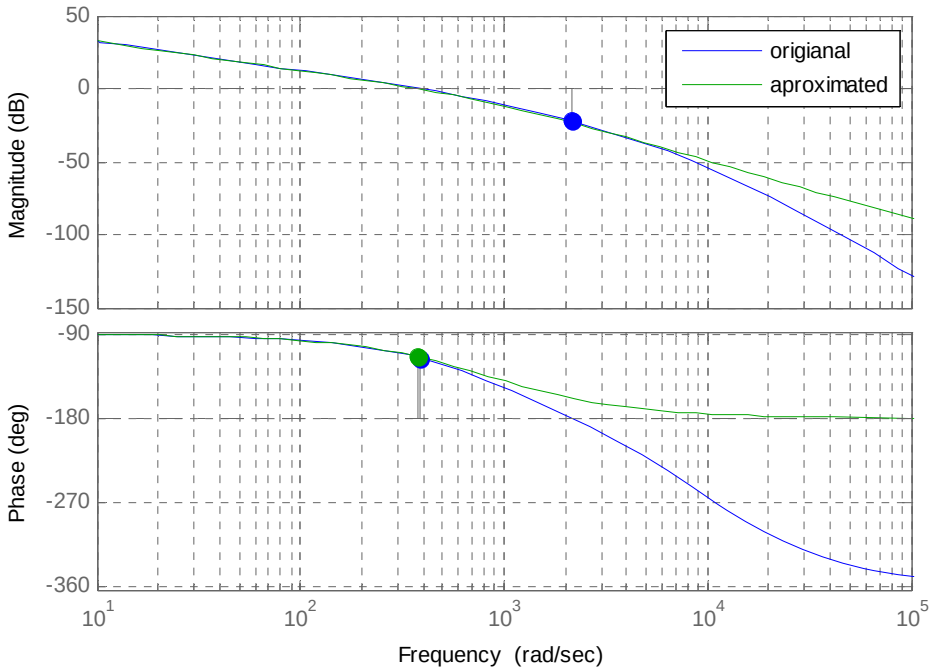

Figure 6-2 Bode Diagram of current control Open loop Transfer function (original, second order approximation)

For real time implementation of controllers on DSP, the discrete z domain equivalent of G_{OL_i} is considered.

$$G_{OL_i}(s) = 3.4313\ \frac{1}{0.008235s}\ \frac{1}{1+0.0012s}$$

$$G_{OL_i}(Z) = \frac{0.006574\,z\ +\ 0.006219}{z^2\ -\ 1.846\,z\ +\ 0.8465} \qquad (6.7)$$

For sampling frequency of $f_s = 5$ kHz, the stability limit of the discrete system is shown figure below, and is compared to its continuous s domain equivalent.

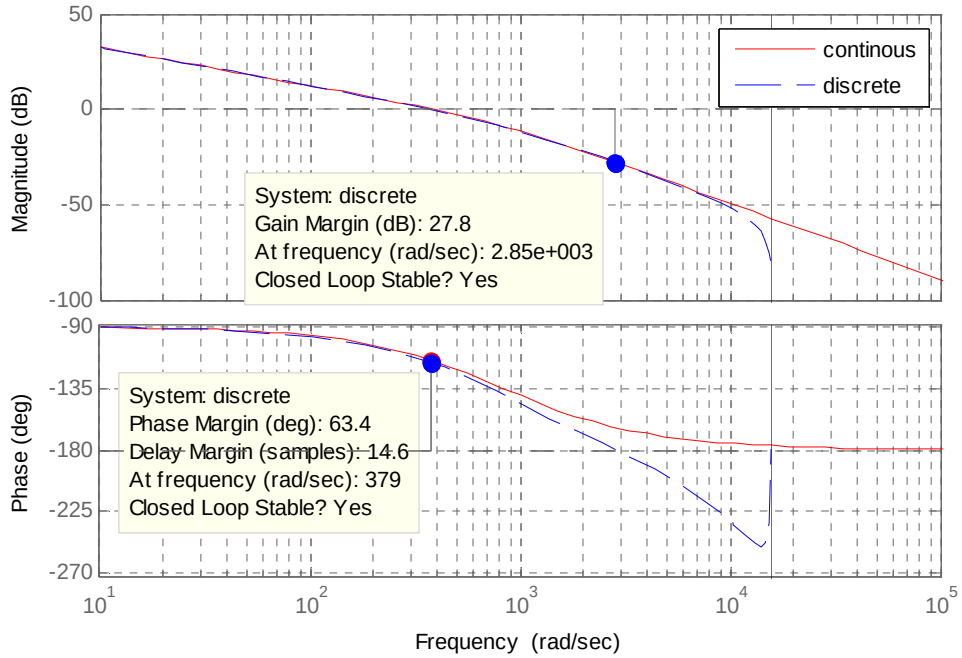

Figure 6-3 Bode Diagram of Current-open loop Transfer function (discrete, continuous)

Digital implementation of regulator deteriorates the stability margins of the equivalent continuous system. The digital implementation of the designed current controller, the second order approximation, has Gain margin of 27.7 dB and Phase margin of 63.4 deg. Therefore, the closed system is stable.

Now the time response of the current control is tested, and it has an Overshoot of 4.32%, Rise time of 3.6 ms and Settling time (within 2%) of 10 ms

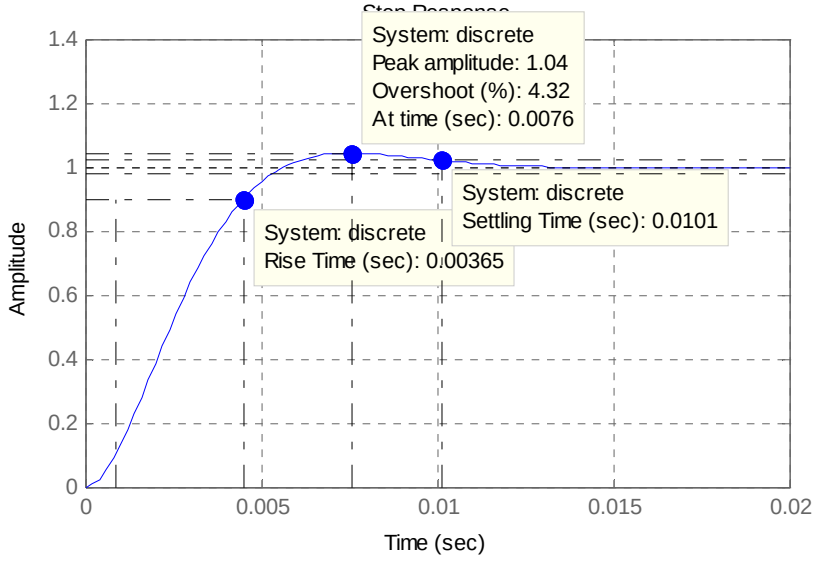

Figure 6-4 Discrete Step response of Current control Loop

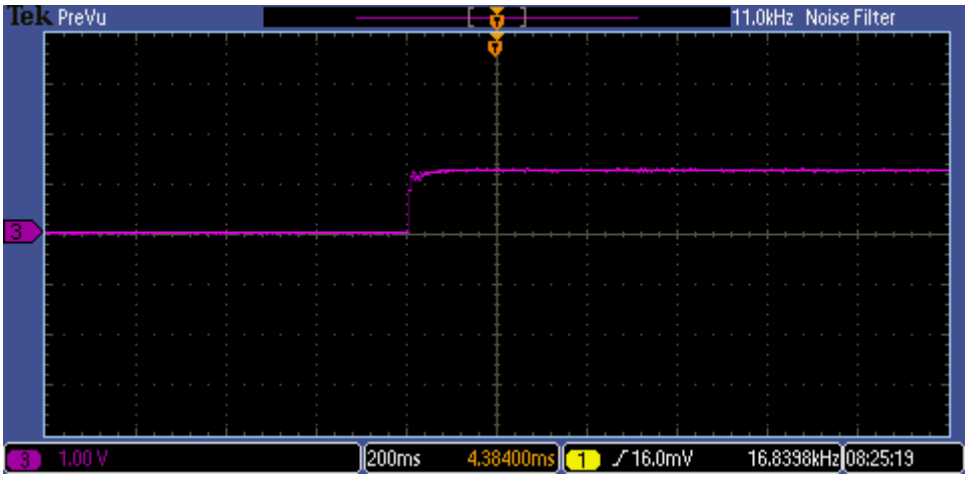

Figure 6-5 Step response of Current control loop (step change of 0 to 0.5 pu)

The laboratory measured current control loop time response is over damped.

6.2.2. Torque Controller Test

The torque of six phase machine is shown (4.15) and (4.18)

Since the peak value of the back emf of the generator is chosen as the base voltage, the per unit permanent magnet flux becomes 1, $\psi_m = 1$ which makes the per unit torque equal to per unit current. Or simply the torque constant $k_T = 1$

6.2.3. Speed Controller Test

From section 4.2.3, the speed controller open loop transfer function, also calculated time constants are given. It is summarized as follows

$$G_{ol\omega}(s) = \left(k_{p\omega}\,\frac{1+T_{i\omega}\,s}{T_{i\omega}\,s}\right)\frac{k_T}{1+T_{eq}\,s}\,\frac{1}{T_m\,s}\,\frac{1}{1+T_{d\omega}\,s}\,\frac{1}{1+T_{f\omega}\,s}$$

$$T_s = 10T_{sw} = 2\ ms;\ 10\ times\ the\ switching\ time$$

$$T_{d\omega} = 0.01T_s = 0.02\ ms \qquad (6.8)$$

$$T_{f\omega} = 2.274\ ms$$

$$T_{eq} = 2T_{isum} = 2.4\ ms$$

$$T_{\omega sum} = T_{eq} + T_{d\omega} + T_{f\omega} = 2.4 + 0.02 + 2.274 = 4.694\ ms$$

The speed controller parameters are calculated using symmetric optimum method, as is shown below

$$G_{c\omega}(s) = k_{p\omega}\ \frac{1 + T_{i\omega}\, s}{T_{i\omega}\, s}$$

$$T_{i\omega} = 4T_{\omega sum}\ = 18.77\ ms \qquad (6.9)$$

$$k_{p\omega} = \frac{T_m}{2k_{\,T}T_{\omega sum}} = 100.7251T_m = 0.5$$

The total equivalent inertia of the system is estimated to be $J_{eq} = 0.00758\ Kg/m^2$ and in per unit system$T_m = 5$ ms.

Putting the time constants in place, the open loop transfer function f of speed control loop is

$$G_{ol\omega}(s) = \left(0.5\frac{1 + 0.01877s}{0.01877s}\right)\frac{1}{1 + 0.0024s}\frac{1}{1 + 0.00002s}\frac{1}{1 + 0.002274s}\frac{1}{0.005s} \qquad (6.10)$$

$$G_{ol\omega}(s) = \left(0.5\frac{1 + 0.01877s}{0.01877s}\right)\frac{1}{1 + 0.004694s}\frac{1}{0.005s}, approximated$$

Bode diagrams are drawn and the approximated system matches the original system within the stability limits. The stability limits (Phase margin, Gain Margin) are (35.4 deg, 16 dB) and (33.2 deg, infinity dB) for original and approximated speed control loop, as seen in Figure

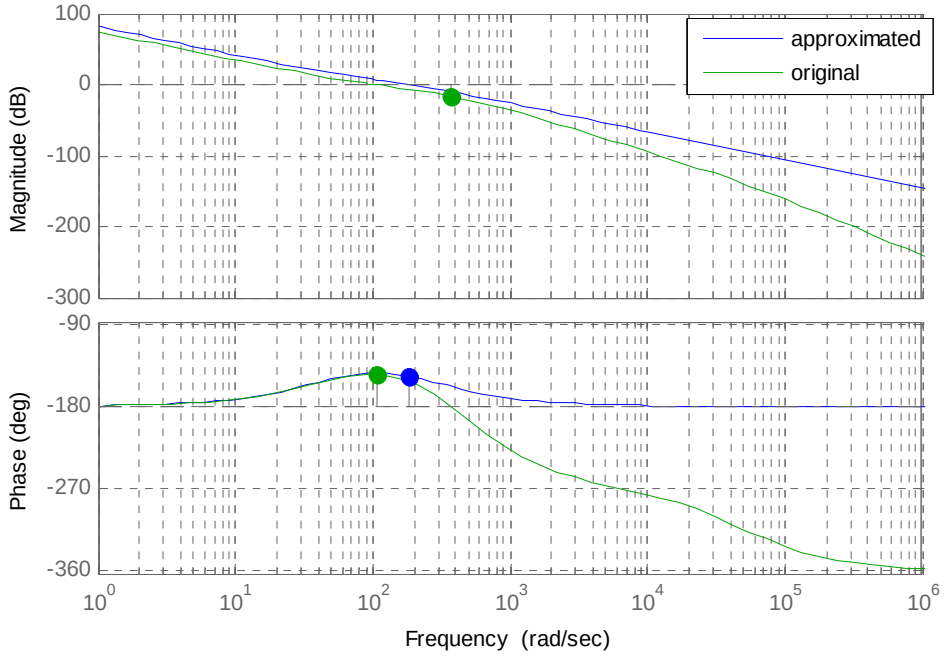

Figure 6-6 Bode Diagram of open loop transfer function of Speed control loop

For real time implementation of controllers on DSP, the discrete z domain equivalent of G_{OL_i} is considered. To see the effect of controller in discrete and continuous frequency domains, the approximated open loop speed loop transfer function is taken and its z domain transfer function is

$$G_{ol\omega}(s) = \left(0.5\frac{1+0.01877s}{0.01877s}\right)\frac{1}{1+0.004694s}\frac{1}{0.005s}$$

$$G_{ol\omega}(Z) = \frac{0.0009678\,z^2 + 0.0009474}{z^3 - 2.958z^2 + 2.917\,z - 0.9583} \qquad (6.11)$$

For sampling frequency of $f_s = 5$ kHz, the stability limit of the discrete system is shown figure below and is compared to its continuous s domain equivalent.

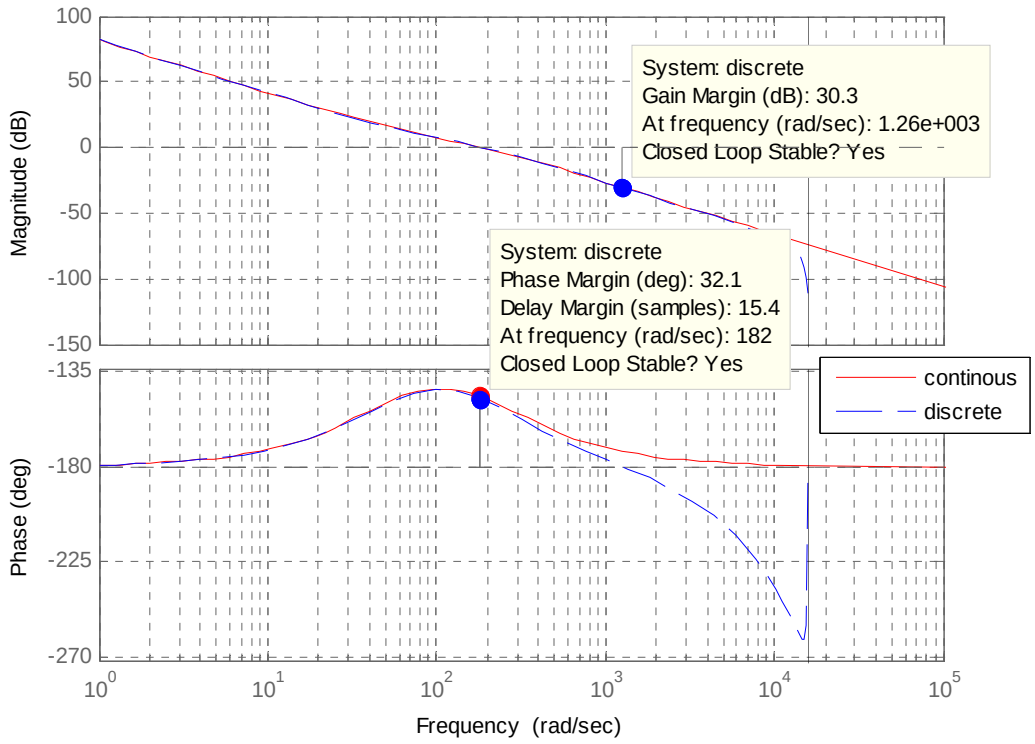

Figure 6-7 Bode Diagram of Speed control-open loop Transfer function (discrete, continuous)

The digital implementation of the designed speed controller-approximated has Gain margin of 30.3 dB and Phase margin of 32.1 deg. Therefore, the closed system is stable. Digital implementation of regulator deteriorates the stability margins of the equivalent continuous system.

In time domain, the step response of the speed control is tested, and it has an Overshoot of 46.5%, Rise time of 6 ms and Settling time (within 2%) of 57 ms

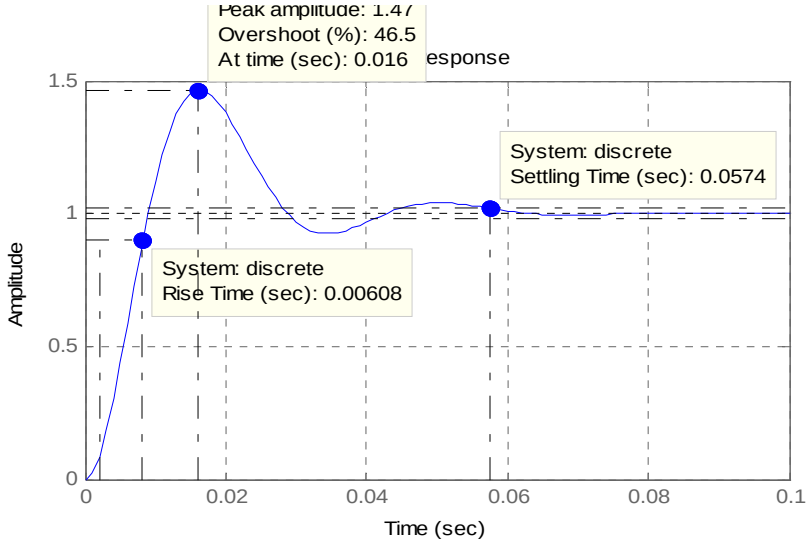

Figure 6-8 Discrete Step response of Speed control Loop- probe 3

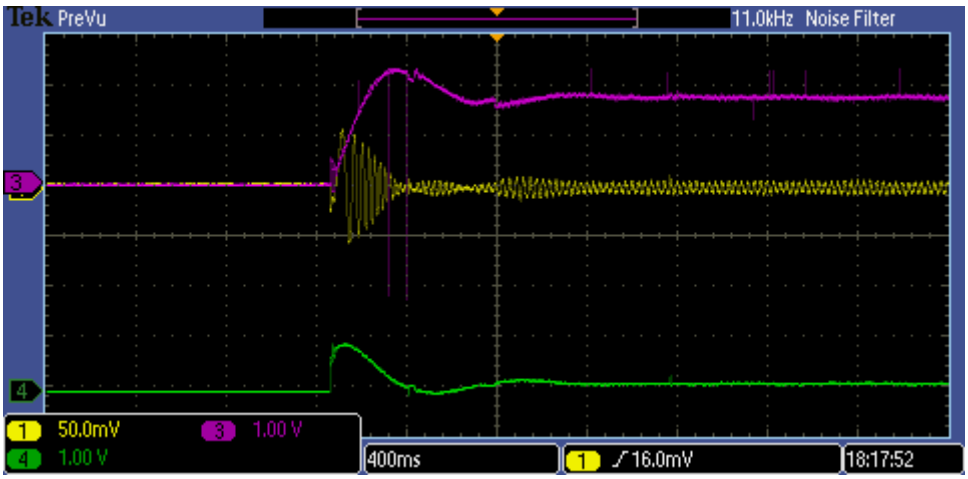

Figure 6-9 Step response of Speed control Loop- probe 3 (step change in speed from 0 to 0.7 pu)

6.2.4. DC link Voltage Controller Tuning

From section 4.2.4, the DC link voltage controller- open loop transfer function and also calculated time constants are given. It is summarized as follows

$$G_{OL_v}(s) = \left(k_{pv}\,\frac{1+T_{iv}\,s}{T_{iv}\,s}\right)\left(\frac{1}{1+T_{vsum}\,s}\right)\left(\frac{1}{T_c\,s}\right) \tag{6.12}$$

$$c = C \cdot Z_{DCb} = 0.573$$

$$T_c = \frac{1}{\omega_b c} = 5.55\, ms$$

$$T_{fv} = 0.02ms$$

$$T_{dv} = 0.01T_{sw} = 0.02ms$$

$$T_{eq} = 2T_{isum} = 2.4\, ms$$

$$T_{vsum} = T_{dv} + T_{eq} + T_{fv} = 2.44\, ms$$

The dc link regulator parameters are calculated using symmetric optimum method, as is shown below

$$G_{cv}(s) = k_{pv}\,\frac{1 + T_{iv}\,s}{T_{iv}\,s}$$

$$T_{iv} = 4T_{vsum} = 9.76\, ms \qquad (6.13)$$

$$k_{pv} = \frac{T_c}{2T_{vsum}} = 1.4,$$

Putting the time constants in place, the open loop transfer function f of dc link control loop is

$$G_{OL_v}(s) = \left(k_{pv}\,\frac{1 + T_{iv}\,s}{T_{iv}\,s}\right)\left(\frac{1}{1 + T_{vsum}\,s}\right)\left(\frac{1}{cs}\right)$$

$$G_{ol\omega}(s) = \left(0.5\,\frac{1 + 0.00976s}{0.00976s}\right)\frac{1}{1 + 0.00244s}\,\frac{1}{0.00555s}, approximated \qquad (6.14)$$

Bode diagrams are drawn and the approximated system matches the original system well within the stability limits. The stability limits are Phase Margin of 36.6 deg and Gain Margin of 37.5 dB as seen Figure below

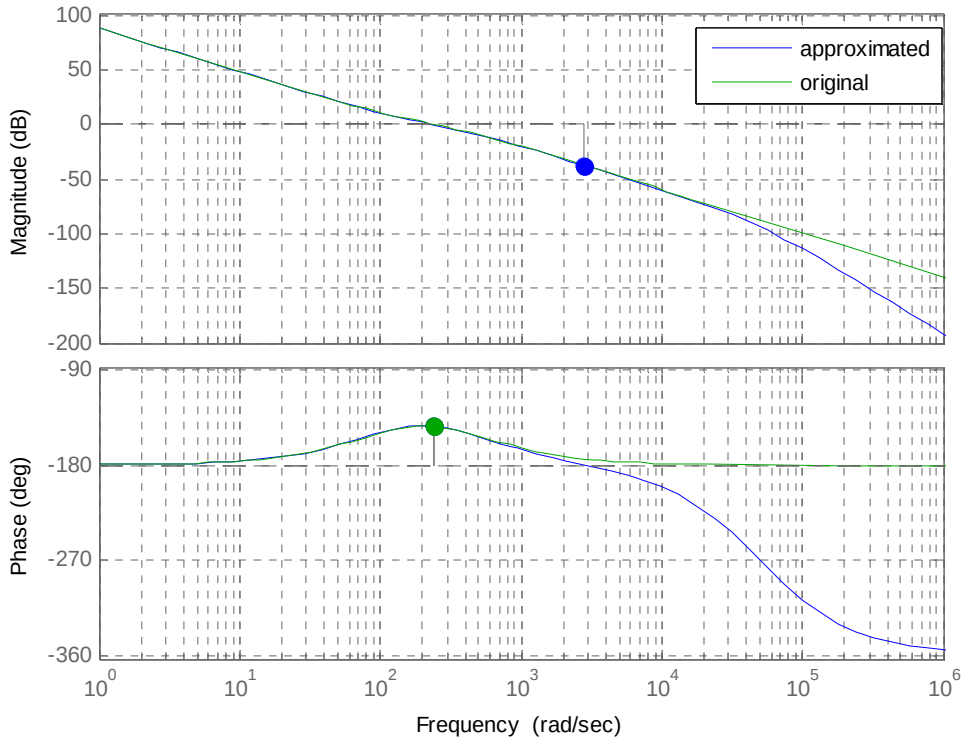

Figure 6-10 Bode Diagram of open loop transfer function of dc link voltage control loop

For real time implementation of controllers on DSP, the discrete z domain equivalent of G_{OL_v} is considered. To see the effect of controller in discrete and continuous frequency domains, the approximated open loop speed loop transfer function is taken and its z domain transfer function is

$$G_{ol\omega}(s) = \left(0.5\frac{1+0.01877s}{0.01877s}\right)\frac{1}{1+0.004694s}\frac{1}{0.005s}$$

$$G_{ol\omega}(Z) = \frac{0.002\,z^2 + 4.554e^{-9}\,z - 0.001945}{z^3 - 2.921z^2 + 2.8243\,z - 0.92133} \qquad (6.15)$$

For sampling frequency of $f_s = 5$ kHz, the stability limit of the discrete system is shown figure below and is compared to its continuous s domain equivalent.

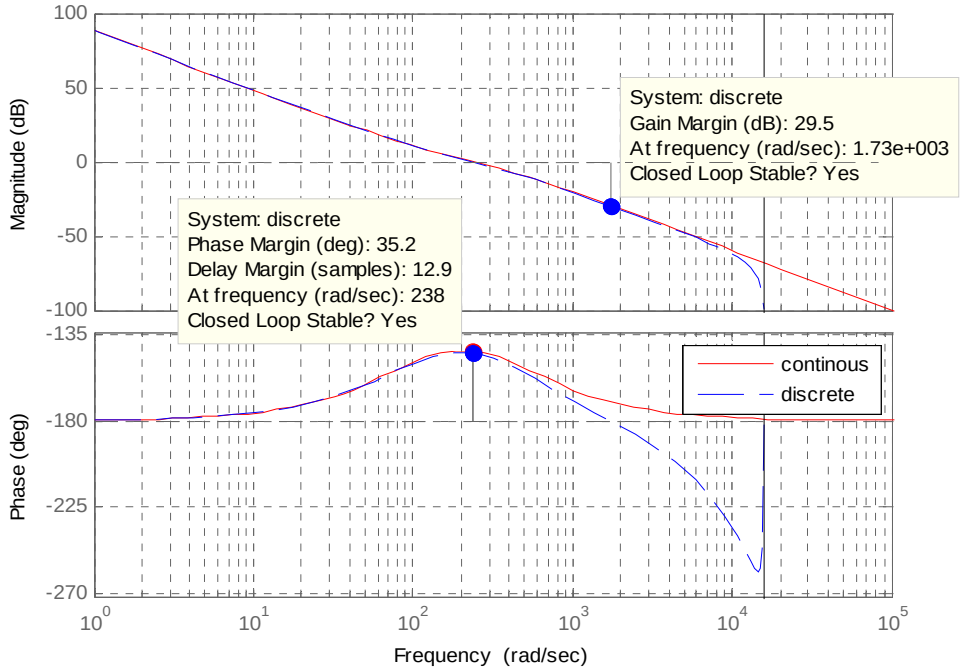

Figure 6-11 Bode Diagram of dc link voltage control-open loop Transfer function (discrete, continuous)

The digital implementation of the designed dc link voltage controller-approximated has Gain margin of 29.5 dB and Phase margin of 35.2 deg. Therefore, the closed system is stable. The gain cross over frequency is 36.6 deg at 238 rad/s(37.88Hz) which is 13 times smaller than the sampling frequency 500Hz .

In time domain, the step response of the speed control is tested, and it has an Overshoot of 43.6%, Rise time of 4.55 ms and Settling time (within 2%) of 33.3 ms.

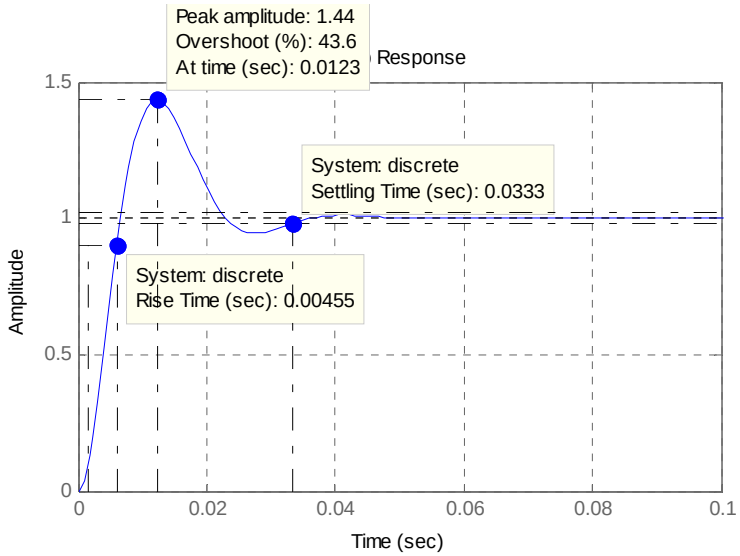

Figure 6-12 Discrete Step response of dc link voltage control Loop- probe

6.3 Rotor angle alignment PM rotor and Starting

An Encoder is used to measure the speed and position of the rotor. This position is not the absolute position. Therefore the position of the rotor flux is unknown. The initial position of the rotor flux has to be known for the proper operation of vector control. Rotor position alignment can be done by applying constant voltage across the stator windings to obtain a constant stator current flowing in the coils which then creates stator flux. The rotor flux automatically aligns itself onto the stator flux and locked there until the stator flux is changed. This position is taken as the initial angle of rotor position.

For six phases PMSM, the rotor alignment is performed with respect to one phase group and keeping the current in the other phase group zero. The stator current vector are set Iq1=0.5, Id1=0 and iq2=0, id2=0; and an arbitrary angular position for inverse park transformation is chosen is to be -90 deg. This lead to an equivalent phase currents Ia=0.5, Ib=Ic= -0.25 and Ix=Iy=Iz=0.

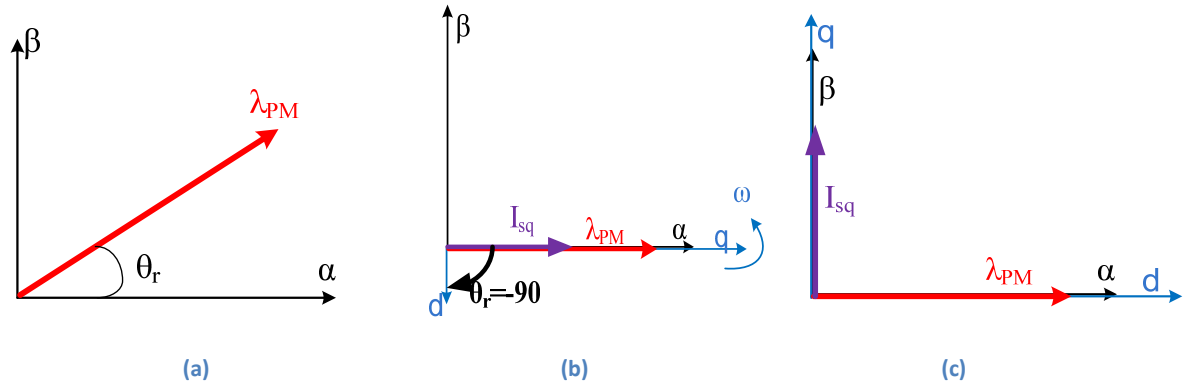

Figure 6-13 initial Rotor alignment step by step pictorial representation

This can be shown in figures, at Figure above (a) the rotor flux is at temporary angle θr. When the rotor align function is activated the values of the stator current vectors are set to Iq1=0.5, Id1=0 and iq2=0, id2=0; and an arbitrary angular position θr =-90 deg. Figure (b) shows rotor flux is known and is aligned to q axis. To align rotor flux with the d axis at start up, 90 electrical degrees is added or simply the stator current (d, q) plane is rotated by 90 deg. Then d axis is aligned rotor flux as seen in figure (c). Now the rotor starts to rotate to catch up with the stator current, meanwhile the control maintains stator current along q axis which leads to a continuous rotation of the rotor.

Experimentally the duration of the rotor alignment time can be adjusted online, Figure blow the first stage when there are no current in the stator windings second stage is alignment stage when dc current is flows through phase group 1. For 1.2 s the rotor is stalled. As it can be seen the value of the stator currents are same as preset values and this makes sure that the machine from heating.

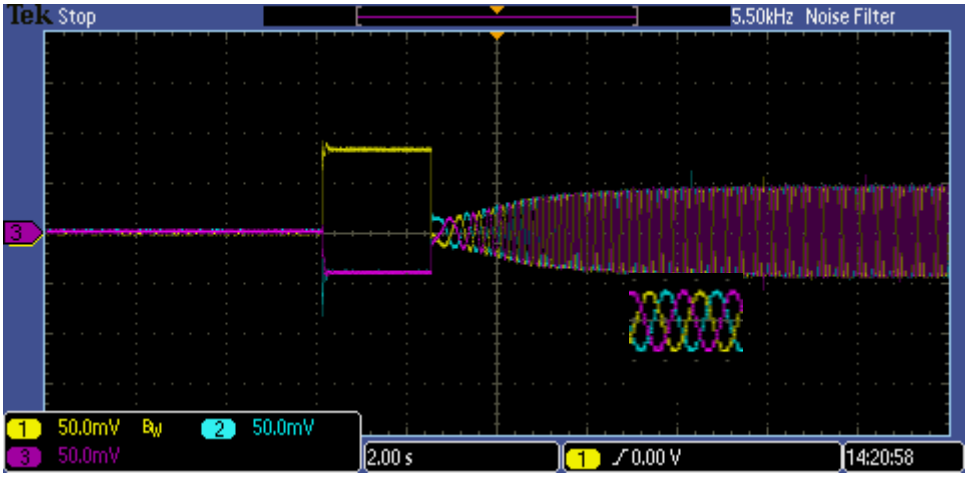

Figure 6-14 stator currents of phase group 1 during starting [probe 100mV/A]

Since phase group 2 is not participated in the alignment process, they are all there during alignment stage. It can be seen that at point where the current in the phase group 1 is step changed, transient current is induced in the phase group 2 to oppose the change in flux.

.

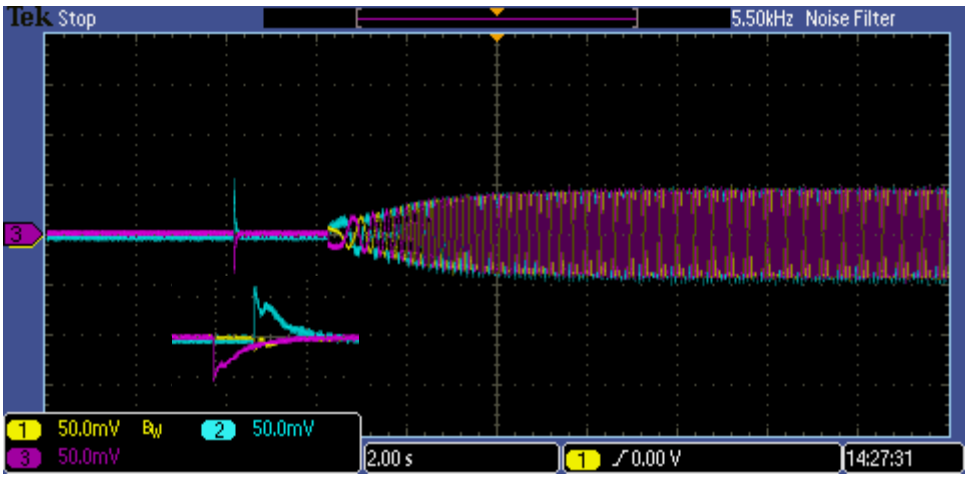

Figure 6-15 stator current of the second phase group during starting [probe 100mV/A]

During startup, the six-phase PMSM can be either torque control mode or speed mode. It is wise to start in speed control mode with no load. This makes sure both speed and stator currents are limited.

6.4 Motor Mode operation

In motor mode operation, the PM machine drives the dc machine. The performance of the control is tested.

6.4.1. Torque Control Mode

Torque control mode is when the output torque of the six –phase PMSM is control variable; the converters operate so that the motor can manage to deliver the preset torque reference. That means speed is free variable within the power limit.

One of the performance indicators of closed loop control is step response.

The step response of the torque can is same as step response of torque producing current in per unit system since pu torque is equal to pu q axis current, see appendix. Step response of torque is given below,

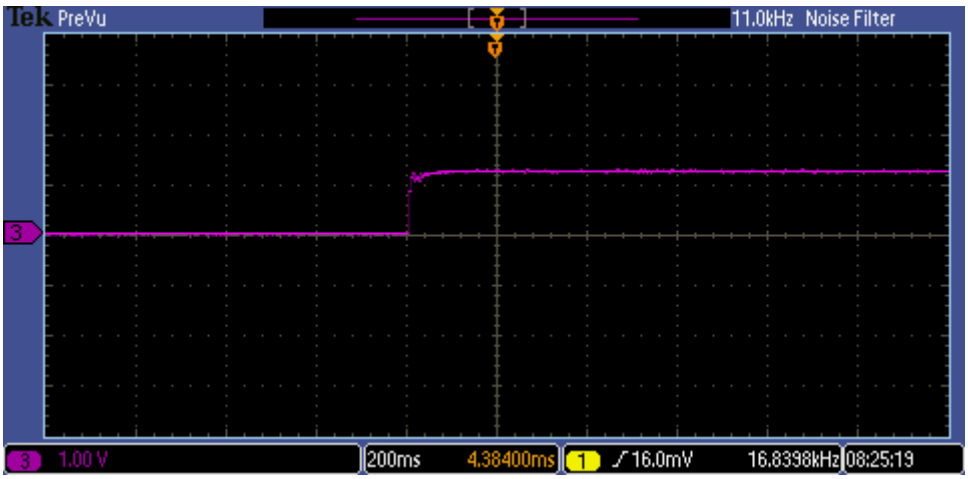

Figure 6-16 step response of torque from 0-0.5 pu (probe-2.5V/pu)

As it can be seen from torque response, the close loop system is over damped. It is a typical characteristic of modulus optimum criteria tuned controller in the system. For safety of the machine it is only 0.5 pu(12 Nm) torque step charge is made. The transient of stator currents have fast response and no overshoot and, are shown in Appendix D .

During normal operation torque reference are ramped to the reference value. It is only in for test purpose in which the control variables change at no time or in step. Therefore, the response of torque controller for different set points is shown below,

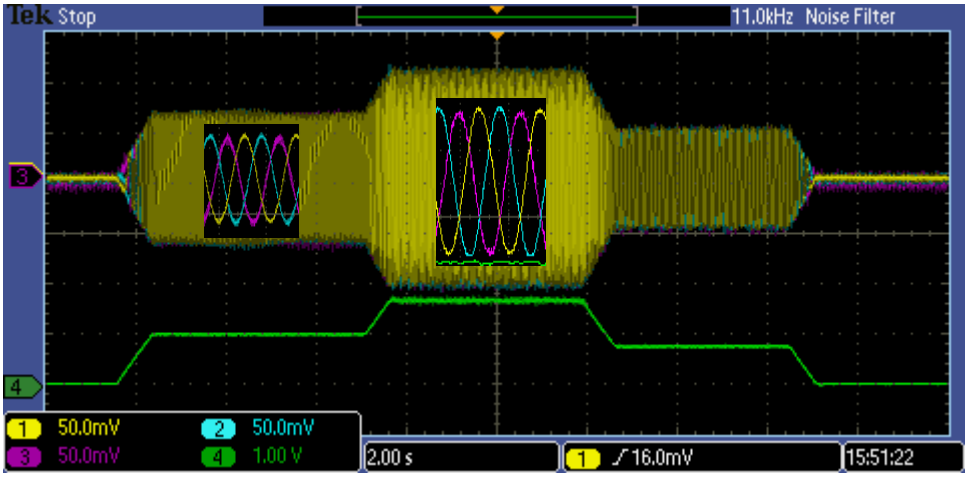

Figure 6-17 Measured stator currents for Change in Torque reference(probe4) in Normal Operation[probe1,2,3 100mV/A, and probe4 2.5V/pu]

Next, constant torque and variable speed operation is done. To do so, the torque is fixed to reference value and the excitation of the dc generator is changed. For test purpose PM torque is set to 0.2 pu and the excitation of the dc machine is reduced by half and then back to previous.

When the excitation of the dc generator is reduced both its back emf and torque decrease from dc machine characteristics. Here, the converter delivers more power so as to keep the torque at set point. This result an increase in speed of PM machine until the current in the dc generator produces torque which equals to set value; speeding up of PM machine increases the induced back emf therefore the controller increases the duty cycle so as to increase the converter output voltage; the reverse process occurs when the excitation increases again. The converter switching voltages, motor speed and torque are measure as shown below

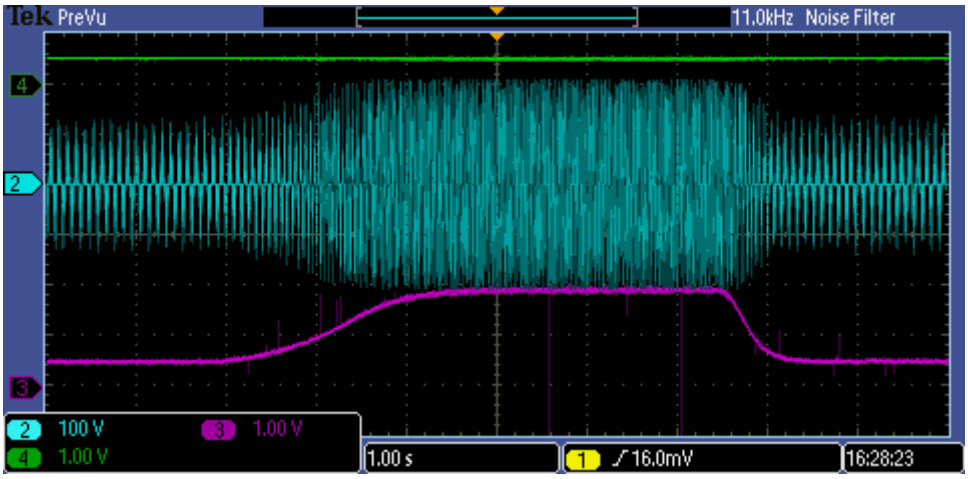

Figure 6-18 Torque (probe4), line voltage (probe2) and speed (probe3) during DC excitation change [probe3, 4-2.5V/pu, probe 2-1/1]

It is possible to change the drive from torque control mode to directly speed control mode. The dynamic behavior of one of the stator current is shown in appendix D.

6.4.2. Speed Control Mode

In Speed control mode, motor speed is the control variable whiles the torque or stator currents are free variable. Speed control loop is the outer control loop to the torque or current control loop. The step change in speed in sequence of [0 0.4 0.7 0] pu is applied to the drive and the measured speed, stator phase a current and torque are measured. Then speed reference is increased, the controller forces the drive system speed to follow the speed command. When the dc machine speed up, its back emf increases then the current delivered to the passive load increases. Thereby demanding more torque from PM machine. The PM machine extracts more current from the converter for sustain increase in speed. Reverse processor occurs for decrease in speed reference.

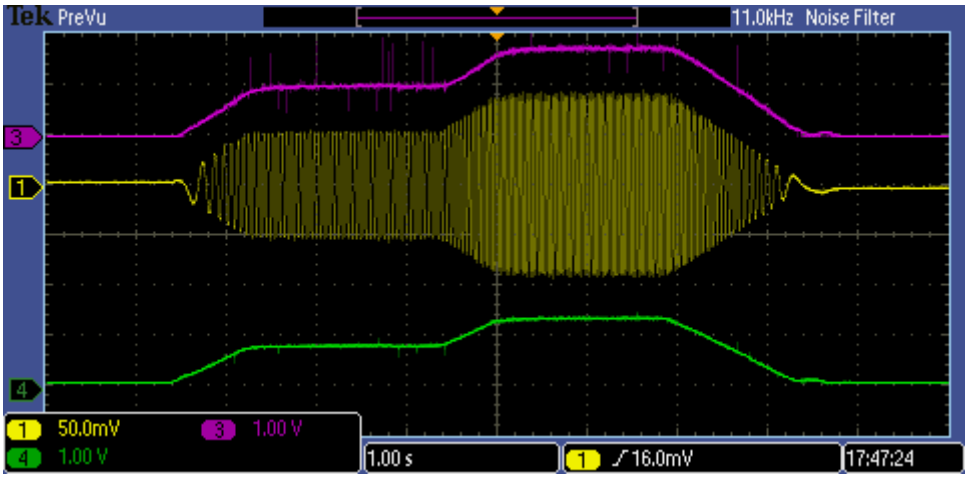

Figure 6-19 Speed(probe3), stator phase current (probe1) and torque(probe3) for step changes in speed,[probe1,2 2.5V/pu, probe1 100mV/A]

Another test event is keeping the speed reference while the load is changing or simple constant speed and variable load operation. This is done by setting speed at a reference value and changing the excitation of the dc machine.

Initially the PM machine is at no load (0.05pu) with zero dc excitation and running at 0.5 pu speed, and then the excitation of the dc machine is varied to full-half-zero excitation manually. This change in excitation results a directly proportional change in torque. An increase in excitation increases the torque of the dc motor and PM motor. This result in an increase output of converter current. Meantime, the dc machine tends to decrease its speed when its excitation increases as it seen in the speed response. When the excitation decreases the dc motor tends to accelerate but the controller keep the speed at the pre set value at steady state. This can be seen in figure below, all the measurements use same probe, unless specified current measurements have scaling factor 100 mV/ A and torque and speed measurements have scaling factor of 2.5V/ pu.

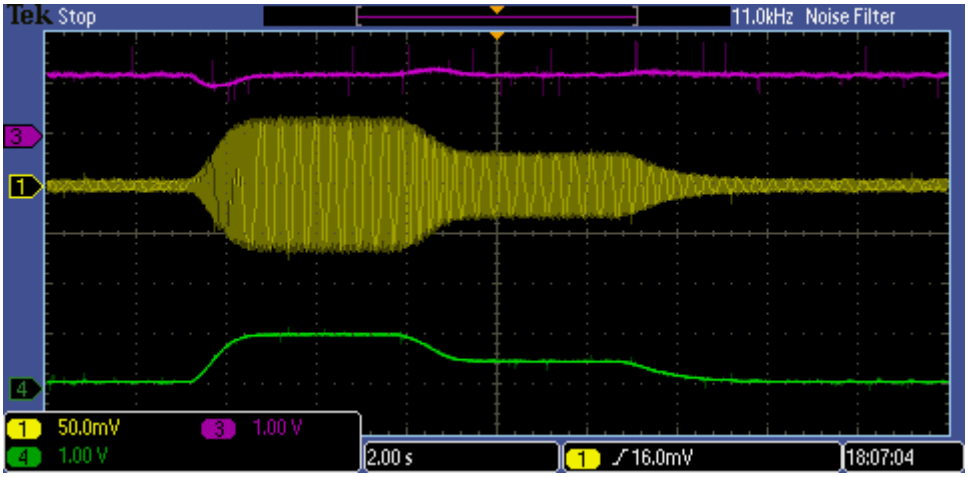

Figure 6-20 constant speed -variable load operation [probe1 speed, probe2 stator phase current, probe3 torque]

The above test is also recorded from Active DSP data logger window, which shows a very fast change since there is no filters included there see Appendix D

6.4.3. Disabling of one Inverter

One of the advantages of this setup its capability to deliver power when one converter is disabled without affecting the other phase group. Two test cases are taken. How the

controller's response during converter failure-disabling to deliver the reference torque or speed.

First case, the six phase machine is running in torque control mode and one of the converters is disabled. For the reference torque 0.5 pu, the six phase machine is running at 0.59 pu speed. The torque reference of each inverter is same as reference torque in pu in separate or dual current controller control, 0.5 pu. When one of the converters disabled, the other inverter provides torque which is equal to its reference. That means the total torque production is reduced by half.

The total torque measurement is taken from torque meter installed on shaft coupling the PM machine and dc machine. Following figure shows when inverter 2 is disabled and the enabled after 4.5 s; while the inverter 2 is disable, torque reference of inverter 2 becomes zero, torque reference of inverter 1 remains unchanged, and the total toque and speed of motor reduced by half.

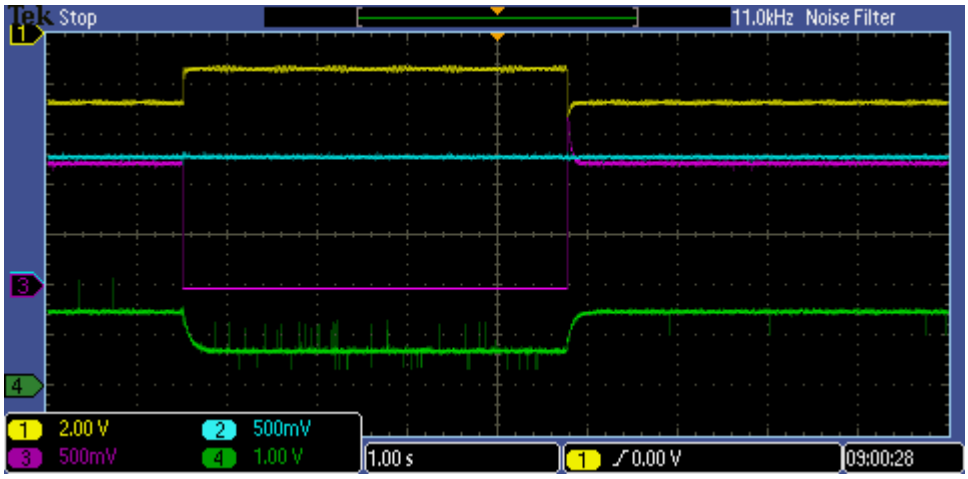

Figure 6-21 disabling and enabling of inverter 2, Measured Iq1 (probe2), Iq2 (probe3), shaft torque (probe1) and speed (probe4) [probe1 5Nm/1V or 5V/pu]

The shaft torque is set so that it negative for generator mode of dc machine or motor mode operation of PM machine. A closer look for transients is given Appendix D.

The Above case is not always true; it depends on structure of control used. For single synchronous rotating current control of six phase machine, even if one of the converts fails, the controller demands total reference torque in what so ever means the current is divided between the twice the pre fault current. These results in current imbalance problems even imbalances are recovered.

The second case which is interesting to see is that when one of the inverters fails whiles the six-phase PM machine is on speed control mode. It is obvious that speed controller is outer while is current (torque) is inner controller. When one of the inverters is disabled, the speed controller does not understand this; and as long as there is error between the reference and measured value, it tries to accumulate the discrepancies and force the converter to follow the reference command. Therefore, the speed controller makes sure that the speed is always at its reference value. The dc machine excitation is kept constant during disabling and enable of inverters. That means the dc machine delivers always delivers constant current as long as the speed is constant (constant back emf). In other word, both the speed and torque of the six phase machine will remain constant at steady state when one of the inverters is disabled. Therefore in order to keep the shaft toque constant in the current in one of the inverters has increase by fold of two. This case is shown by disabling and then enabling of inverter 1 as shown below; initially the generator was operating at reference speed of 0.3 pu(15Hz) speed, and delivering torque of 0.27 pu (7Nm) . Inverter 1 is disabled for 3 s.

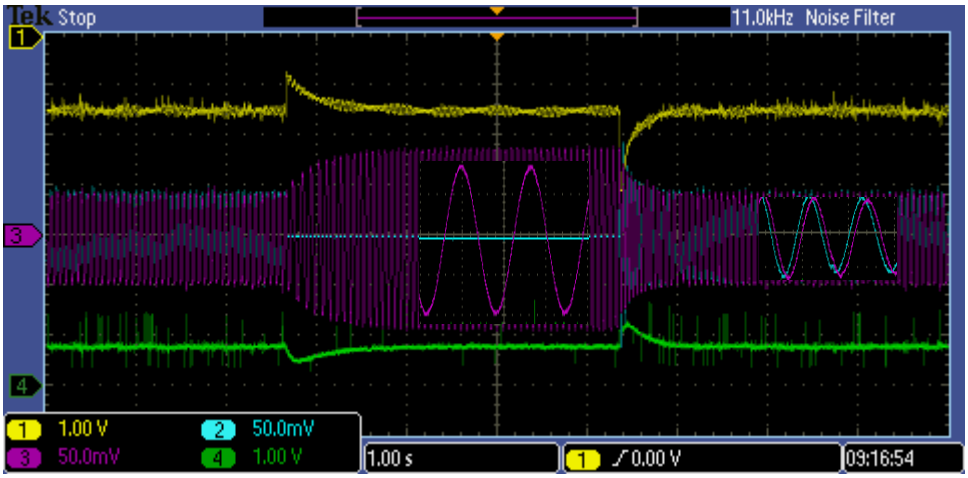

Figure 6-22 disabling of inverter 1 in speed control mode of drive; shaft torque (probe1), phase a stator current of inverter1 (probe2), phase x stator current inverter2 (probe3) & speed (probe4)

There is larger transient or overshoot in the current waveforms as it is reflected on the torque. This is the consequence of symmetric optimum criteria which allow considerable overshoot. But the response is fast enough. See appendix, zoomed in pictures around the disturbance

6.5 Generator Mode operation-Generator Control

In Generator mode operation, the six phase PM machine acts as a generator driven by the dc motor. From the control point of view both motor mode operation and generator mode operation. The only difference is the direction of power flow, power flows from the generator ac to dc. To damp this power a resistor is connected across the dc link.

The dc machine acts can be arranged to act as a constant current source or constant power source element based on how the armature windings are connected to dc source for a fixed excitation. For normal operation the back emf the dc motor is always very small compared to its nominal value since the nominal speed of the PM machine is 8 times smaller than the nominal speed of dc machine. Therefore, by connecting the armature of the dc machine to its nominal value (220V) through a large resistance (50 Ohm), the dc machine acts as a constant current source at fixed excitation for the PM machine. This can emulate the linear region of the power curve of wind turbine generator. The torque change can only be achieved by changing the excitation of the dc machine.

The normal behavior of dc motor can be achieved by connecting a variable dc source directly to the armature windings directly to armature terminals without large armature series resistor. The armature current at zero or low speed operation can be limited by a continuously changing the variable dc source manually.

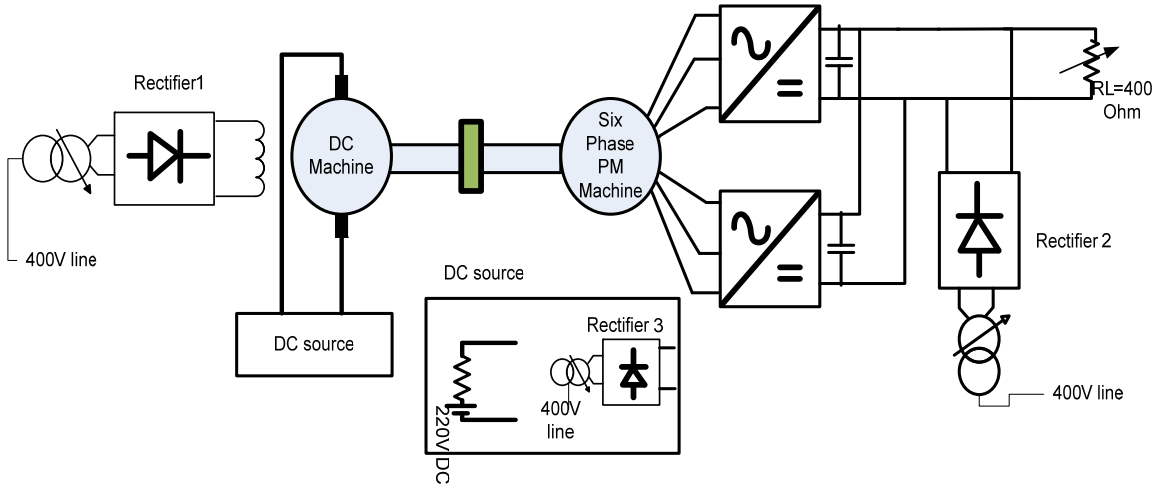

Figure 6-23 setup for generator mode control for a constant dc link voltage

The over view of the laboratory setup is as shown above. The dc link voltage is kept constant by the diode rectifier. A resistive load is connected across the dc link which draws constant power for a constant dc link voltage.

When the six -phase PM machine is at stand still the rectifier delivers full current/power to the load RL. And when the PM generator is operated power flows from the generator to converters; since the load consumes constant power at constant voltage, the rectifier reduces the power delivered to the load. When the power production of the generator increases, the

power production of the rectifier decreases. If generator power production increases above the point where the rectifier contributes nothing, the dc link voltage becomes no more constant. Therefore, the resistance RL is chosen to consume at least the rated power of the generator at rated current.

6.5.1. Speed Control Mode

As it is discussed above, the dc motor armatures are connected to 220V dc through a 50 Ohm armature series resistor, the motor acts as torque source. At constant speed operation is maintained by the converter, the only way to control the power transfer is by changing the input torque by varying the excitation of the dc machine.

To calculate the total power transfer from the two converters to the resistive load RL, the current from the output of the rectifier is measure. In the other way the power delivered by the generator is equal to the power saved by the Rectifier2. Following table shows when the excitation of the dc machine is varied from zero to full while the six-phase PMSG is maintained at 0.3 pu speed.

Table 6-3 Measured Generator torque and rectifier current –by varying dc excitation at 0.3 pu speed

Generator Torque	0.622	0.6	0.565	0.533	0.508	0.483	0.461	0.447	0.431	0.42
Rectifier2 Current	0.025	0	-0.05	-0.1	-0.15	-0.2	-0.25	-0.3	-0.35	-0.39

Similarly, for 0.5 pu speed operation and excitation change from zero to full is shown below

Table 6-4 Measured Generator Torque and rectifier current by varying excitation at 0.5 pu speed

Generator Torque	0.646	0.602	0.533	0.466	0.404	0.383	0.293	0.243	0.195	0.172
Rectifier2 Current	0.003	0	-0.05	-0.1	-0.15	-0.2	-0.25	-0.3	-0.35	-0.38

Both tests show that the current contribution from the rectifier decrease when the torque of the PM machine is increased (sign generator mode operation).

From the two tables the power contribution from the rectifier which is inversely proportional to the power delivered by the six-phase PMSG.

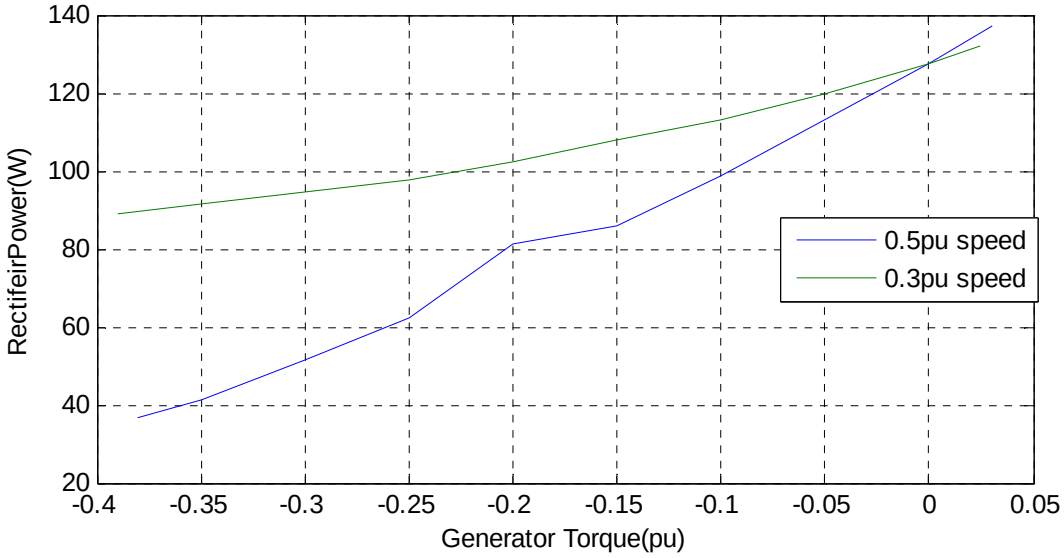

Figure 6-24 Power delivered by the rectifier to the Load

This emulates the linear range of the power curve of wind turbine.

6.5.2. Disabling of one Inverter

The system can operate successfully one one inverter is failed.

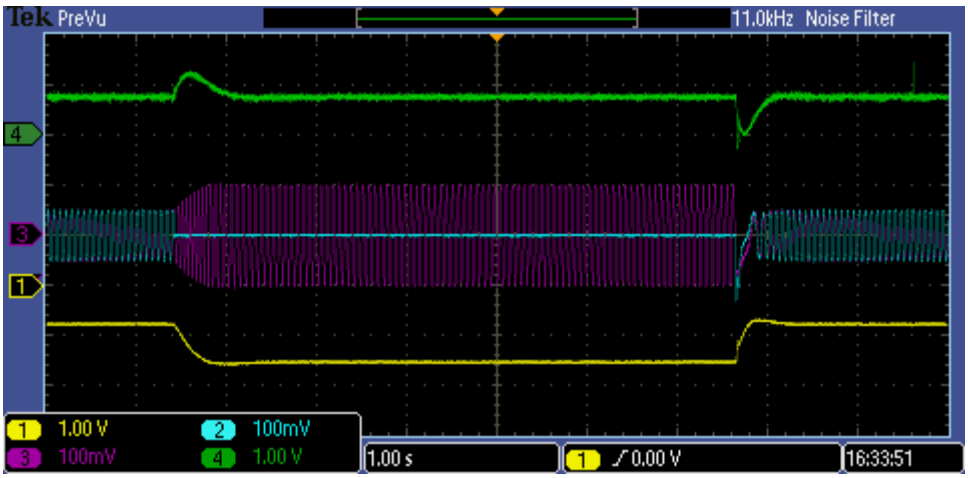

Figure 6-25 inverter 1 disabled, probe2 current a

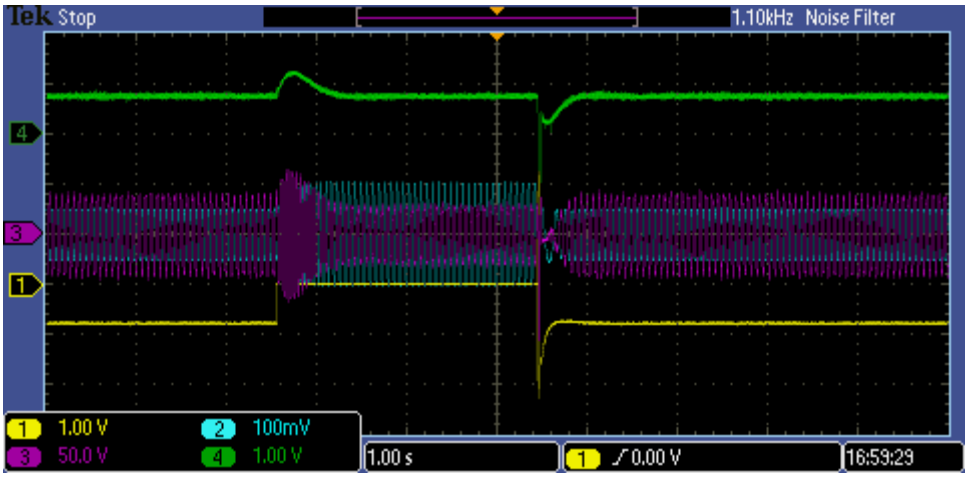

Figure 6-26 inverter 1 disable, probe2 current in the phase group 2

6.5.3. Torque Control Mode

When the dc motor operates as a constant torque, torque control mode is of no interest. Both the source and load as a constant torque operation results in either acceleration or stall of the generator. The generator accelerates when the reference torque, acts as load, is smaller than the dc motor torque and the generator stalls when the reference torque is of is larger.

Therefore, in order to have a continuous change is torque without acceleration or stalling the setup is modified by changing the supply of the dc motor to a variable voltage source (Rectifier3) and no series resistance. In this case, the dc motor acts as a constant power source.

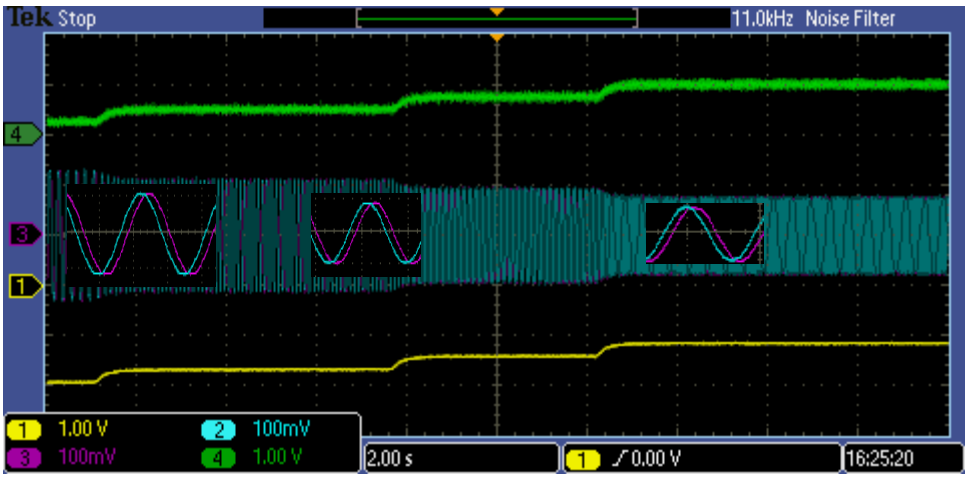

Figure 6-27 Measured shaft torque(probe1) , stator phase a current (probe2) , stator phase x current and speed (probe4) [probe1 5V/pu]

Decreasing the reference load torque increases the speed of the drive. Initially the dc motor is delivering power to the converter and has reached steady state. When the converter decreases its torque demand, the dc motor tends to accelerate which increases its back emf. This results in smaller armature current, since the back emf is comparable to the armature voltage. Then the dc motor reduces its torque. A close up near a the disturbance are shown in Appendix D

6.6 Generator Mode operation –DC voltage Control

In the case of grid connected wind turbine, there are two control strategies. The first strategy is when grid side converter controls the dc link and the machine side converter controls the generator. This is most common method. And the second strategy is when the machine side converter controls the dc link voltage and the grid side converter controls the generator power. Therefore, this control is studied for completeness, and show the capability of the proposed converter topology.

6.6.1. Performance of DC link Controller

Test case 1: changing the excitation of dc motor at constant dc link voltage control

Reference dc link voltage is set to 0.5 pu and the generator was operating at 0.43 u speed. The dc motor excitation increases from half excitation to full excitation.

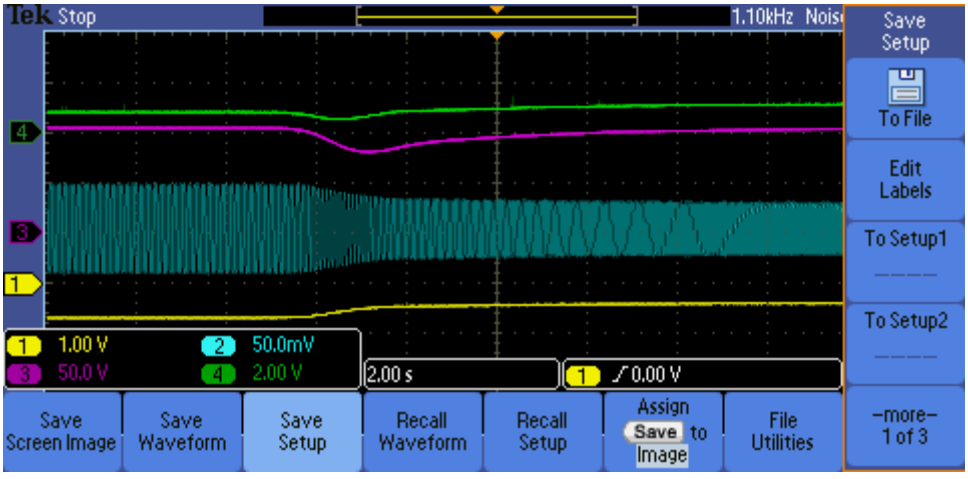

Figure 6-28 constant dc link variable load operation

The dc link voltage step change is also shown in figure below

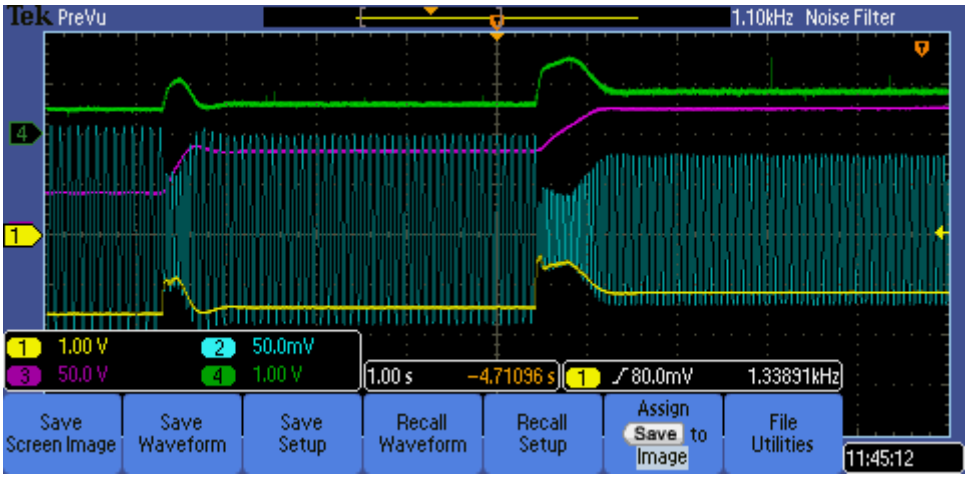

Figure 6-29 DC link voltage changes

7 Conclusion and Further work

Conclusion

Offshore wind energy system has to be lighter in weight, more compact in size and more reliable in operation. In this project, six phase permanent magnet synchronous generator-six leg converter system is proposed for offshore wind energy conversion system.

The optimal angle difference between the two three phase groups is 30 degree. The PM generator at hand was originally three phase machine. Rewinding of stator coils is done in order to obtain six phase machine with a separation angle between phase groups as close to 30 degree. And 33.2725 degree is the nearest angle which is possible to obtain in symmetrical systems of each phase group. This theoretical angle difference perfectly matches with that is tested in the laboratory.

Six phase PMSG having 33.2725 degree difference is modeled.

Design of vector control of six phase PMSG is developed using both a single synchronous rotating frame current control and dual synchronous rotating frame current control. For a single layer concentrated winding six phase PMSG, the coupling inductance is very small compared to self inductance. This makes the current and speed control loops same in both control strategies.

Vector control strategy, zero d axis control, is also tested when six phase machine operate as a Motor. Torque control and speed control operation is archived.

Vector control strategy, zero d axis control, is also tested when six phase machine operate as a generator. Torque control and speed control operation is archived. The linear part of the wind turbine power curve is emulated by making the dc machine constant torque source controlled by its excitation.

In wind energy system, the machine side converter has always not been used for generator speed or torque control. Dc link control using six phase converter is designed and implemented. Dc link voltage control was not as robust as speed control of generator. A very large disturbance may bring the system unstable.

All the currents, speed and dc link controller parameters which are designed and tested in MATLAB fits to the practical implementation values. This shows the assumptions and the approximations of the control loops are very close to the real system.

Both sinusoidal and space vector modulation is tested and compared. Space vector modulation of the two six phase converters has shown better dc link utilization but no superior advantages in terms of harmonic minimization.

The harmonic in the dc link current shows little improvement. This may be because of the poor generator design.

The disabling of one inverter is tested. And the system has shown good performance. This is a proof that the proposed configuration can improve the reliability of the system. The harmonic in the currents did not have considerable difference. This also shows that that concentrated winding generators has better fault tolerant capability.

Further works:

In this, project vector control strategy is achieved. In this short time it is not possible to investigate many detail characteristics. Having this as a foundation, the following points can be listed out for further work

- Implementation of actual drive trail and wind turbine model
- Implementation of sensor less vector control technique
- Investigating control strategy for fault tolerant operation
- Comparison with other control strategies (direct torque control or direct power control)
- Integrating with Grid and Comparing overall system performance
- Analyzing grid side fault and fault ride thorough capability

References:

[1] Wind Energy Association, "Wind energy-- the facts: a guide to the technology, economics and future of wind power" 2009

[2] World Wind Energy Report 2010 http://www.wwindea.org/home/images/stories/pdfs/worldwindenergyreport2010_s.pdf

[3] Z. Lubosny, "Wind Turbine Operation in Electric Power Systems" , 2003

[4] The European Wind Energy Association offshore fact sheet http://www.ewea.org/fileadmin/swf/factsheet/9_offshore.pdf

[5] D. D. Chase, H. C. Forbes, "Double Winding Generator Solves Breaker Problem", Electrical World, New York, N. Y., 1928, pp. 1183-86.

[6] Philip L. Alger, E. H. Freiburghouse, D. D. Chase, "Double Windings For Turbine Alternators", AIEE Transactions, vol. 49, Jan. 1930, pp. 226-44.

[7] R. Robert, J Dispaux and J. Dacier. "Improvement of Turbo Alternators Efficiency", Cigre Meeting, June 8-18, 1966.

[8] E. F. Fuchs, and L. T. Rosenberg, "Analysis of an alternator with two displaced stator windings," IEEE Transactions on Power Apparatus and Systems, Vol. 93, No. 6, pp. 1776-1786, 1974,

[9] R. H. Nelson, P. C. Krause, "Induction machine analysis for arbitrary displacement between multiple winding sets", IEEE Transactions on Power Apparatus and Systems, Vol. PAS-93, pp. 841-848, 1974

[10] Thomas Marin Jahns, "Improved Reliability In Solid State Drives For Large Asynchronous AC Machine By Means of Multiple Independent Phase Drive Units" Ph.D. dissertation, MIT, VOL I. April 1978

[11] R. F. Schiferl, C. M. Ong., "Six-phase synchronous machine with AC and DC stator connection part I: equivalent circuit representation and steady-state analysis", IEEE Transactions on Power Apparatus and Systems, Vol. PAS-102, No. 8, August 1983.

[12] R.F. Schiferl, C. M. Ong , "Six Phase Synchronous Machine with AC and DC Stator Connections - I I: Harmonic Studies and Proposed Uninterruptable Power Supply

Scheme," IEEE Transactions on Power Apparatus and Systems, Vol. PAS 102, No. 8, pp. 2694-2693 ,August 1983.

[13] M. Abbas, R. Christen, and T. Jahns, “Six-phase voltage source inverter driven induction motor”, Conference record of 18 th annual meeting of IEEE industry application society, pp. 503-511, 1983.

[14] L. Parsa, “On advantages of multi-phase machines,” IEEE 2005, pp. 1574-1579

[15] Levi, E. “Multiphase Electric Machines for Variable-Speed Applications”, Industrial Electronics, IEEE Transactions on pp. 1893 - 1909 , Vol. 55 , May 5, 2008.

[16] D. Vizireanu, S. Brisset, X. Kestelyn, P. Borchet, Y. Milet, and D. Laloy, “Investigation on multi-star structures for large power direct-drive wind generator,” Electr. Power Compon. Syst., Vol. 35, No. 2, pp. 135–152, 2007.

[17] Sheng-Nian Yeh, Jonq-Chin Hwang, Ming-Chih Hsieh, Li-Hsiu Chen “Development of Wind Power Control System for Six-Phase Permanent-Magnet Synchronous Generators”

[18] Janne Kinnunen, “Direct-On-Line Axial Flux Permanent Magnet Synchronous Generator Static and Dynamic Performance”, Ph.D. dissertation, Lappeenranta University of Technology, November 2007.

[19] Jan Machowski, Janusz W. Bialek, James R. Bumby, “Power System Dynamics stability and control” second Edition,2008

[20] N. Mohan, “Electric Drives An Integrative Approach”, Edition 2003

[21] Mohan, N., T.M. Undeland, and W.P. Robbins, “Power Electronics: Converters, Applications, and Design”, John Wiley & Sons, Inc., New York, 1995

[22] John A. Houldsworth, Duncan A. Grant, “The Use of Harmonic Distortion to Increase the Output Voltage of a Three-Phase PWM Inverter”, IEEE Transactions on Industry Applications, Vol. Ia-20, No. 5, Pp. 1224-1228, September/October 1984

[23] Van der Broeck, Skudelny, H.C., Stanke, G.: “Analysis and Realisation of a Pulse Width Modulator Based on Voltage Space Vectors”, Conf.Rec. 1986 Annual Meeting IEEE-IAS, Denver/USA, pp. 244-251.

[24] Jin-Woo Jung, “ PROJECT #2 SPACE VECTOR PWM INVERTER”, Mechatronic Systems Laboratory Department Of Electrical And Computer Engineering, The Ohio State University, February 2005.

[25] Wei-Feng Zhang, Yue-Hui Yu, “Comparison of Three SVPWM Strategies” Journal Of Electronic Science And Technology Of China, Vol. 5, No. 3, September 2007 Pp. 283-287

[26] Yifan Zhao, A. Lipo, “Space vector PWM control of Dual Three Phase Induction Machine using vector space decomposition”, IEEE Trans. Industry Applications Vol 31 No 5,pp. 1100-1109, Oct 1995

[27] Yanhui He, Yue Wang, Jinlong Wu, Yupeng Feng, Jinjun Liu “A Comparative Study of Space Vector PWM Strategy for Dual Three-Phase Permanent-Magnet Synchronous Motor Drives” IEEE 2010, pp 915-919

[28] R Krishnan, “Permanent Magnet Synchronous and Brushless DC Motor Drives”, CRC Press 2010

[29] Jeffrey W. Umland, Mohammed Safiuddin , “Magnitude and Symmetric Optimum Criterion for the Design of Linear Control Systems What is it and how does it compare with the others?”, IEEE 1988, pp. 1796-1802

[30] T. Sebastain, G.R. Slemon, “Transient Modeling and Performance of Variable-Speed Permanent Magnet Motors”,IEEE Transactions On Industry Applications, Vol.25, No.1 pp. 101-106, January/February 1989

[31] Kjell Ljøkelsøy , Library of IP modules, building blocks for FPGA based converter control system, 2010-06-14.

[32] Ljokelsoy, K., Kolstad H, “Application note -20 kW IGBT omformer. Beskrivelse ” Sintef Enegiforskning AS,Trondheim, Norway, 2002

[33] Datasheet - http://www.lem.com/docs/products/la%20205-t%20sp16.pdf

[34] Datasheet-http://www.lem.com/docs/products/lv%2025-600%20sp2.pdf

[35] DRIVECOM Nutzergruppe e.V, ” DRIVECOM-Profile Drive Engineering 22” 26 May 1995

[36] ActiveDSP A/s,” ActiveDSP - User Manual A TOOL FOR REAL TIME MONITORING, OPERATION AND MAINTENANCE OF EMBEDDED SYSTEMS”, 2008

Appendix

A. Transformation Matrices

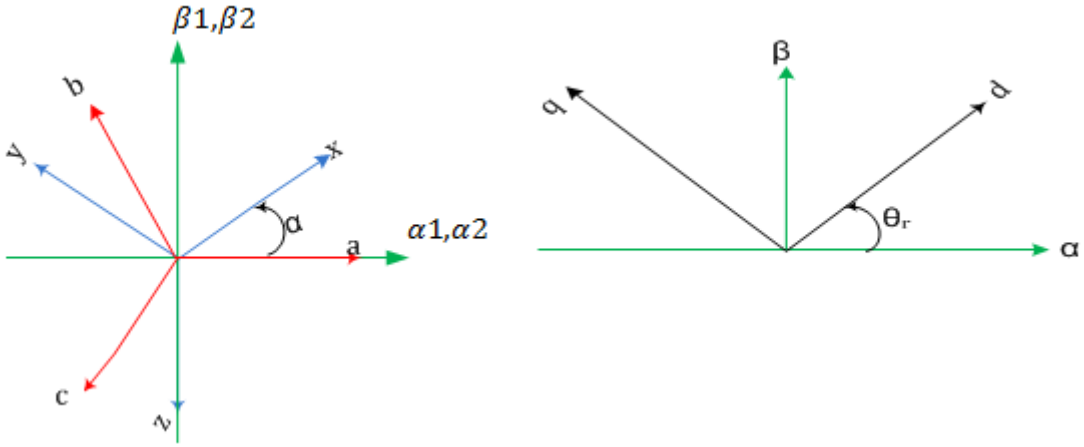

Figure A- 1 phase, stationary and rotating reference frames

Clarke Transformation-the voltage invariant park transformation T_3

$$[T_3] = \frac{2}{3}\begin{bmatrix} 1 & -1/2 & -1/2 \\ 0 & \sqrt{3}/2 & -\sqrt{3}/2 \\ 1/2 & 1/2 & 1/2 \end{bmatrix} \qquad (A1.1)$$

$$\begin{bmatrix} w_{\alpha 1} \\ w_{\beta 1} \\ w_{o1} \end{bmatrix} = [T_3]\begin{bmatrix} w_a \\ w_b \\ w_c \end{bmatrix}$$

Inverse Clarke

$$[T_3]^T = \begin{bmatrix} 1 & 0 & 1 \\ -1/2 & \sqrt{3}/2 & 1 \\ -1/2 & -\sqrt{3}/2 & 1 \end{bmatrix} \qquad (A1.2)$$

$$\begin{bmatrix} w_a \\ w_b \\ w_c \end{bmatrix} = [T_3]^T \begin{bmatrix} w_{\alpha 1} \\ w_{\beta 1} \\ w_{o1} \end{bmatrix}$$

Modified Clarke transformation

$$[T_{3M}] = \frac{2}{3}\begin{bmatrix} \cos\alpha & \cos(\alpha+120) & \cos(\alpha+240) \\ \sin\alpha & \sin(\alpha+120) & \sin(\alpha+240) \\ 1/2 & 1/2 & 1/2 \end{bmatrix} \qquad (A1.3)$$

$$\begin{bmatrix} w_a \\ w_b \\ w_c \end{bmatrix} = [T_{3M}]\begin{bmatrix} w_{\alpha 1} \\ w_{\beta 1} \\ w_{o1} \end{bmatrix}$$

Inverse Modified Clarke transformation

$$[T_{3M}]^T = \frac{2}{3}\begin{bmatrix} cos\ \alpha & sin\,\alpha & 1 \\ cos\,(\alpha+120) & sin\,(\alpha+120) & 1 \\ cos\,(\alpha+240) & sin\,(\alpha+240) & 1 \end{bmatrix}$$

$$\begin{bmatrix} w_a \\ w_b \\ w_c \end{bmatrix} = [T_{3M}]^T \begin{bmatrix} w_{\alpha 1} \\ w_{\beta 1} \\ w_{o1} \end{bmatrix} \qquad \textit{(A1.4)}$$

Park Transformation-Rotating Transformation

$$[\mathrm{T_r}] = \begin{bmatrix} cos\theta_r & sin\theta_r \\ -sin\theta_r & cos\theta_r \end{bmatrix}$$

$$\begin{bmatrix} w_d \\ w_q \end{bmatrix} = [\mathrm{T_r}] \begin{bmatrix} w_\alpha \\ w_\beta \end{bmatrix} \qquad \textit{(A1.5)}$$

Inverse Park-Inverse rotating Transformation

$$[\mathrm{T_r}]^{\mathrm{T}} = \begin{bmatrix} cos\theta_r & -sin\theta_r \\ sin\theta_r & cos\theta_r \end{bmatrix}$$

$$\begin{bmatrix} w_\alpha \\ w_\beta \end{bmatrix} = [\mathrm{T_r}]^{\mathrm{T}} \begin{bmatrix} w_d \\ w_q \end{bmatrix} \qquad \textit{(A1.6)}$$

Six phase Transformation

$$[T_6] = \frac{1}{3}\begin{bmatrix} 1 & cos\,4\alpha & cos\,8\alpha & cos\,\alpha & cos\,5\alpha & cos\,9\alpha \\ 0 & sin\,4\alpha & sin\,8\alpha & sin\,\alpha & sin\,5\alpha & sin\,9\alpha \\ 1 & cos\,8\alpha & cos\,4\alpha & cos\,5\alpha & cos\,\alpha & cos\,9\alpha \\ 0 & sin\,8\alpha & sin\,4\alpha & sin\,5\alpha & sin\,\alpha & sin\,9\alpha \\ 1 & 1 & 1 & 0 & 0 & 0 \\ 0 & 0 & 0 & 1 & 1 & 1 \end{bmatrix} \qquad \textit{(A1.7)}$$

$$[\mathrm{T_6}]^{-1} = [\mathrm{T_6}]^{\mathrm{T}}$$

Twelve phase two phase real component transformation is $[\mathrm{T_{12}}]$ -power invariant

$$[T_{12}] = \frac{2}{\sqrt{12}}\begin{bmatrix} \frac{\sqrt{2}}{2} & \frac{\sqrt{2}}{2} & \frac{\sqrt{2}}{2} & \frac{\sqrt{2}}{2} & \frac{\sqrt{2}}{2} & \frac{\sqrt{2}}{2} & \frac{\sqrt{2}}{2} & \frac{\sqrt{2}}{2} & \frac{\sqrt{2}}{2} & \frac{\sqrt{2}}{2} & \frac{\sqrt{2}}{2} & \frac{\sqrt{2}}{2} \\ 1 & cos\alpha & cos2\alpha & cos3\alpha & cos4\alpha & cos5\alpha & -1 & cos7\alpha & cos8\alpha & cos9\alpha & cos10\alpha & cos11\alpha \\ 1 & cos2\alpha & cos4\alpha & cos6\alpha & cos8\alpha & cos10\alpha & 1 & cos2\alpha & cos4\alpha & cos6\alpha & cos8\alpha & cos10\alpha \\ 1 & cos3\alpha & cos6\alpha & cos9\alpha & cos12\alpha & cos3\alpha & -1 & cos9\alpha & cos12\alpha & cos3\alpha & cos6\alpha & cos9\alpha \\ 1 & cos4\alpha & cos8\alpha & cos12\alpha & cos4\alpha & cos8\alpha & 1 & cos4\alpha & cos8\alpha & cos12\alpha & cos4\alpha & cos8\alpha \\ 1 & cos5\alpha & cos10\alpha & cos3\alpha & cos8\alpha & cos\alpha & -1 & cos11\alpha & cos4\alpha & cos9\alpha & cos2\alpha & cos7\alpha \\ \frac{\sqrt{2}}{2} & -\frac{\sqrt{2}}{2} & \frac{\sqrt{2}}{2} & -\frac{\sqrt{2}}{2} & \frac{\sqrt{2}}{2} & -\frac{\sqrt{2}}{2} & \frac{\sqrt{2}}{2} & -\frac{\sqrt{2}}{2} & \frac{\sqrt{2}}{2} & -\frac{\sqrt{2}}{2} & \frac{\sqrt{2}}{2} & -\frac{\sqrt{2}}{2} \\ 0 & sin5\alpha & sin10\alpha & sin3\alpha & sin8\alpha & sin\alpha & 0 & sin11\alpha & sin4\alpha & sin9\alpha & sin2\alpha & sin7\alpha \\ 0 & sin4\alpha & sin8\alpha & sin12\alpha & sin4\alpha & sin10\alpha & 0 & sin4\alpha & sin8\alpha & sin12\alpha & sin4\alpha & sin8\alpha \\ 0 & sin3\alpha & sin6\alpha & sin9\alpha & sin12\alpha & sin3\alpha & 0 & sin9\alpha & sin12\alpha & sin3\alpha & sin6\alpha & sin9\alpha \\ 0 & sin2\alpha & sin4\alpha & sin6\alpha & sin8\alpha & sin10\alpha & 0 & sin2\alpha & sin4\alpha & sin6\alpha & sin8\alpha & sin10\alpha \\ 0 & sin\alpha & sin2\alpha & sin3\alpha & sin4\alpha & sin5\alpha & 0 & sin7\alpha & sin7\alpha & sin7\alpha & sin10\alpha & sin11\alpha \end{bmatrix}$$

B. Per Unit system

In this work, all quantities except time and angle are scaled to a common system. The scaling factors are based on three quantities: No load terminal voltage(E_n), nominal stator current (I_n) and nominal stator frequency of the PMSG.

Physical quantity	Base quantity	Per unit quantity
Voltage (V)	$V_b = \frac{\sqrt{2}}{\sqrt{3}} E_n$	$v = \frac{V}{V_b}$
Current (I)	$I_b = \sqrt{2} I_n$	$i = \frac{\mathrm{I}}{I_b}$
Resistance (R), Reactance (X), Inductance (L)	$Z_b = \frac{V_b}{I_b}$	$r = \frac{R}{Z_b}, x = \frac{X}{Z_b}, l = \frac{L}{Z_b}$
Frequency (f)	$f_b = f_n$	$n = \frac{f}{f_b}$
Angular Speed(ω_r)	$\omega_b = 2\pi f_b$	$n = \frac{\omega_r}{\omega_b}$
Mechanical Speed(N)	$N_b = 60\frac{f_n}{p}$	$n = \frac{N}{N_b}$
Power ($S\ in\ VA$)	$S_b = 6 V_b I_b$	$s = \frac{S}{S_b}$
Torque (M)	$M_b = \frac{\mathrm{P}}{2}\frac{S_b}{\omega_b}$	$m = \frac{M}{M_b}$
Flux Linkages(λ)	$\lambda_b = \frac{V_b}{\omega_b}$	$\psi = \frac{\lambda}{\lambda_b}$

Since the transformation used in this work is voltage invariant, the base system in the three phase system and two phase system (α, β) &(d, q)are same except the power.

$$V_b{}^2 = V_d{}^2 + V_q{}^2$$

$$I_b{}^2 = I_d{}^2 + I_q{}^2$$

The base value for the DC link voltage is taken to be two times the base value of the AC Voltage, $V_{DC\_b} = 2V_b$.

The base value for the DC link current can be derived from the power balance.

$$P = V_{DC}I_{DC} = 6VIcos\varphi = 2\frac{3}{2}(V_dI_d + V_qI_q)$$

In the case of $I_d = 0$ control,

$$P = V_{DC}I_{DC} = 6VIcos\varphi = 2\frac{3}{2}(V_qI_q)$$

Then the DC link current base value becomes,

$$I_{DC\_b} = \frac{6V_bI_bcos\varphi_b}{V_{DC\_b}} = 2\frac{3}{2}\left(\frac{V_{q\_b}I_{q\_b}}{V_{DC\_b}}\right) = 2\frac{3}{2}\left(\frac{V_bI_b}{2V_b}\right) = \frac{3}{2}I_b$$

$$I_{DC1\_b} = I_{DC2\_b} = \frac{3}{4}I_b$$

Generator Model in Per Unit system

Six phase PMSG Model as two three phase PMSG using dual synchronous rotating frame

$$v_{d1} = r_si_{d1} + l_d\frac{di_{d1}}{dt} - n \cdot x_q \cdot i_{q1}$$
$$v_{q1} = r_si_{q1} + l_q\frac{di_{q1}}{dt} + n \cdot x_d \cdot i_{d1} + n \cdot \psi_m \quad \textit{(A1.8)}$$

$$v_{d2} = r_si_{d2} + l_d\frac{di_{d2}}{dt} - n \cdot x_q \cdot i_{q2}$$
$$v_{q2} = r_si_{q2} + l_q\frac{di_{q2}}{dt} + n \cdot x_d \cdot i_{d2} + n \cdot \psi_m \quad \textit{(A1.9)}$$

$$\mathrm{m_e} = \frac{1}{2}\psi_m(i_{q1} + i_{q2}) \quad \textit{(A1.10)}$$

Or

$$\mathrm{m_e} = \frac{1}{2}\left(i_{q1} + i_{q2}\right)$$

$\psi_m = 1$ - Since the base voltage is taken to be the back emf and the permanent magnet at it rated value and is not demagnetized.

When the six-phase PMSG Model as using single synchronous rotating frame or vector space decomposition, $l_d \frac{di_{d1}}{dt}$

$$v_d = r_s i_d + l_s \frac{di_d}{dt} - n \cdot x_s \cdot i_q$$

$$v_q = r_s i_q + l_s \frac{di_q}{dt} + n \cdot x_s \cdot i_d + n \cdot \psi_m$$

$$v_{x^-} = r_s i_{x^-} + l_s \frac{di_{x^-}}{dt} - n \cdot x_s \cdot i_{y^-}$$

$$v_{y^-} = r_s i_{y^-} + l_s \frac{di_{y^-}}{dt} + n \cdot x_s \cdot i_{x^-} \qquad \textit{(A1.11)}$$

$$v_{z1^-} = r_s i_{z1^-} + l_s \frac{di_{z1^-}}{dt} - n \cdot x_s \cdot i_{z2^-}$$

$$v_{z2^-} = r_s i_{z2^-} + l_s \frac{di_{z2^-}}{dt} + n \cdot x_s \cdot i_{z1^-}$$

$$\mathrm{m_e} = \psi_m \cdot i_q = i_q \qquad \textit{(A1.12)}$$

$\psi_m = 1$ - Since the base voltage is taken to be the back emf and the permanent magnet at it rated value and not demagnetized.

DC link Model in per unit

The base system for the DC link are based on the base DC voltage and base DC current.

Physical quantity	Base quantity	Per unit quantity
DC link Voltage (V_{dc})	$V_{DC_b} = 2V_b$	$v_{dc} = \frac{V_{dc}}{V_{DC_b}}$
DC link Current (I_{dc})	$I_{DC_b} = \frac{3}{2} I_b$	$i_{dc} = \frac{I_{dc}}{I_{DC_b}}$
Resistance (R), Capacitance (C),	$Z_{DC_b} = \frac{V_{DC_b}}{I_{DC_b}}$	$r = \frac{R}{Z_{DC_b}}, c = \frac{1}{\omega_b C \cdot Z_{DC_b}}$

Using the above base, the dc link model becomes

$$i_c = i_{dc} - i_L$$

$$i_c = c\frac{dv_{dc}}{dt}, \qquad \textit{(A1.13)}$$

$$i_L = \frac{v_{dc}}{r}$$

For $I_d = 0$ control, the power balance equation,

$$i_{dc} = \frac{v_q}{v_{dc}} i_q \qquad \textit{(A1.14)}$$

C. Modulation

Vector space decomposition, active and zero vector selection

Sector 1: 45, 41, 9, 11 63

	z	y	x	c	b	a
T_0	1	1	1	1	1	1
T_1	1	0	1	1	0	1
T_2	1	0	1	0	0	1
T_3	0	0	1	0	0	1
T_4	0	0	1	0	1	1

Sector 2: 41, 9, 11, 27 56

	z	y	x	c	b	a
T_0	1	1	1	0	0	0
T_1	1	0	1	0	0	1
T_2	0	0	1	0	0	1
T_3	0	0	1	0	1	1
T_4	0	1	1	0	1	1

Sector 3: 9, 11, 27, 26 0

	z	y	x	c	b	a
T_0	0	0	0	0	0	0
T_1	0	0	1	0	0	1
T_2	0	0	1	0	1	1
T_3	0	1	1	0	1	1
T_4	0	1	1	0	1	0

Sector 4: 11, 27, 26, 18 07

	z	y	x	c	b	a
T_0	0	0	0	1	1	1
T_1	0	0	1	0	1	1
T_2	0	1	1	0	1	1
T_3	0	1	1	0	1	0
T_4	0	1	0	0	1	0

Sector 5: 27, 26, 18, 22 63

	z	y	x	C	b	a
T_0	1	1	1	1	1	1
T_1	0	1	1	0	1	1
T_2	0	1	1	0	1	0
T_3	0	1	0	0	1	0
T_4	0	1	0	1	1	0

Sector 6: 26, 18, 22, 54 56

	z	y	x	c	b	a
T_0	1	1	1	0	0	0
T_1	0	1	1	0	1	0
T_2	0	1	0	0	1	0
T_3	0	1	0	1	1	0
T_4	1	1	0	1	1	0

Sector 7: 18, 22, 54, 52 0

	z	y	x	c	b	a
T_0	0	0	0	0	0	0
T_1	0	1	0	0	1	0
T_2	0	1	0	1	1	0
T_3	1	1	0	1	1	0
T_4	1	1	0	1	0	0

Sector 8: 22, 54, 52, 36 07

	z	y	x	c	b	a
T_0	0	0	0	1	1	1
T_1	0	1	0	1	1	0
T_2	1	1	0	1	1	0
T_3	1	1	0	1	0	0
T_4	1	0	0	1	0	0

Sector 9: 54, 52, 36, 37 63

	z	y	x	c	b	a
T_0	1	1	1	1	1	1
T_1	1	1	0	1	1	0
T_2	1	1	0	1	0	0
T_3	1	0	0	1	0	0
T_4	1	0	0	1	0	1

Sector 11: 36, 37, 45, 41 56

	z	y	x	c	b	a
T_0	0	0	0	0	0	0
T_1	1	0	0	1	0	0
T_2	1	0	0	1	0	1
T_3	1	0	1	1	0	1
T_4	1	0	1	0	0	1

Sector 10: 52, 36, 37, 45 56

	z	y	x	c	b	a
T_0	1	1	1	0	0	0
T_1	1	1	0	1	0	0
T_2	1	0	0	1	0	0
T_3	1	0	0	1	0	1
T_4	1	0	1	1	0	1

Sector 12: 37, 45, 41, 9 07

	z	y	x	c	b	a
T_0	0	0	0	1	1	1
T_1	1	0	0	1	0	1
T_2	1	0	1	1	0	1
T_3	1	0	1	0	0	1
T_4	0	0	1	0	0	1

D. Motor Mode Operation of 6 Phase PMSG

Stator current transients at step change of torque (of magnitude 0.5 up or from 0 to 12 Nm)

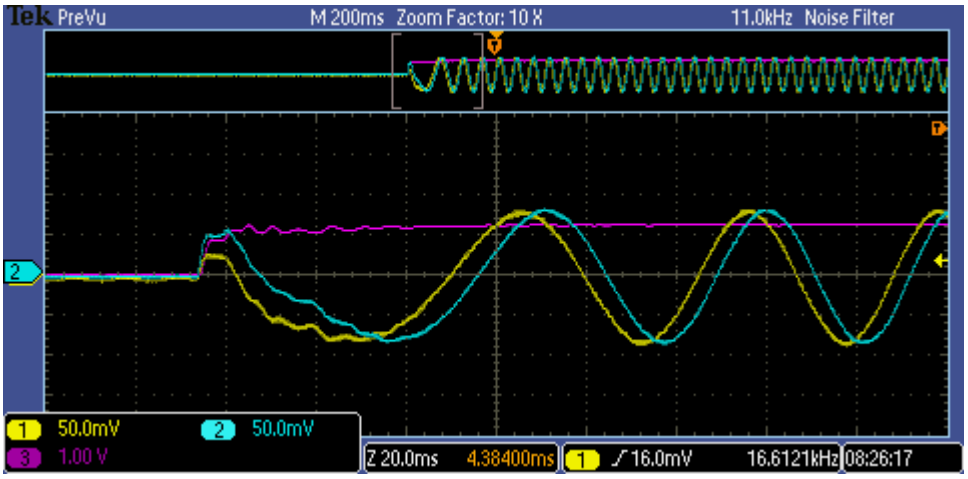

Figure A 1 Step Torque Response and Transient Currents in phase a(probe3), and phase x(probe2)

Changing from speed control mode to speed control mode transients

Initially the motor 0.2 pu control mode in torque mode, then control is changed to speed control mode with speed set value of 0.4 pu;

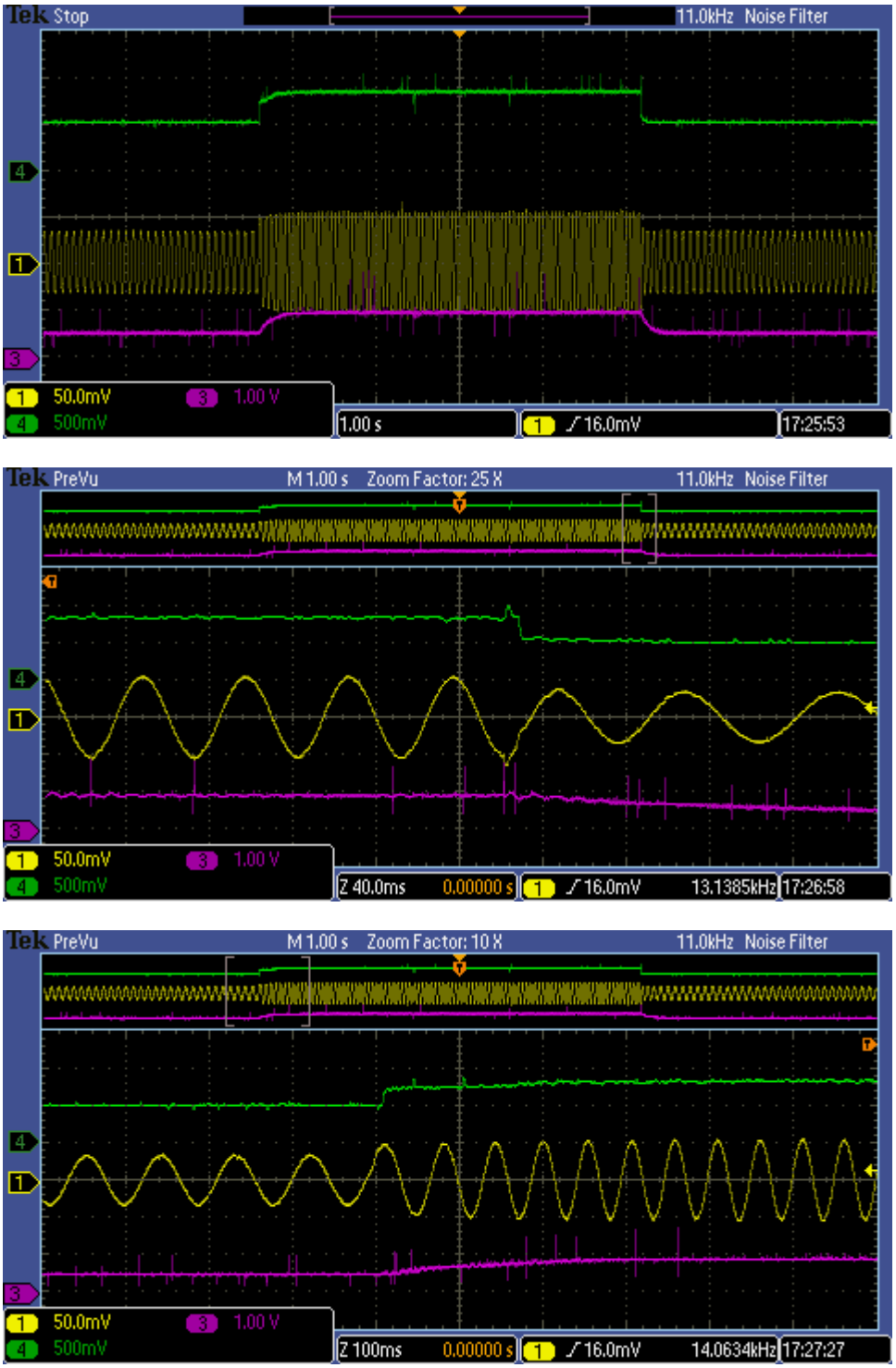

Figure A 1 Stator Current Transients to a change from torrque control to speed control mode

Constant speed variable load operation

The first excition is change from zero to half, and second the excitation is changed from zero to full and to half then to zero at constant speed of 0.5 pu operation of the drive

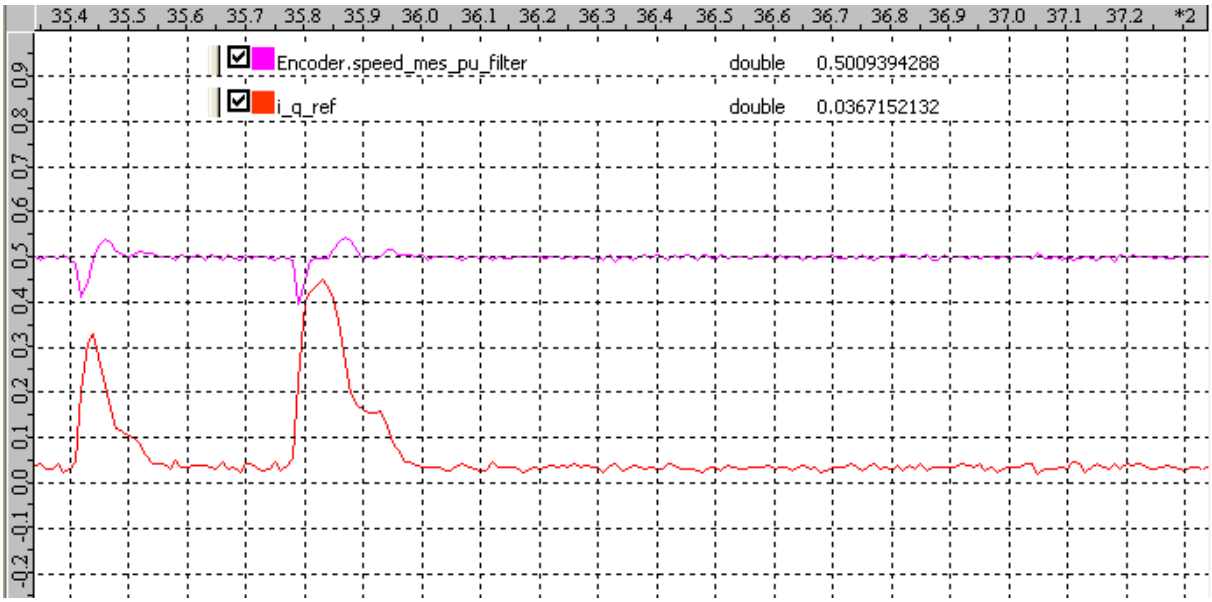

Figure A 2 encoder speed and torque (red)-at constant speed and variable exitaiton operation

Disabling one inverter in Torque control Mode

First the Motor is operating in torque control mode, torque of 0.5 pu and speed of 0.59 pu

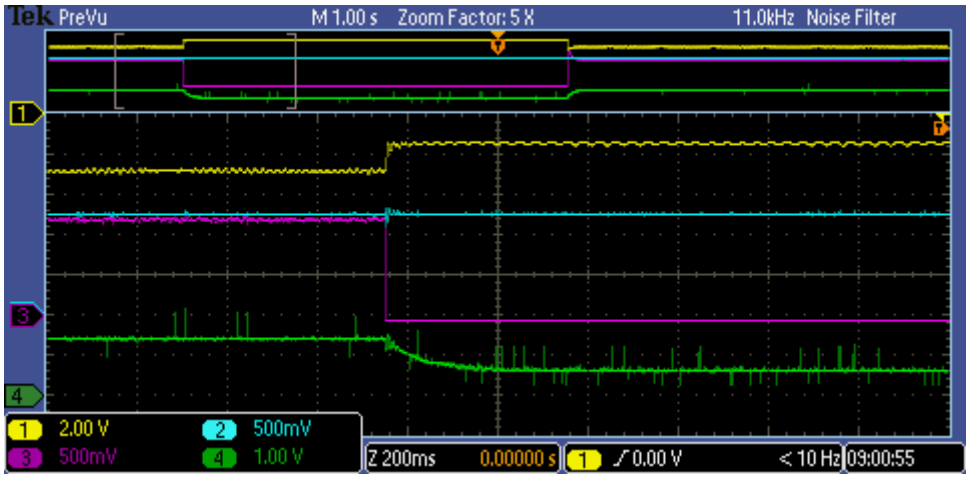

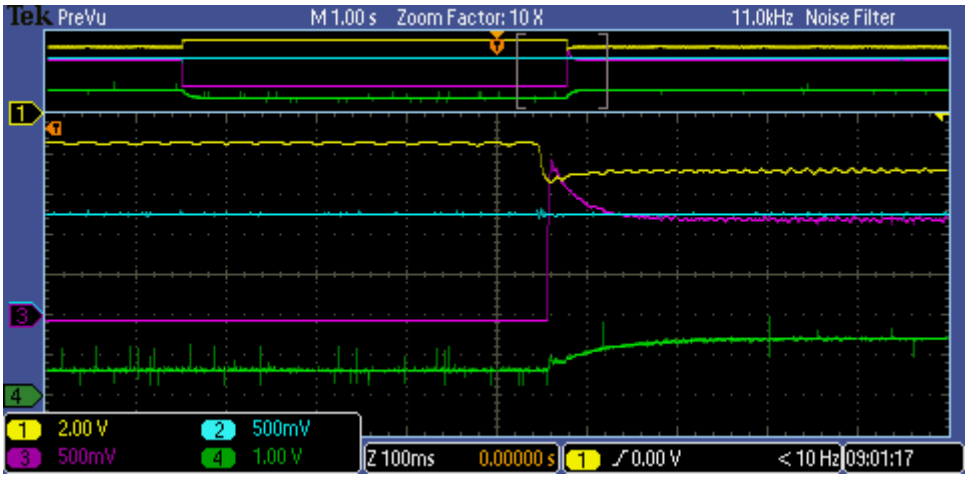

Figure A 3 Transients in speed and Torque when inverter 1 is disabled

Disabling one inverter in speed control mode

Initially the PM machine was running at reference 0.3 pu speed and load torque of 0.27 pu(7NM) torque, then inverter 1 is disable and enabled

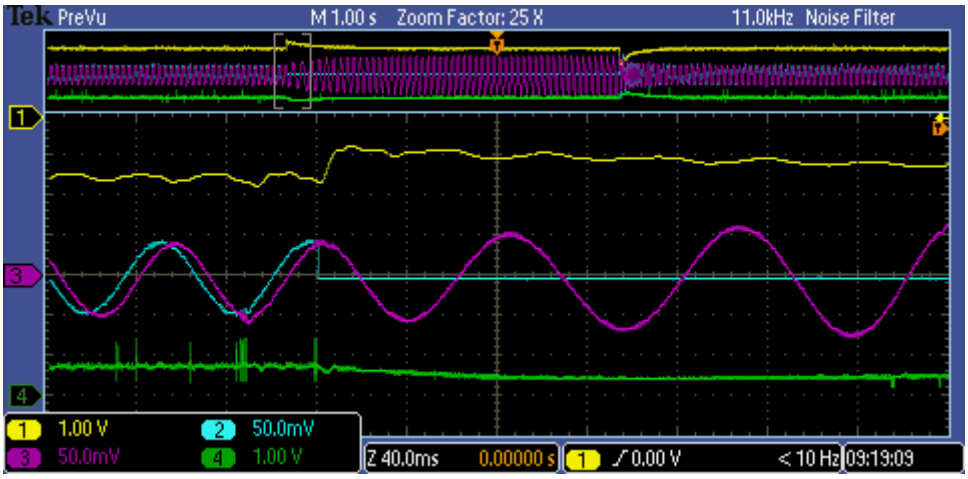

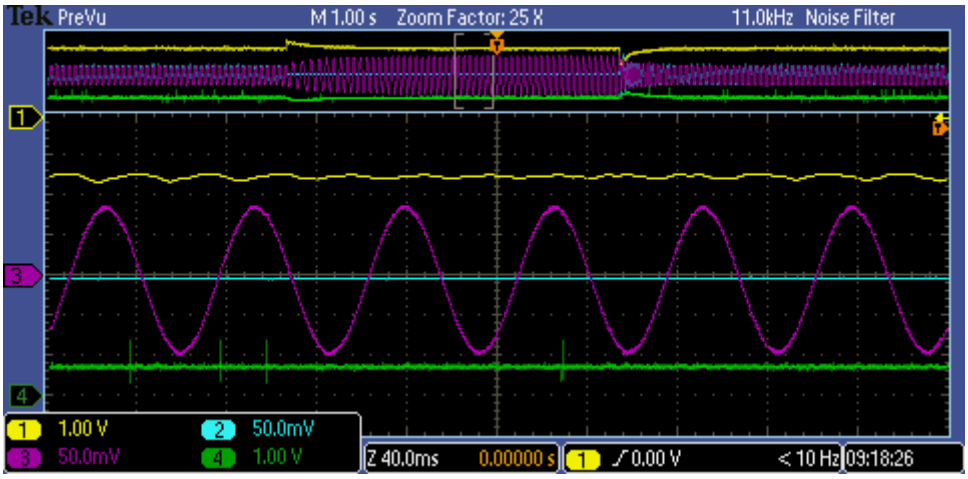

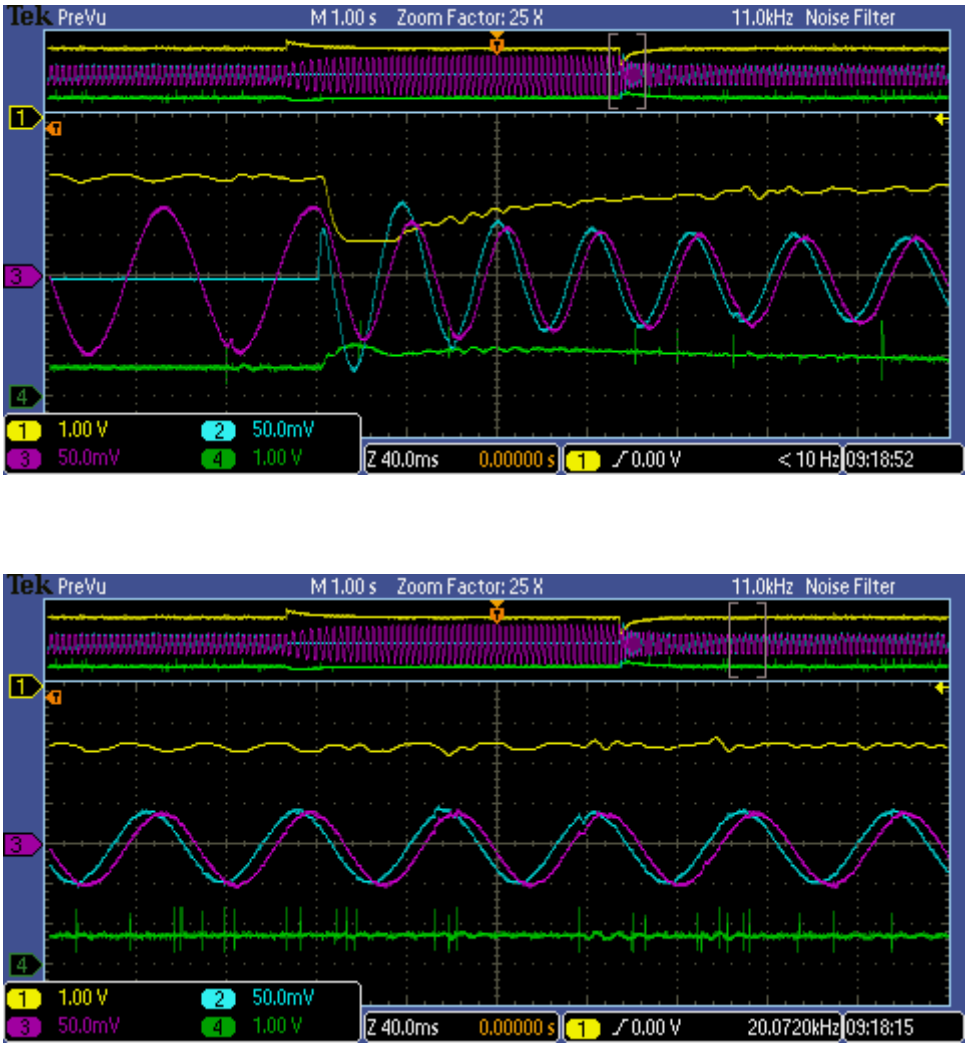

Figure A 4 Disabling of inverter 1 while drive is in speed control mode

E. Generator Mode operation of 6 Phase PMSG

F. Mathlab Codes

Matlab code for current open loop

```
Ts=0.0002;% Sampling Time

Ti=0.008235;
Tv=0.0001;
Tf=0.001;
Kpp=3.4313;
Tprod=Tv*Tv*Ti*Ti*Tf;
num=Kpp*Ti/Tprod*[1 1/Ti];
denum=poly([-1/Tv -1/Tv -1/Tf -1/Ti 0]);
bd=tf(num, denum);
figure(1)
bode(bd)
num2=[3.4313/(Ti*(Tf+2*Tv))];
denum2=poly([0 -1/(Tf+2*Tv)]);
bd2=tf(num2, denum2);
figure(2)
%bode(bd2)

gd = c2d(bd2, Ts)
bode(bd2,'r',gd,'b--')
```

Matlab code for Speed open loop

```
Jeq=0.005;
Tiw=0.01877;
Tieq=0.0024;
Td=0.00002;
Twsum=0.004694;
Tf=0.00227;
Kpw=0.5;
Ts=0.0002; % sampling Time
Tprod=Tiw*Tieq*Tf*Jeq*Td;
num=Kpw*Tiw/Tprod*[1 1/Tiw];
denum=poly([-1/Td -1/Tieq -1/Tf 0 0]);
bd=tf(num, denum);
figure(1)
bode(bd)
num2=Kpw*Tiw/(Ti*Twsum*Jeq)*[1 1/Tiw];
denum2=poly([0  0 -1/(Twsum)]);
bd2=tf(num2, denum2);
figure(2)
%bode(bd2)

gd = c2d(bd2,0.0002)
bode(bd2,'r',gd,'b--')
```

Matlab code for voltage control loop

```
Kpv=0.7;
c=0.0033;%3300uF
Tiv=0.00976;
Tieq=0.0024;
Tdv=0.00002;
Tvsum=0.00244;
Tfv=0.00002;

Tprod=Tiv*Tieq*Tfv*c*Tdv;
num=Kpv*Tiv/Tprod*[1 1/Tiv];
denum=poly([-1/Tdv -1/Tieq -1/Tfv 0 0]);
bd=tf(num, denum);
figure(1)
bode(bd)
num2=Kpv*Tiv/(Tiv*Tvsum*c)*[1 1/Tiv];
denum2=poly([0  0 -1/(Tvsum)]);
bd2=tf(num2, denum2);
figure(2)
%bode(bd2)

gd = c2d(bd2,0.0002)
bode(bd2,'r',gd,'b--')
clspd=tf(num2,[1])/(tf(num2,[1])+tf(denum2,[1]))
figure(3)
step(clspd,0.1)
figure(4)
bode(clspd,c2d(clspd,0.0002))
```

C++ code SVPWM

```
void SVM_Modulation3p(float va_ref,float vb_ref)
    {
    vdc_invTime=0.5/(PUVoltages.U_dc_1);//*INVERTER_PARM.Tsw--- Normalized
here
   // float va_ref,vb_ref;
    float X,Y,Z;
    float va,vb,vc;

    X=vb_ref;// X=abs(vbref)
    Y=0.5*(vb_ref + SQRT3*va_ref);
    Z=0.5*(vb_ref - SQRT3*va_ref);
     //Modified inverse park transformation
     va=vb_ref;
     vb=0.5*(SQRT3*va_ref - vb_ref);
     vc=0.5*(-SQRT3*va_ref - vb_ref);
     //----------------------------------------
     int A, B, C;
         if(va>0) A=1; else A=0;
         if(vb>0) B=1; else B=0;
         if(vc>0) C=1; else C=0;

         float t1=0,t2=0;
```

```
        int sector;
        int N=A+2*B+4*C;

        switch (N)
        {
        case 3: // sector 1
            t1=X; t2=-Z; sector=1;break; // interchange t1 and t2 here
        case 1: // sector 2
            t1=Y; t2=Z;sector=2;break;
        case 5: // sector 3
            t1=-Y; t2=X;sector=3;break;// interchange t1 and t2 here
        case 4: // sector 4
            t1=Z; t2=-X;sector=4;break;
        case 6: // sector 5
            t1=-Z; t2=-Y;sector=5;break;//interchange t1 and t2 here
        case 2: // sector 6
            t1=-X; t2=Y;sector=6;break;
        default:
            sector=0;
        }
    //-------------------------

            float w0,w1,w2;// one time of each phase

            w0=(float)(1.0-t1-t2)/2.0;
            w1=w0+t1;
            w2=w1+t2;
        float ta_on=0,tb_on=0,tc_on=0;
            // sector phase time calculation
           // odd sector
           switch(sector)
            {
           case 1: //100 110
               ta_on=w2; tb_on=w1; tc_on=w0; break;
           case 2:// 110 010
               ta_on=w1; tb_on=w2; tc_on=w0; break;
           case 3:// 010 011
               ta_on=w0; tb_on=w2; tc_on=w1; break;
           case 4:// 011 001
               ta_on=w0; tb_on=w1; tc_on=w2; break;
           case 5:// 001 101
               ta_on=w1; tb_on=w0; tc_on=w2; break;
           case 6:// 101 100
               ta_on=w2; tb_on=w0; tc_on=w1; break;
           default:
           ta_on=0,tb_on=0,tc_on=0;


            }
      //--------------------------------

            DwellTime.a=SQRT3*vdc_invTime*(ta_on-0.5);//;
            DwellTime.b=SQRT3*vdc_invTime*(tb_on-0.5);//*
            DwellTime.c=SQRT3*vdc_invTime*(tc_on-0.5);//


    }
```

G. Paper presented at IEEE PES Trondheim PowerTech 19-24 June 2011, Norway

Vector Control of Direct Drive Six Phase Permanent Magnet Synchronous Generators

Nahome Alemayehu A., R. Zaimeddine, Bing Liu and Tore Undeland

Norwegian University of Science and Technology, Trondheim, Norway

Abstract—**this paper presents the vector control of six phase permanent magnet synchronous generator which is directly connected to a six leg converter. A mathematical model of the machine has been developed using the generalized two phase real component transformation. Dual synchronous d-q current control is employed so as to eliminate current imbalances. The six legs the converter are controlled to extract the maximum power from the wind turbine with reduced torque pulsation, reduced harmonics and minimum stator losses using vector space decomposition space vector modulation. Matlab® Simulink is used for simulation.**

Index Terms— orthogonal subspace transformation, multi leg converter, six phase permanent magnet machines, space vector pulse width modulation, vector control, vector space decomposition.

I. Introduction

MULTI Phase machines provides several advantages such as : reduction of amplitude of pulsating torque and increased pulsating frequency; reduction of current per phase for the same rated voltage; lowering the dc-link current harmonics; reducing the stator copper loss ; improving reliability and give additional degree of freedom[1]-[3]. Permanent magnet synchronous generators known to have higher power density, higher efficiency, more stable and secure during normal operation. Off shore wind energy system needs to be more reliable and lighter than on shore wind energy system. Therefore, Multiphase PMSGs have become attractive for large off shore wind farm.

Multiphase machines drives, motors, has been used as in Electric Vehicles(EV), hybrid EV, aerospace, ship propulsion, and high-power applications in which the requirements are not cost oppressive when compared to the overall system[1]-[4]. Reference [2] gives thorough survey related to Multiphase drives in various subcategories, and including the application of Multiphase machines for electric generation.

In [5] parallel connection of converters in modular way is investigated to allow the use of classical converters. The application of multiphase PMSG for wind is also shown in [6] that the two three phase windings are controlled independently.

In this paper the six-phase PMSG has two groups of three phase windings which are separated by 30 degrees. The arrangement of the six phases and definition of reference frames is shown in Fig. 1.

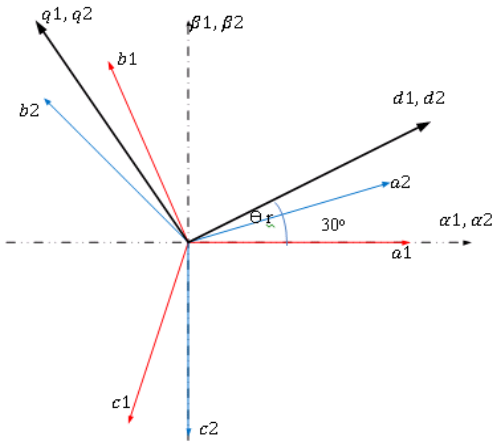

Fig. 1 Six phase machine-arrangement of stator windings

II. System Description

The proposed wind energy conversion system along with the control scheme is shown in Fig. 2. It is assumed that the average DC link voltage is kept constant by the grid side converter which is modeled by constant dc ideal voltage source.

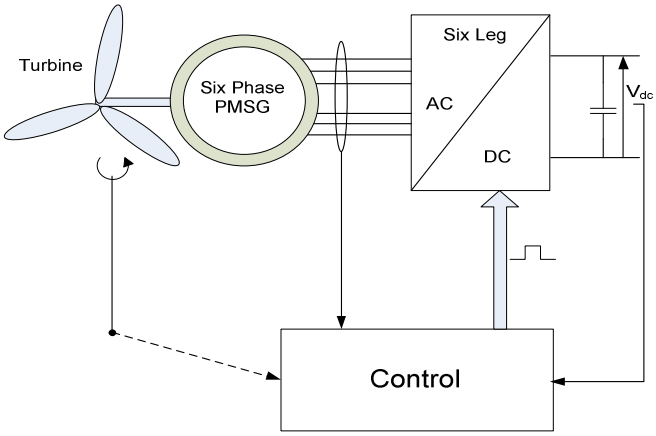

Fig. 2. System topology

A. Wind turbine

The power extracted from wind by turbine is given by

$$P_t = \frac{1}{2} C_p \rho A v_w^{\,3} \quad (1)$$

Where ρ is the air density, A is the area swept out by the turbine blades, v_w is the wind velocity, and C_p is the power coefficient. C_p is a function of the pitch angle β and of the tip speed ratio λ, shown in Fig. 3. Tip speed ratio is the ratio of turbine speed at the tip of a blade to wind velocity.

$$\lambda = \frac{\omega R}{v_w} \quad (2)$$

where R is the turbine radius, and ω is the turbine angular speed.

For a given wind turbine, the maximum power extracted can be tracked by adjusting the speed of the generator either using maximum power tracking or the optimal tip speed ratio.

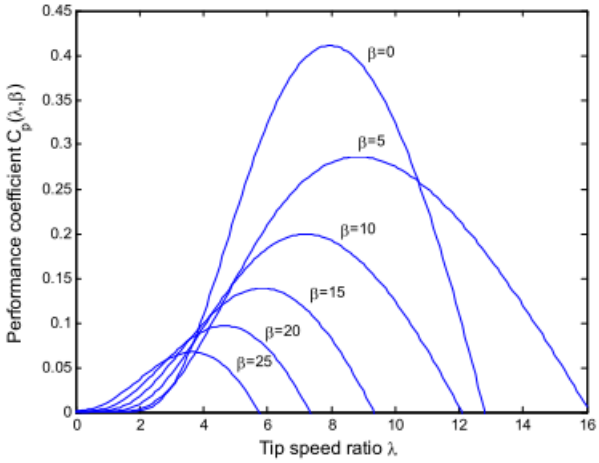

Fig. 3. Power (performance) coefficient as function of λ and β [7].

B. Six Phase PMSG Modeling

By neglecting the magnetic saturation and core losses, and assuming a sinusoidal air gap flux, the voltage equations of generator in phase quantities are

$$[\mathrm{V_s}] = [\mathrm{R_s}][\mathrm{i_s}] + \mathrm{p}\cdot([\mathrm{L_s}][\mathrm{i_s}]) + \mathrm{p}\cdot([\lambda_{\mathrm{sM}}]) \quad (2)$$

$$[\lambda_{\mathrm{sM}}] = \lambda_{\mathrm{M}}\left[\cos\theta_{\mathrm{r}} \;\; \cos\left(\theta_{\mathrm{r}} - \tfrac{2\pi}{3}\right) \;\; \cos\left(\theta_{\mathrm{r}} + \tfrac{2\pi}{3}\right) \;\; \cos\left(\theta_{\mathrm{r}} - \pi 6\right) \;\; \cos\theta\mathrm{r} - 5\pi 6 \;\; \cos\theta\mathrm{r} - 3\pi 2\mathrm{T}\right] \quad (3)$$

where the voltage and current are defines as

$\mathrm{V_s} = [\mathrm{V_{a1}}\ \mathrm{V_{b1}}\ \mathrm{V_{c1}}\ \mathrm{V_{a2}}\ \mathrm{V_{b2}}\ \mathrm{V_{c2}}]^{\mathrm{T}}$

$i_s = [i_{a1}\, i_{b1}\ i_{c1}\ i_{a2}\ i_{b2}\ i_{c2}]^T$;

λ_M is the permanent magnet flux linkage, θ_r is the angle between magnetic axis of phase 'a' and rotating magnetic field , as shown in Fig. 1., and $p\cdot(\,) = \frac{d(\,)}{dt}$.

The resistance term and the inductance terms of (2) are given by (4); for Surface Mounted PMSG the pulsatory components of the magnetizing inductance of stator windings are zero. Mutual leakage inductance is ignored and has little effect on torque pulsation and voltage harmonic distortion since the separation angle between the two sets of three phase windings is 30°, [8].

$$[R_s] = \begin{bmatrix} r_s & 0 & 0 & 0 & 0 & 0 \\ 0 & r_s & 0 & 0 & 0 & 0 \\ 0 & 0 & r_s & 0 & 0 & 0 \\ 0 & 0 & 0 & r_s & 0 & 0 \\ 0 & 0 & 0 & 0 & r_s & 0 \\ 0 & 0 & 0 & 0 & 0 & r_s \end{bmatrix} \quad (4a)$$

$$[L_s] = L_l \begin{bmatrix} 1 & 0 & 0 & 0 & 0 & 0 \\ 0 & 1 & 0 & 0 & 0 & 0 \\ 0 & 0 & 1 & 0 & 0 & 0 \\ 0 & 0 & 0 & 1 & 0 & 0 \\ 0 & 0 & 0 & 0 & 1 & 0 \\ 0 & 0 & 0 & 0 & 0 & 1 \end{bmatrix} + L_1 \begin{bmatrix} 1 & -1/2 & -1/2 & \sqrt{3}/2 & -\sqrt{3}/2 & 0 \\ -1/2 & 1 & -1/2 & 0 & \sqrt{3}/2 & -\sqrt{3}/2 \\ -1/2 & -1/2 & 1 & -\sqrt{3}/2 & 0 & \sqrt{3}/2 \\ \sqrt{3}/2 & 0 & -\sqrt{3}/2 & 1 & -1/2 & -1/2 \\ -\sqrt{3}/2 & \sqrt{3}/2 & 0 & -1/2 & 1 & -1/2 \\ 0 & -\sqrt{3}/2 & \sqrt{3}/2 & -1/2 & -1/2 & 1 \end{bmatrix} \quad (4b)$$

Where $\mathrm{r_s}$, L_l and L_1 are resistance, leakage reactance and magnetizing reactance of a stator winding respectively.

Using generalized two phase real component transformation or vector space decomposition theory, the original six dimensional space representation of the machine is mapped to three orthogonal two dimensional subspaces, [16]. The power invariant transformation matrix is used to map phase quantities to orthogonal subspace quantities, which is

$$[T_6] = \frac{1}{\sqrt{3}} \begin{bmatrix} 1 & \cos 4\theta & \cos 8\theta & \cos\theta & \cos 5\theta & \cos 9\theta \\ 0 & \sin 4\theta & \sin 8\theta & \sin\theta & \sin 5\theta & \sin 9\theta \\ 1 & \cos 8\theta & \cos 4\theta & \cos 5\theta & \cos\theta & \cos 9\theta \\ 0 & \sin 8\theta & \sin 4\theta & \sin 5\theta & \sin\theta & \sin 9\theta \\ 1 & 1 & 1 & 0 & 0 & 0 \\ 0 & 0 & 0 & 1 & 1 & 1 \end{bmatrix} \quad (5)$$

where $\theta = \frac{\pi}{6}$

Applying transformation $[\mathrm{T_6}]$ to (2) and (3), the vector space decomposition variable can be written as

$$[\mathrm{V_{vsd}}] = [\mathrm{R_s}][\mathrm{i_{vsd}}] + [\mathrm{L_{vsd}}]\mathrm{p}\cdot([\mathrm{i_{vsd}}]) + \omega_{\mathrm{r}}[\lambda_{\mathrm{vsd}}] \quad (6)$$

$$[\lambda_{\mathrm{vsd}}] = \sqrt{3}\lambda_{\mathrm{M}}\omega_{\mathrm{r}}[-\sin\theta_{\mathrm{r}}\ \cos\theta_{\mathrm{r}}\ 0\ 0\ \ 0\ 0]^{\mathrm{T}} \quad (7)$$

where $\omega_{\mathrm{r}} = \frac{d\theta_{\mathrm{r}}}{dt}$

$[V_{vsd}] = [V_\alpha\, V_\beta\ V_x\ V_y\ V_{z1}\ V_{z2}]^T$ $[\,i_{vsd}] = [i_\alpha\, i_\beta\ i_x\, i_y\, i_{z1}\ i_{z2}]^T$

And

$$[\mathrm{L_{vsd}}] = \begin{bmatrix} \mathrm{L_\alpha} & 0 & 0 & 0 & 0 & 0 \\ 0 & \mathrm{L_\alpha} & 0 & 0 & 0 & 0 \\ 0 & 0 & \mathrm{L_l} & 0 & 0 & 0 \\ 0 & 0 & 0 & \mathrm{L_l} & 0 & 0 \\ 0 & 0 & 0 & 0 & \mathrm{L_l} & 0 \\ 0 & 0 & 0 & 0 & 0 & \mathrm{L_l} \end{bmatrix} \quad (8a)$$

$$\mathrm{L_\alpha} = 3\mathrm{L_1} + \mathrm{L_l} \quad (8b)$$

As seen above the voltage and flux equations are as a function of rotor position. This can be eliminated by using

reference transformation, T_r.

$$T_r = \begin{bmatrix} \cos\theta_r & -\sin\theta_r \\ \sin\theta_r & \cos\theta_r \end{bmatrix} \quad (9a)$$

$$\begin{bmatrix} W_\alpha \\ W_\beta \end{bmatrix} = T_r \begin{bmatrix} W_d \\ W_q \end{bmatrix} \quad (9b)$$

where W is dummy variable which can be voltage, current or flux. Therefore, the machine model in the synchronous rotating frame, applying rotational transformation T_r on (6) and (7), become

1) Machine model in (d,q) subspace

$$V_d = r_s i_\alpha + L_\alpha \, p \cdot (i_d) - \omega_r L_\alpha \, i_q \quad (10a)$$

$$V_q = r i_\beta + L_\alpha p \cdot (i_q) + \omega_r L_\alpha \, i_d + \omega_r \sqrt{3} \lambda_M \quad (10b)$$

2) Machine model in (x, y) subspace

$$\begin{bmatrix} V_x \\ V_y \end{bmatrix} = \begin{bmatrix} r_s + L_l \, p \cdot ( ) \\ r_s + \ L_l p \cdot ( ) \end{bmatrix} \begin{bmatrix} i_x \\ i_y \end{bmatrix} \quad (11)$$

3) Machine Model in (z_1, z_2) subspace

$$\begin{bmatrix} V_{z1} \\ V_{z2} \end{bmatrix} = \begin{bmatrix} r_s + L_l \, p \cdot ( ) \\ r_s + L_l p \cdot ( ) \end{bmatrix} \begin{bmatrix} i_{z1} \\ i_{z2} \end{bmatrix} \quad (12)$$

As seen from (11) and (12), the current components in (x, y) and (z_1, z2) are limited to stator resistor and stator leakage inductance. These currents do not contribute to electromechanical energy conversion but losses. Thereby the electromechanical energy conversion variables are mapped in the only (d,q) subspace. This makes the modeling of the machine and torque calculation simpler. The electro-magnetic torque expression can be calculated from the air gap power. The air gap power is the part of input power which does not contribute to resistive loss or rate of change of stored energy in the inductances.

$$P_{ag} = P_{el} - P_{loss} - P_{rateChangeStoredMagnetic}$$

$$P_{ag} = \omega_r \sqrt{3} \lambda_M i_q \quad (13)$$

And if there are P poles, the electrical torque T_e is

$$T_e = \frac{P_{ag}}{\omega_m} = \frac{P}{2} \sqrt{3} \lambda_M i_q = K \, i_q \quad (14)$$

C. Six Leg Converter

Using more legs means, power is shared by the many legs so that the current stress of each switch can be reduced compared with a three-phase converter. Besides six leg converters give more freedom to choose switching states which helps for optimal operation of the generator. Fig. 4, shows the generic scheme of six leg converter.

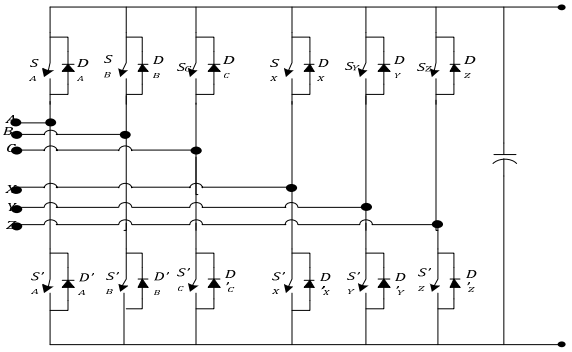

Fig. 4. Schematic of six leg converter

Only one of the power switches of the same leg can operate in the "ON" state to avoid the short circuit of the DC-link. The switching function can be represented in terms of the upper switch of each leg as $f(S_{a1}, S_{b1}, S_{c1}, S_{a2}, S_{b2}, S_{c2})$.

Applying the transformation matrix $[T_6]$ on the phase voltages of the converter, the converter voltages with respect to the stationary reference frame given by

$$\begin{bmatrix} V_\alpha \\ V_\beta \\ V_x \\ V_y \\ V_{z1} \\ V_{z2} \end{bmatrix} = \frac{V_{dc}}{\sqrt{3}} \begin{bmatrix} 1 & -\frac{1}{2} & -\frac{1}{2} & \frac{\sqrt{3}}{2} & \frac{-\sqrt{3}}{2} & 0 \\ 0 & \frac{\sqrt{3}}{2} & \frac{-\sqrt{3}}{2} & \frac{1}{2} & \frac{1}{2} & -1 \\ 1 & -\frac{1}{2} & -\frac{1}{2} & -\frac{\sqrt{3}}{2} & \frac{\sqrt{3}}{2} & 0 \\ 0 & -\frac{\sqrt{3}}{2} & \frac{\sqrt{3}}{2} & \frac{1}{2} & \frac{1}{2} & -1 \\ 0 & 0 & 0 & 0 & 0 & 0 \\ 0 & 0 & 0 & 0 & 0 & 0 \end{bmatrix} \begin{bmatrix} S_{a1} \\ S_{b1} \\ S_{c1} \\ S_{a2} \\ S_{b2} \\ S_{c2} \end{bmatrix} \quad (15)$$

The converter and the machine are connected without neutral line and is taken in account, [9]. The switching voltages (z_1, z_2) subspace is zero since the neutral points are isolated. The vector space diagram converter of the converter voltages on (α,β) and (x, y) subspace are shown in Fig. 5. and Fig. 6.

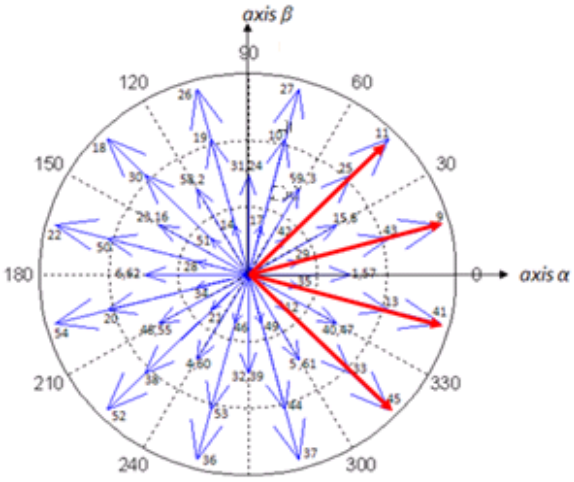

Fig. 5. Converter voltage on (α,β) subspace; 0, 7, 56, 63 are zero states

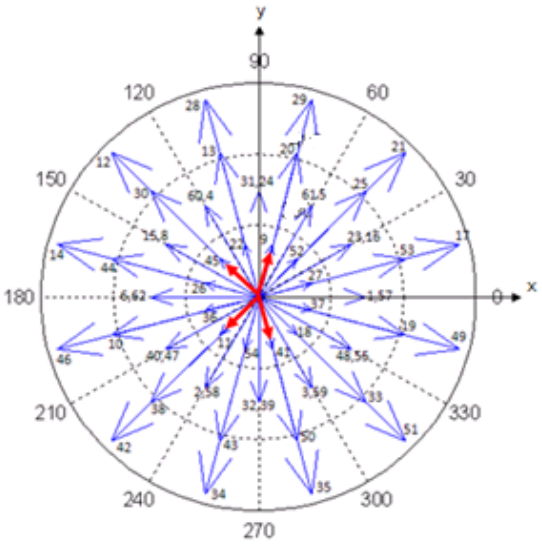

Fig. 6. Converter voltage on (x, y) subspace; 0, 7, 56, 63 zero states

D. Space Vector PWM

The vector space decomposition technique is of priority. As shown in Fig. 5 and Fig. 6, the largest voltages (outer most) on (α,β) become smallest (inner most) voltages on (x, y) subspace. The medium voltages have the same magnitude on both(α,β) and (x, y) subspaces. Hence, the largest voltages are chosen as active voltage thereby the switching control is simplified to 12 sectors. To minimize losses in the (x, y) subspaces four active vector and one zero vector are chosen to build the space vector in(α,β) subspace. The red vectors in Fig. 5 and Fig. 6 shows the four active voltages when the resultant vector lies on the first sector $(-\frac{\pi}{12}, \frac{\pi}{12})$.

Imposing on the converter that average zero volt-seconds of the switching vectors on (x, y) subspace and at same time equaling the average volt-seconds of switching vectors on (α,β) to that of the reference voltages at the output of the inner current controller, further reduction in losses can be achieved. The time duration of the four active vectors and one zero vector is calculated this way, [9].

$$\begin{bmatrix} V_\alpha^{\,1} & V_\alpha^{\,2} & V_\alpha^{\,3} & V_\alpha^{\,4} & V_\alpha^{\,0} \\ V_\beta^{\,1} & V_\beta^{\,2} & V_\beta^{\,3} & V_\beta^{\,4} & V_\beta^{\,0} \\ V_x^{\,1} & V_x^{\,2} & V_x^{\,3} & V_x^{\,4} & V_\alpha^{\,0} \\ V_y^{\,1} & V_y^{\,2} & V_y^{\,3} & V_y^{\,4} & V_\beta^{\,0} \\ 1 & 1 & 1 & 1 & 1 \end{bmatrix} \begin{bmatrix} T_1 \\ T_2 \\ T_3 \\ T_4 \\ T_0 \end{bmatrix} = \begin{bmatrix} T_s V_\alpha^{\,*} \\ T_s V_\beta^{\,*} \\ 0 \\ 0 \\ T_s \end{bmatrix} \quad (15)$$

Where, $V_k^{\,i}$ is the projection of the i^{th} voltage on the k-plane and T_i is the dwelling time of the vector $V_k^{\,i}$ over a sampling period T_s.

The switching sequence of the gate signals are generated according to the dwelling time of the five vectors. Zero vector has to be selected carefully so that only one of the leg change state not more than two in a sampling period.

E. Vector Control

Vector control decouples field flux and armature flux so that they can be controlled separately to control torque or current and power or speed independently. The current control forms an inner loop while seep control forms the outer control for the case considered. The vector control is applied in the synchronous rotating frame so as to use simple PI regulators will result in zero steady-state error since the steady-state currents are dc currents

The vector space decomposition approach of vector control has been used to control dual three phase induction machines [9]-[13]. Though using single current controller makes the design easier and need less number of PI regulators, it can not observe the current imbalance. Therefore, to do away with this problem, dual current controller is preferred. The control schematics of the proposed system is shown in Fig. 7

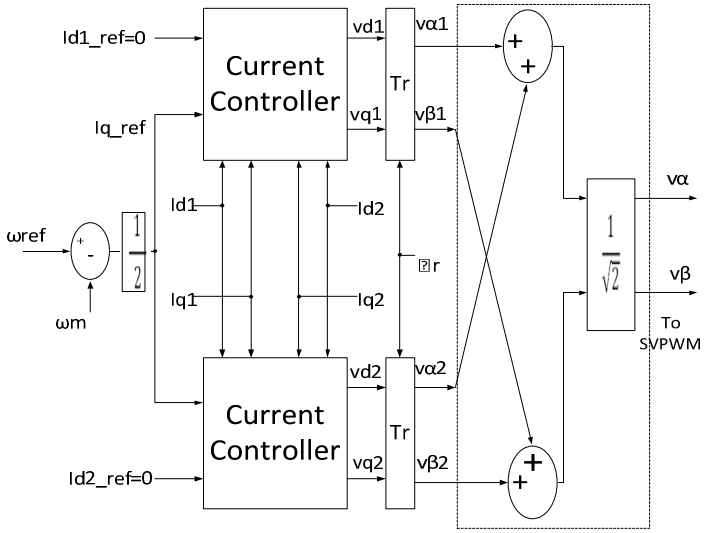

Fig. 7. Control Schematics, with dual synchronous current control

To design dual current control for each three phase group, the generator voltage equations are derived with respect to synchronous rotating reference frames $(d1, q1)$ and $(d2, q2)$ see Fig.1.

$$V_{d1} = r_s i_{d1} + L_d\, p \cdot i_{d1} + M_d p \cdot i_{d2} - \omega_r L_q i_{q1} - \omega_r M_q i_{q2}$$

$$V_{q1} = r_s i_{q1} + L_q\, p \cdot i_{q1} + M_q p \cdot i_{q2} + \omega_r L_d i_{d1} + \omega_r M_d i_{d1} + \omega_r \sqrt{\frac{3}{2}}\, \lambda_M \quad (16a)$$

$$V_{d2} = r_s i_{d2} + L_d\, p \cdot i_{d2} + M_d p \cdot i_{d1} - \omega_r L_q i_{q2} - \omega_r M_q i_{q1}$$

$$V_{q2} = r_s i_{q2} + L_q\, p \cdot i_{q2} + M_q p \cdot i_{q1} + \omega_r L_d i_{d2} + \omega_r M_d i_{d1} + \omega_r \sqrt{\frac{3}{2}}\, \lambda_M \quad (16b)$$

There is strong coupling between the voltage equations. Since the d and q axis currents are constant at steady state, the current control can be simplified and also control structures is identical for d1 and d2 axes as well as q1 and q2 axes.

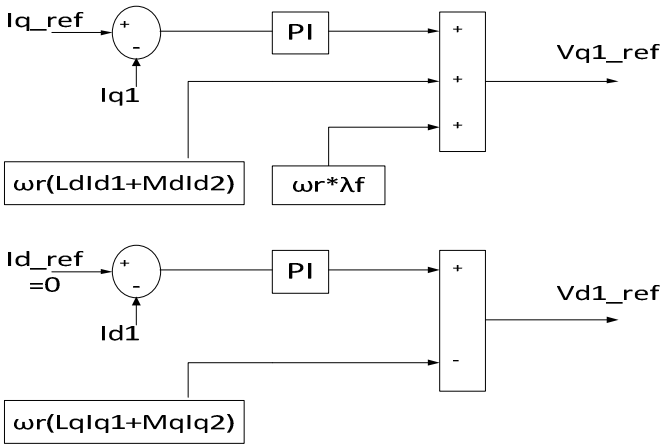

Fig. 8. Block diagram of the current controllers

By introducing feed forward compensation and assuming fast switching, the inner current controllers can be considered as separate closed loops (decoupled current loop), in which linear control theory can be applied. The Modulus optimum criterion is used to find the PI controller the current control loop. The detailed analysis of synchronous frame decoupled current control can be found in many literatures, [14]-[15]. So, it is not repeated here.

The outer controller, show in Fig. 7, is speed control. The reference speed is assumed to come from maximum point power tracking. The Symmetric Optimum criterion is employed to find the parameters of the PI controller. The permanent magnet flux linkage is at rated value and there is no need to use field weakening; the d axis current reference is kept zero which helps to fully utilize the stator current for torque or power extraction from the turbine.

III. RESULTS

Independent control of torque and speed is obtained. The average DC link voltage is kept constant as if grid side converter were connected.

The response of the generator-converter is tested first keeping the torque constant at -16 Nm and the reference speed is changed from 100 rad/s to 50 rad/s at 0.4 sec and then to 100 rad/is at 0.68 sec..

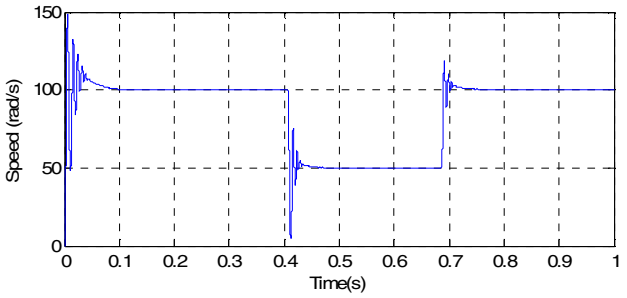

(a) Generator rotor speed

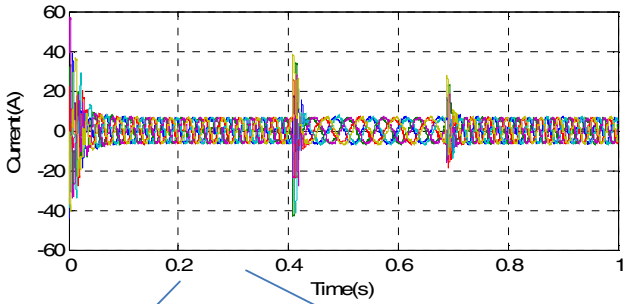

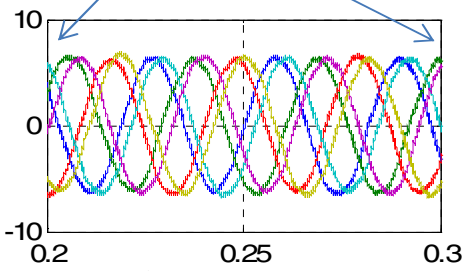

(b) Generator Stator Currents.

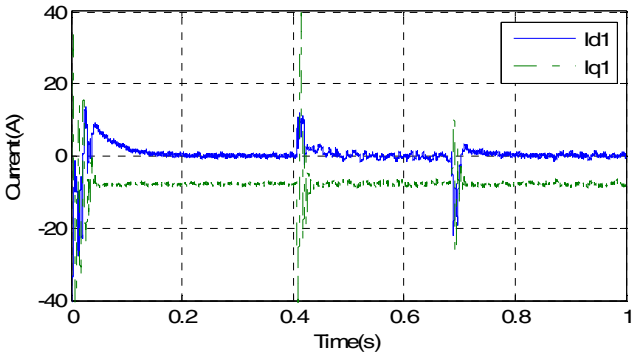

(c) d and q axis stator currents of phases (a1,b1,c1).

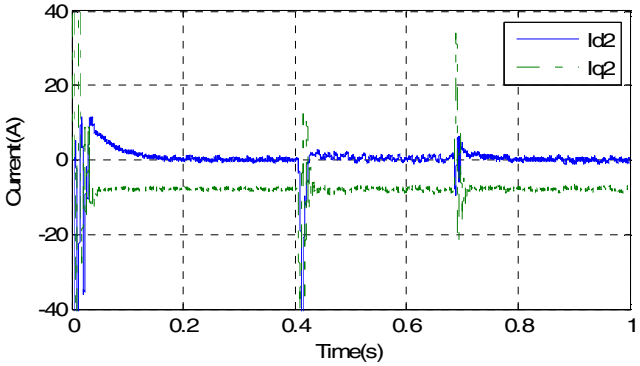

(d) d and q axis stator currents of phases(a2,b2,c2)

Fig. 9. Responses of vector controlled six phase PMSG- vector space decomposition SVPWM of six leg converter to speed change.

Similarly, the system performance is tested for torque change of torque from -16Nm to -10 Nm at 0.6 sec and again to -10 Nm at 0.96 sec as shown below.

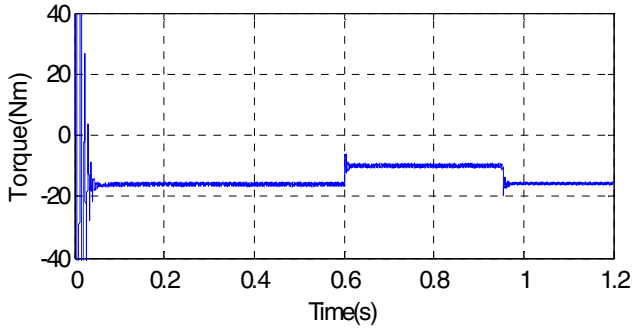

(a) Electrical Torque

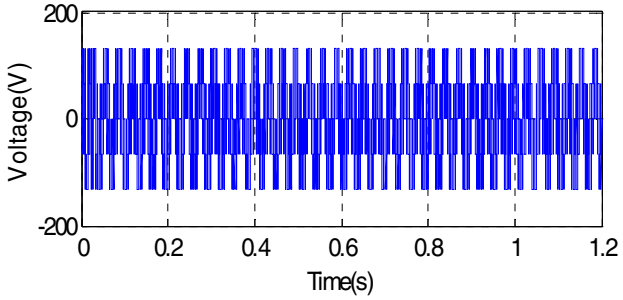

(b) Generator phase voltage/converter output

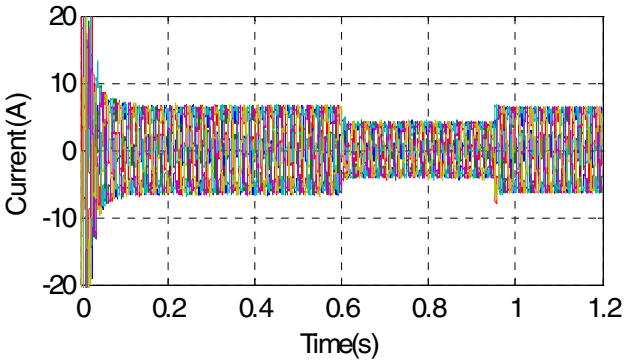

(c) Generator phase currents

IV. CONCLUSION

The use of vector space decomposition or generalized two phase real component transformation makes the modeling of six phase machines easier and also equivalent to that of three phase machines.

The dual synchronous current controller maintains the current in the two groups of three phase systems equal if there is current difference between them.

Having six leg converter increases the controllability of the converter using vector space decomposition SVPWM which results in reduced losses and ripple in the stator and Dc link current.

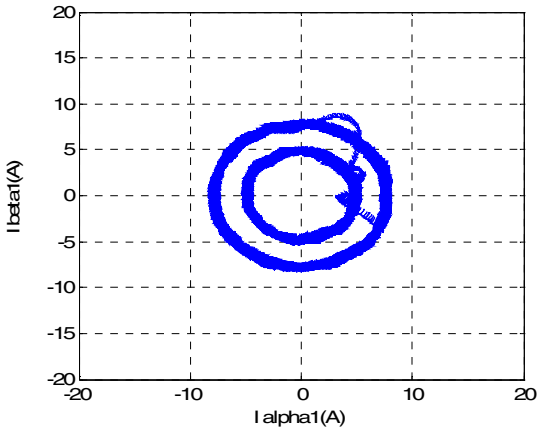

(d) Stator currents of phases(a1,b1,c1) referred to stationary axis (α1,β1)- radii of the circles is proportional to torque

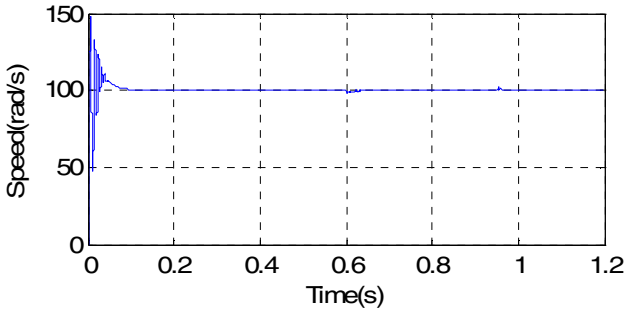

(e) Rotor Speed

Fig. 10. Responses of vector controlled six phase PMSG- vector space decomposition SVPWM of six leg converter to torque change.

V. REFERENCES

[1] L. Parsa, "On advantages of multi-phase machines," IEEE 2005, pp. 1574-1579

[2] Levi, E. "Multiphase Electric Machines for Variable-Speed Applications", *Industrial Electronics, IEEE Transactions on* pp. 1893 - 1909 , Vol. 55 , May 5, 2008

[3] Marcelo Godoy Simões, and Petronio Vieira, Jr., "A High-Torque Low-Speed Multiphase Brushless Machine—A Perspective Application for Electric Vehicles", IEEE TRANSACTIONS ON INDUSTRIAL ELECTRONICS, VOL. 49, NO. 5, OCT. 2002, pp. 1154-1164

[4] Leila Parsa and Suman Dwari "An Optimal Control Technique for Multiphase PM Machines Under Open-Circuit Faults'', IEEE TRANSACTIONS ON INDUSTRIAL ELECTRONICS, VOL. 55, NO. 5, MAY 2008.

[5] D. Vizireanu, S. Brisset, X. Kestelyn, P. Borchet, Y. Milet, and D. Laloy, "Investigation on multi-star structures for large power direct-drive wind generator," Electr. Power Compon. Syst., vol. 35, no. 2, pp. 135–152, 2007.

[6] Sheng-Nian Yeh, Jonq-Chin Hwang, Ming-Chih Hsieh, Li-Hsiu Chen "Development of Wind Power Control System for Six-Phase Permanent-Magnet Synchronous Generators"

[7] M. J. Duran , F. Barrero , S. Toral , M. Arahal , R. Gregor , R. Marfil "Multi-phase generators viability for offshore wind farms with HVDC transmission"

[8] Schiferl, R. F , and Ong, C. M., "Six Phase Synchronous Machine with AC and DC Stator Connections - I I: Harmonic Studies and Proposed Uninterruptable Power Supply Scheme," IEEE Transactions on Power Apparatus and Systems, Vol. PAS 102, No. 8, pp. 2694-2693

[9] Yifan Zhao, A. Lipo, "Space vector PWM control of Dual Three Phase Induction Machine using vector space decomposition", IEEE Trans. Industry Applications Vol 31 No 5,pp. 1100-1109, Oct 1995

[10] M.B.R. Corria, C.B. Jacobina, C.R. da Silva, A.M.N. Lima, E.R.C. da Silva' "Vector and Scalar Modulation for Six-Phase Voltage Source Inverters", IEEE 2003, pp. 562-567

[11] Yanhui He, Yue Wang, Jinlong Wu, Yupeng Feng, Jinjun Liu "A Comparative Study of Space Vector PWM Strategy for Dual Three-Phase Permanent-Magnet Synchronous Motor Drives" IEEE 2010, pp 915-919

[12] Radu Bojoi, Mario Lazzari, Francesco Profumo, "Digital Field-Oriented Control for Dual Three-Phase Induction Motor Drives ", IEEE TRANS. ON INDUSTRY APPLICATIONS, VOL39, NO. 3, MAY/JUNE 2003

[13] Bojoi, EProfumo, A. Tenconi , "Digital Synchronous Frame Current Regulation for Dual Three-phase Induction Motor Drives", IEEE 2003, pp 1475-1480

[14] Rusong Wu, S.B. Dewan, G.R. Slemon, "A PWM AC to DC Converter with Fixed Switching Frequency", IEEE 1998, pp. 706-711

[15] Vladimir Blasko, "A New Mathematical Model and Control of a Three-Phase AC–DC Voltage Source Converter", IEEE Transactions on POWER ELECTRONICS, VOL. 12, NO. 1, PP. 116-123,JAN 1997.

Dissertations:

[16] Thomas Marin Jahns "IMPROVED RELIABILITY IN SOLID STATE DERIVES FOR LARGE ASYNCHRONOUS AC MACHINES BY MEANS MULTIPLE INDEPENDENT PHASE DRIVE UNITS" Ph.D. dissertation, MIT April 1978 VOL I.